Radiation from acceleration Particles in relativistic jets with shocks and shear-flow

Ken Nishikawa ***UAHuntsville/Physics***

Collaborators:
P. Hardee (*Univ. of Alabama, Tuscaloosa*)
I. Duţan (*Institute of Space Science, Rumania*)
B. Zhang (*Univ. Nevada, Las Vegas*)
A. Meli (*Unv. of Gent*)
E. J. Choi (*KAIST*)
K. W. Min (*KAIST*)
J. Niemiec (*Institute of Nuclear Physics PAN*)
Y. Mizuno (*Goethe-Universität Frankfurt am Mein*)
M. Medvedev (*Univ. of Kansas*)
Å. Nordlund (*Niels Bohr Institute*)
J. Frederiksen (*Niels Bohr Institute*)
H. Sol (*Meudon Observatory*)
M. Pohl (*U-Potsdam/DESY*)
D. H. Hartmann (*Clemson Univ.*)
J. Gómez (*IAA, CSIC*)

Astro Coffee, June 2, 2015

Outline of talk

1. **Introduction and Weibel instability**
2. **Recent 3-D particle simulations of relativistic jets**
   *** $e^{\pm}$pair jet into $e^{\pm}$pair, $\gamma = 15$ and electron-ion ($m_i/m_e = 20$) into electron-ion $\gamma = 15$ shock structures**
3. **Magnetic field generation and particle acceleration in kinetic Kelvin-Helmholtz instability** (Nishikawa et al. 2014, ApJ, arXiv:1405.5247)
4. **Global jet simulations with shock and KKHI**
5. **Synthetic spectra in shocks generated by the Weibel instability**
6. **Acceleration in recollimation shock**
7. **Summary**
8. **Future plans**

Key Scientific questions

- How do shocks in relativistic jets evolve?
- How do magnetic fields affect shocks and reconnection?
- How are particles accelerated?
- What are the dominant radiation processes?
- How do 3-D relativistic PIC simulations reveal the dynamics of shock fronts and transition regions (CD and RS)?
- How do shocks in relativistic jets evolve in various ambient plasma- and magnetic field configurations?
- How do magnetic fields generated by the Weibel instability contribute to the emerging radiation?
- How do velocity shears generate magnetic fields and accelerate particles?
- How the Weibel instability and kKHI affect the evolution of shock with global jets?

Plasmas in the Universe

* The major constituents of the universe are made of plasmas.
* When the temperature of gas is more than 10^4K, the gas becomes fully ionized plasmas (4^{th} phase of matter).
* Plasmas are applied to many astrophysical phenomena.
* Plasmas are investigated in several ways
  * particle-in-cell (PIC) (microscopic)
  * magnetohydrodynamics, MHD (macroscopic)
  * hybrid (fluid electron and kinetic ions)
  * MHD with test particles (fluid mixed with particles)
  * particles with photons (more realistic simulations)

3D Relativistic particle-in-cell code

Kinetic processes are included in this code

- Particle acceleration can be investigated
- Synthetic spectrra of radiation can be calculated
- Simulation system size is limited due to necessity of resolving Debye length (Skin depth)
- Global dynamics of plasma such as large jets cannot be simulated

This simulation method is complimentary to MHD method which will be described briefly later

Terminal Hotspots

Kino & Takahara 04

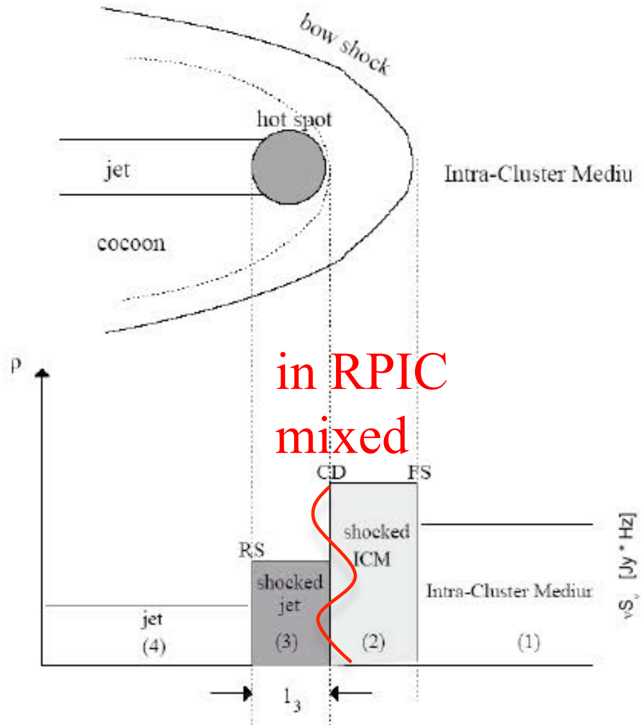

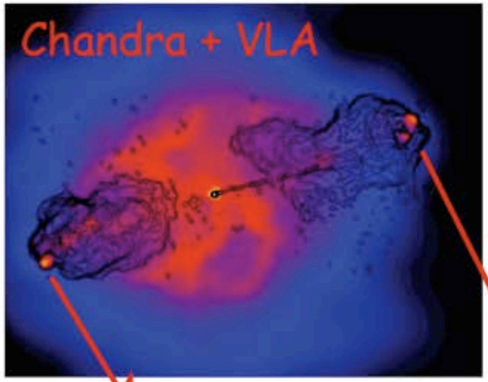

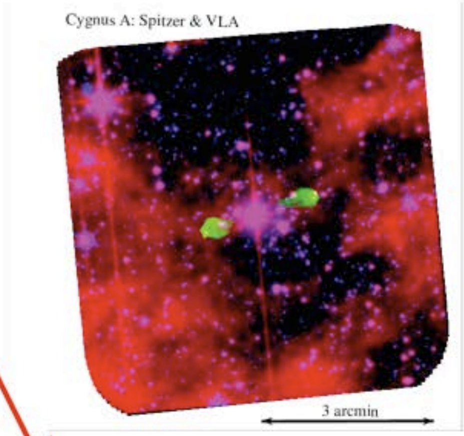

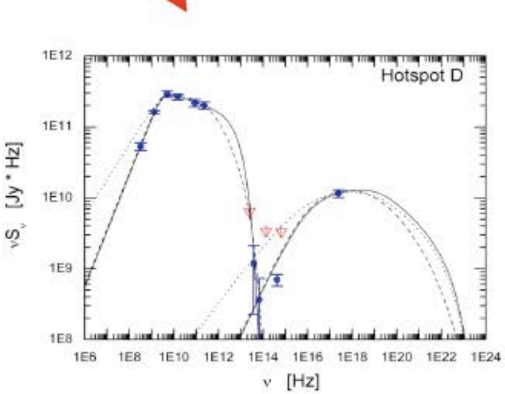

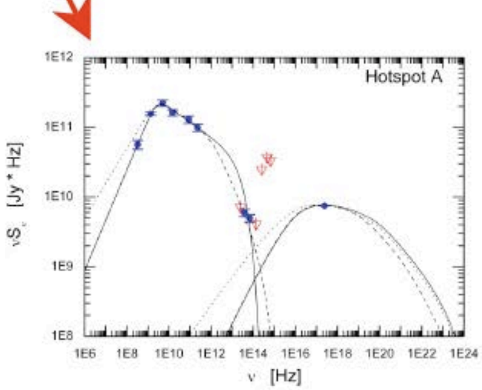

Hotspots in powerful radio sources are understood as the terminal regions of relativistic jets, where bulk kinetic power transported by the outflows from the active centers is converted at a strong shock (formed due to the interaction of the jet with the ambient gaseous medium) to the internal energy of the jet plasma.

Hotspots of exceptionally bright radio galaxy Cygnus A (d_L = 250 Mpc) can be resolved at different frequencies (VLA, Spitzer, Chandra), enabling us to understand how (mildly) relativistic shocks work (LS+ 07).

from the talk by L. Stawarz

Gamma-ray bursts

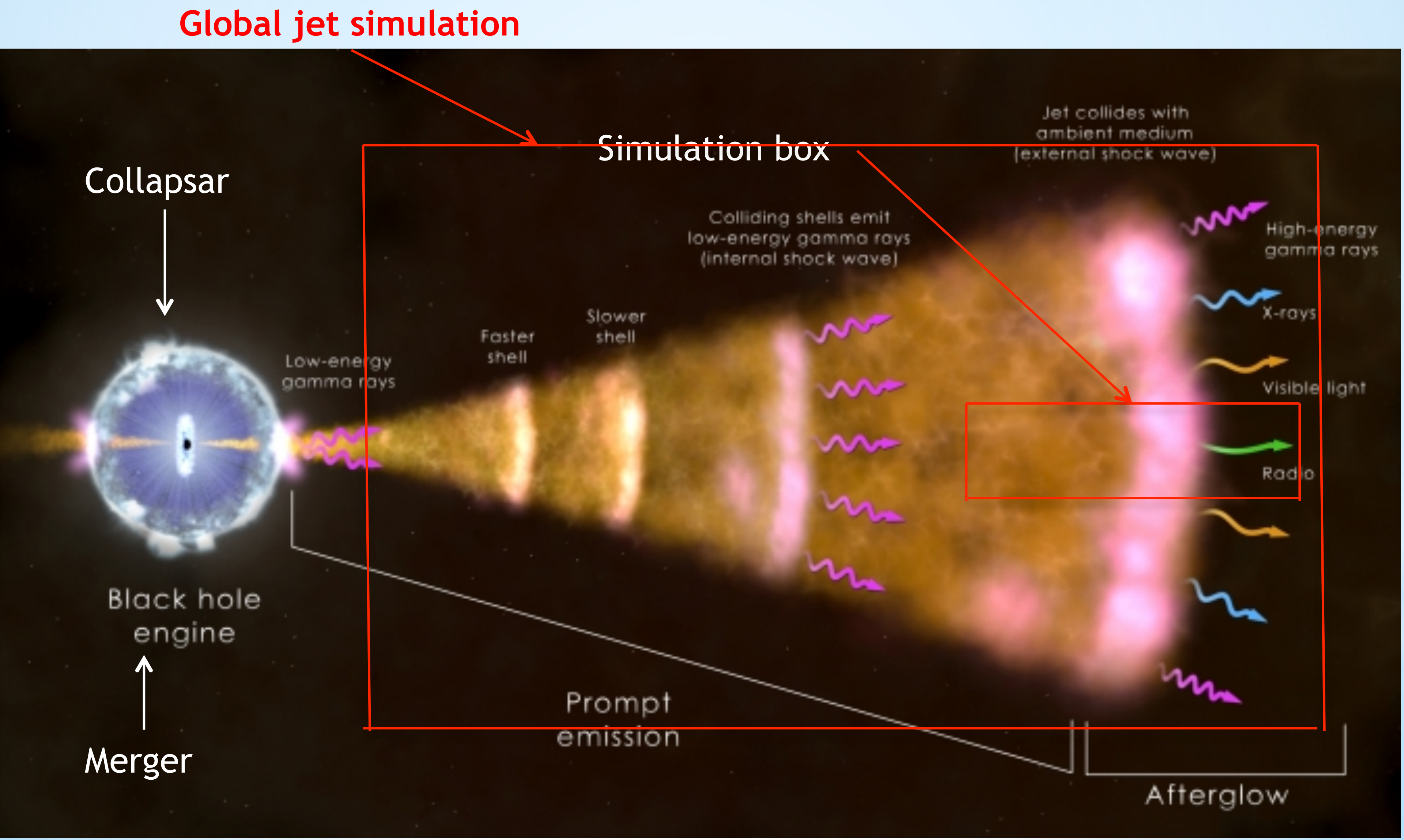

3-D simulation

with MPI code

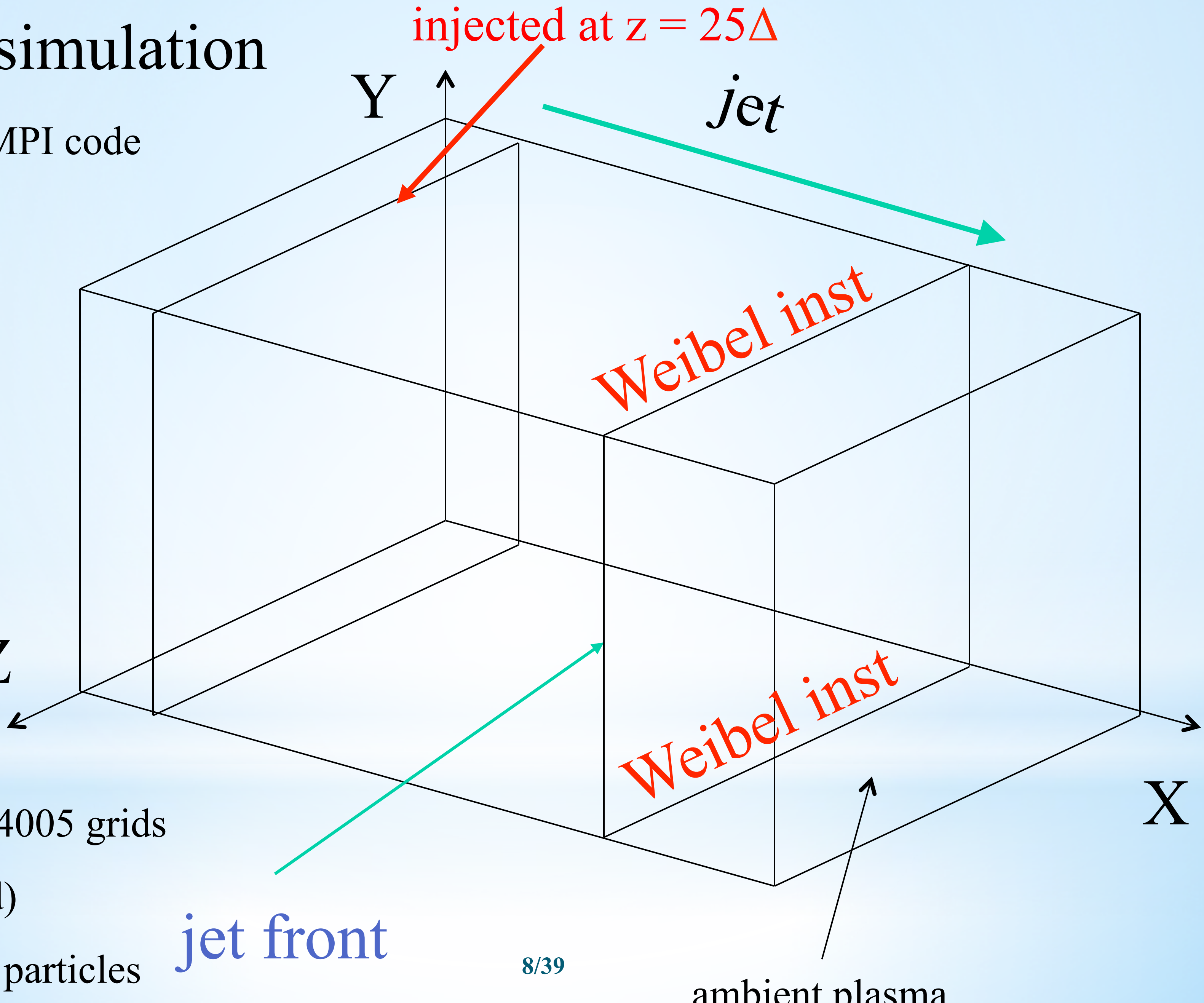

131×131×4005 grids

(not scaled)

1.2 billion particles

Collisionless shock

Electric and magnetic fields created self-consistently by particle dynamics randomize particles

(Buneman 1993)

$$\partial B / \partial t = -\nabla \times E$$
$$\partial E / \partial t = \nabla \times B - J$$
$$dm_0 \gamma v / dt = q(E + v \times B)$$
$$\partial \rho / \partial t + \nabla \bullet J = 0$$

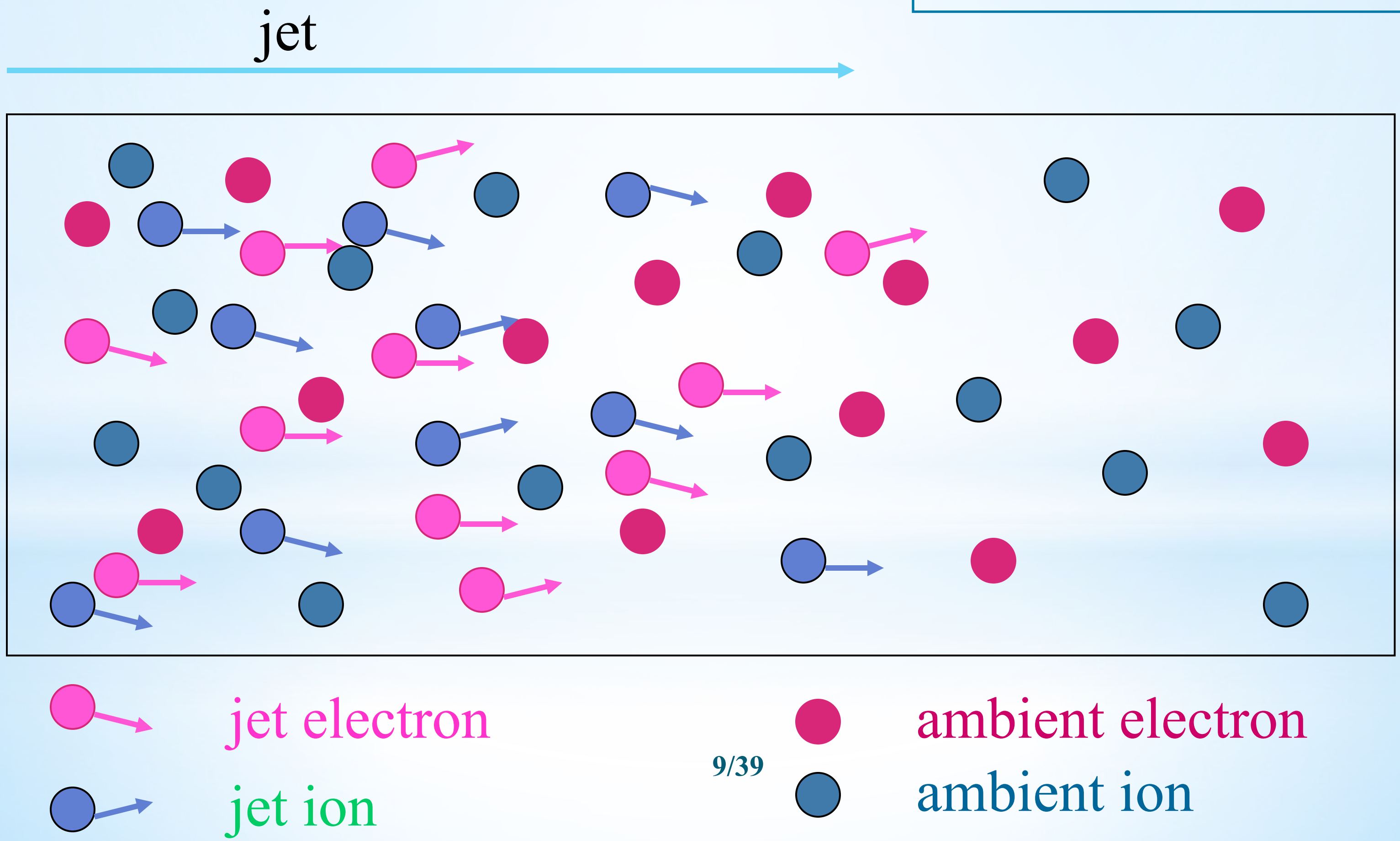

Weibel instability

current filamentation

Time:
$\tau = \gamma_{sh}^{1/2}/\omega_{pe} \approx 21.5$
Length:
$\lambda = \gamma_{th}^{1/2}c/\omega_{pe} \approx 9.6\Delta$

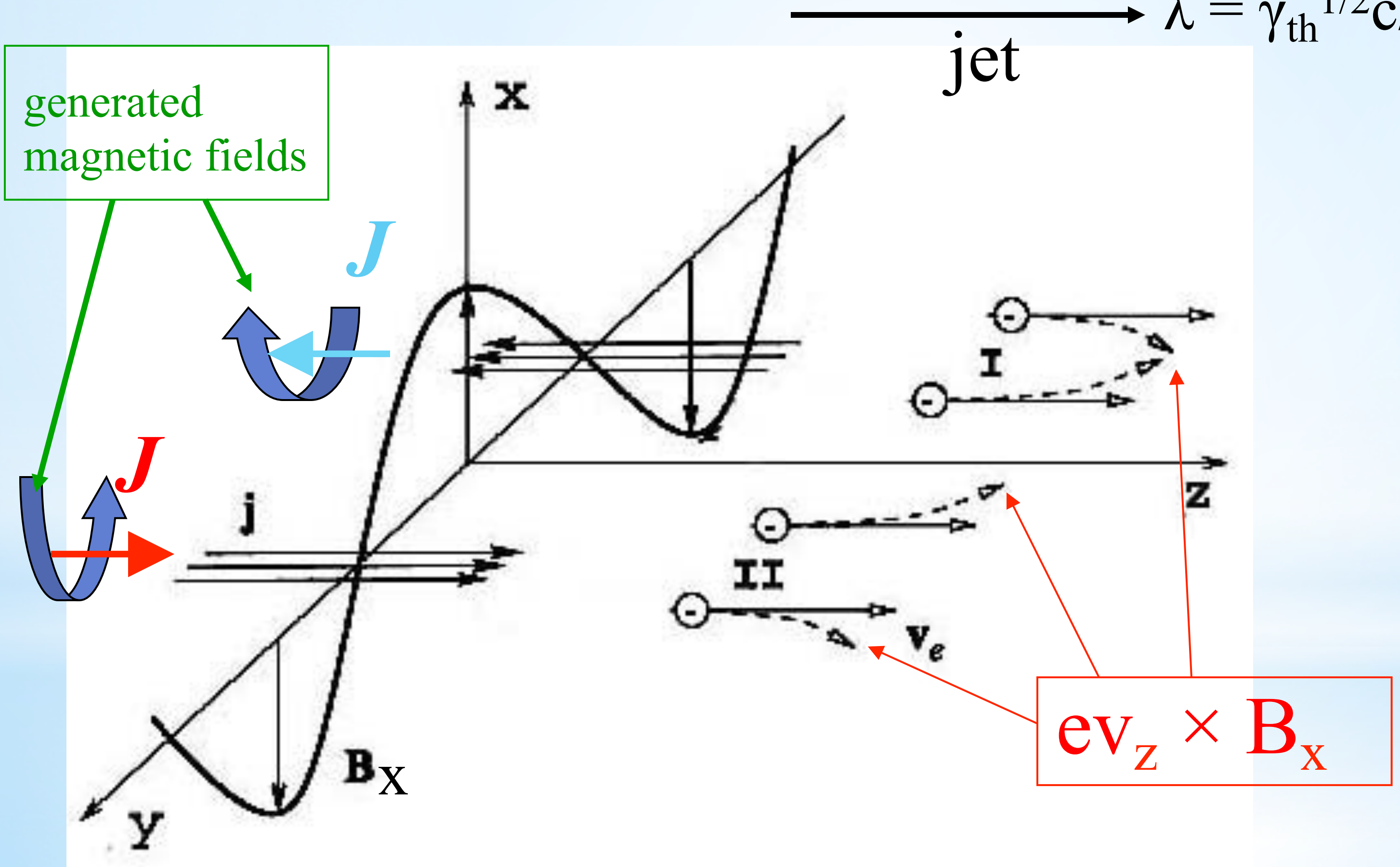

(electrons)

(Medvedev & Loeb, 1999, ApJ)

Evolution of B_x due to the Weibel instability

el-positron γ= 15 (B)

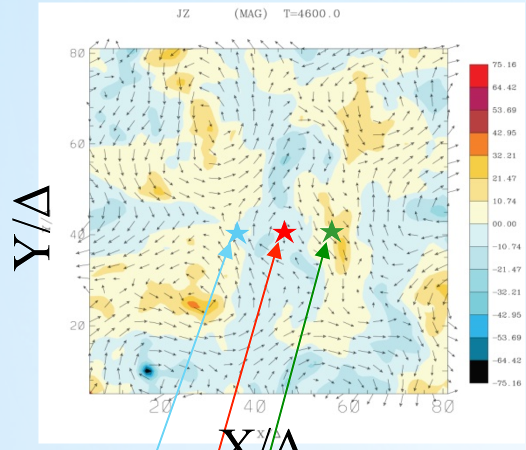

(*convective instability*)

$\omega_{pe}t = 59.8$

at Y = 43Δ

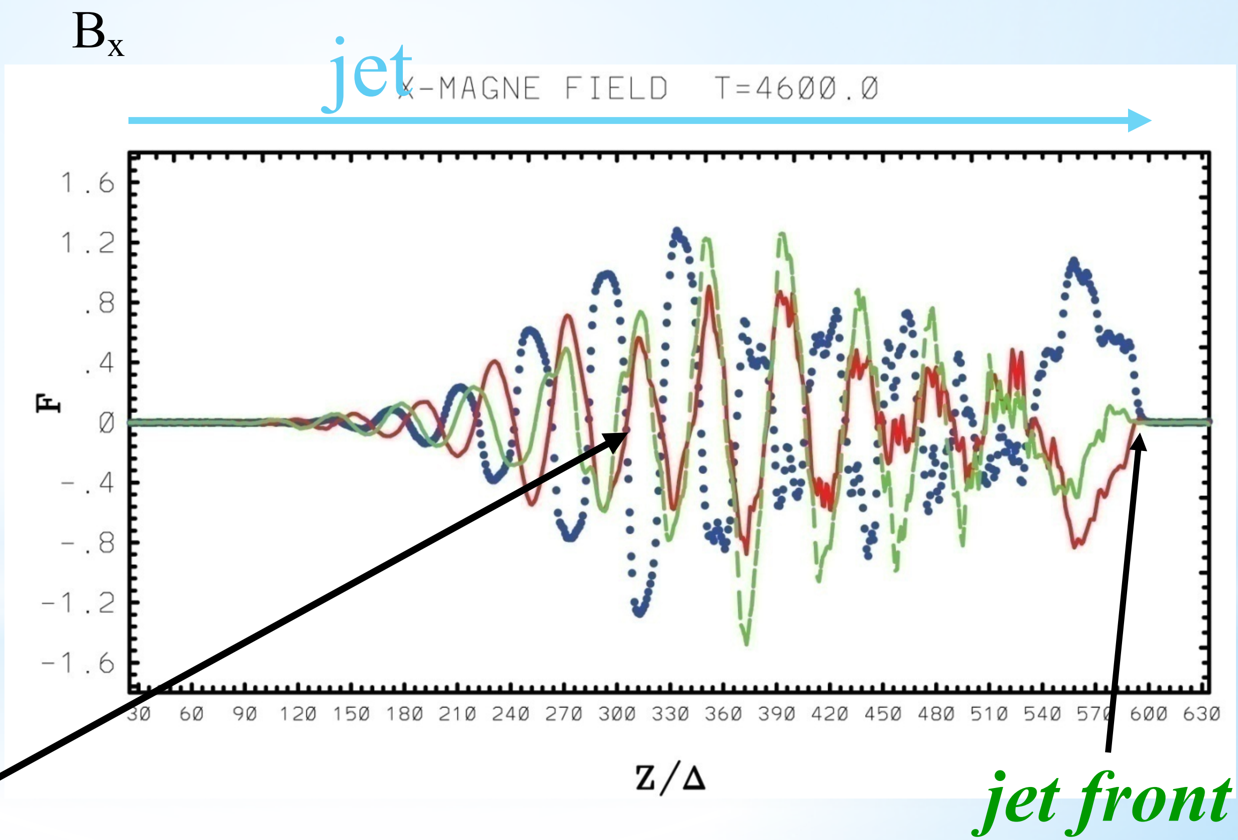

Blue X = 33 Δ
Red X = 43 Δ
Green X = 53 Δ

see movie b51.avi

Weibel instability

(Nishikawa et al. 2005)

Ion Weibel instability

ion current

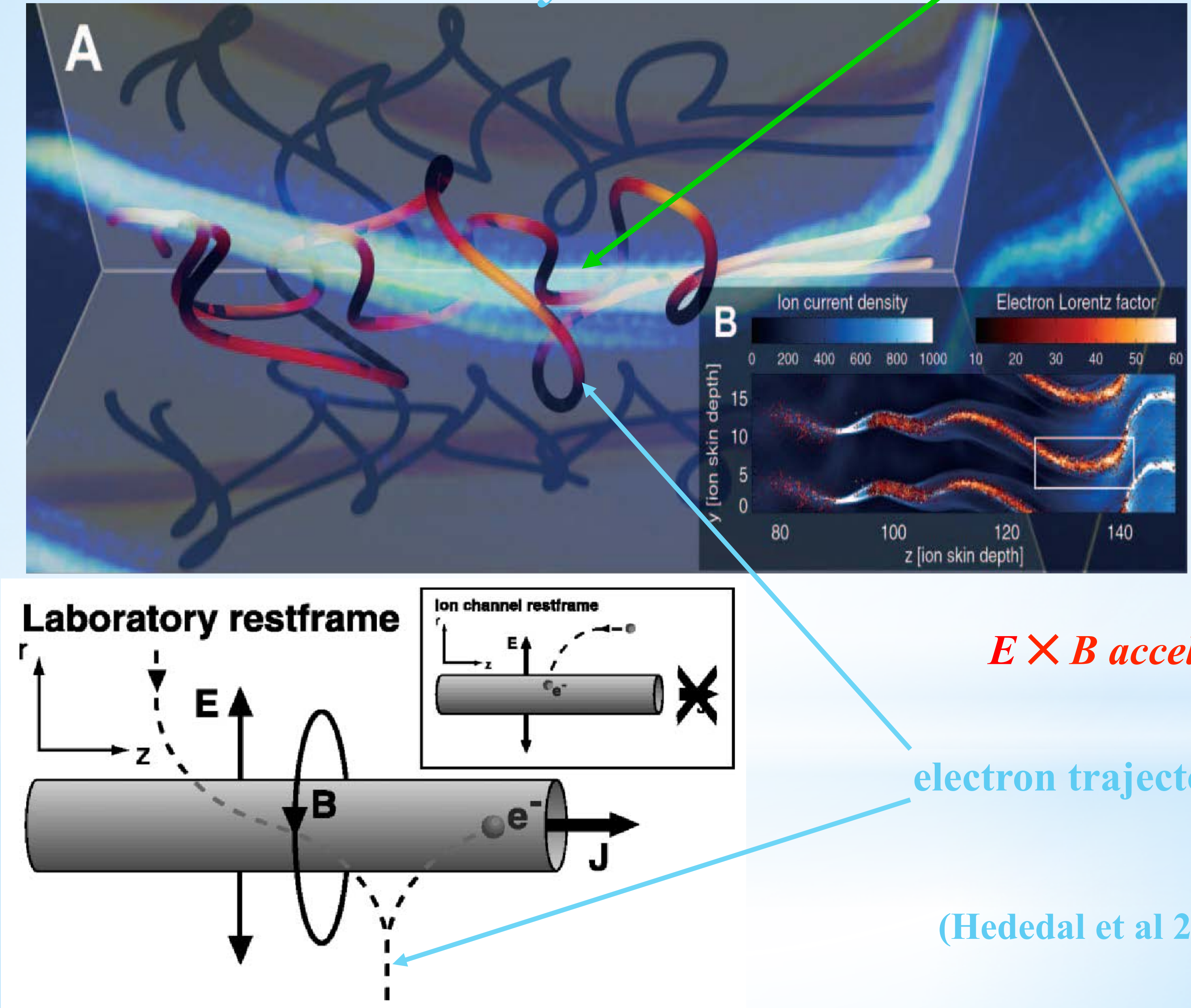

E × B acceleration

electron trajectory

(Hededal et al 2004)

3-D isosurfaces of z-component of current J_z for narrow jet ($\gamma v_{||}$=12.57)

electron-ion ambient $t = 59.8\omega_e^{-1}$

$-J_z$ (red), $+J_z$ (blue),

magnetic field lines (white)

see movie apf62jzB.avi

Particle acceleration due to the local reconnections during merging current filaments at the nonlinear stage

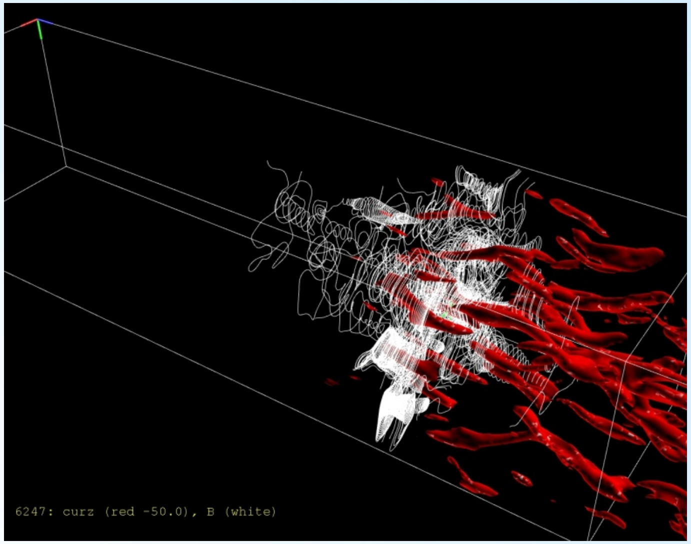

thin filaments

merged filaments

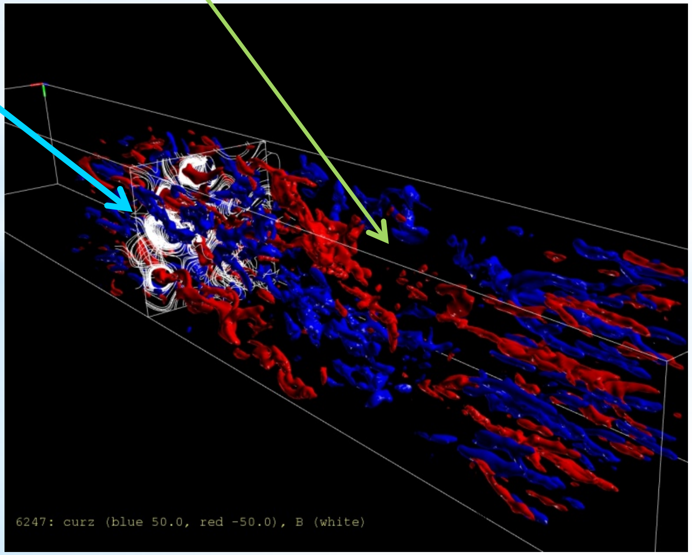

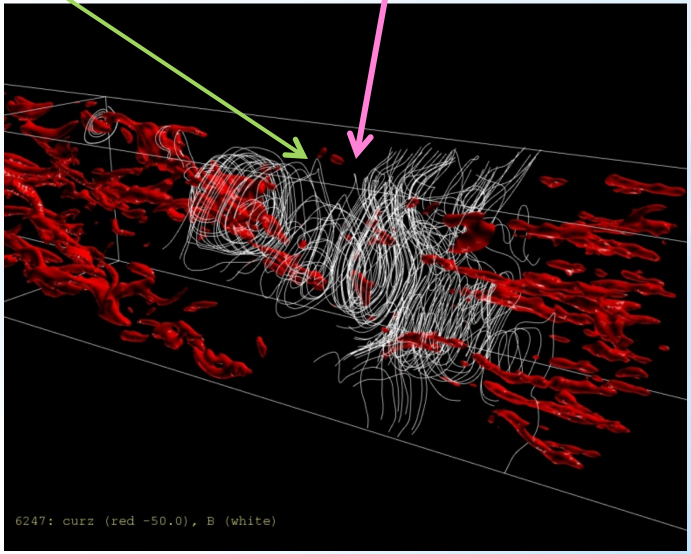

Shock velocity and bulk velocity

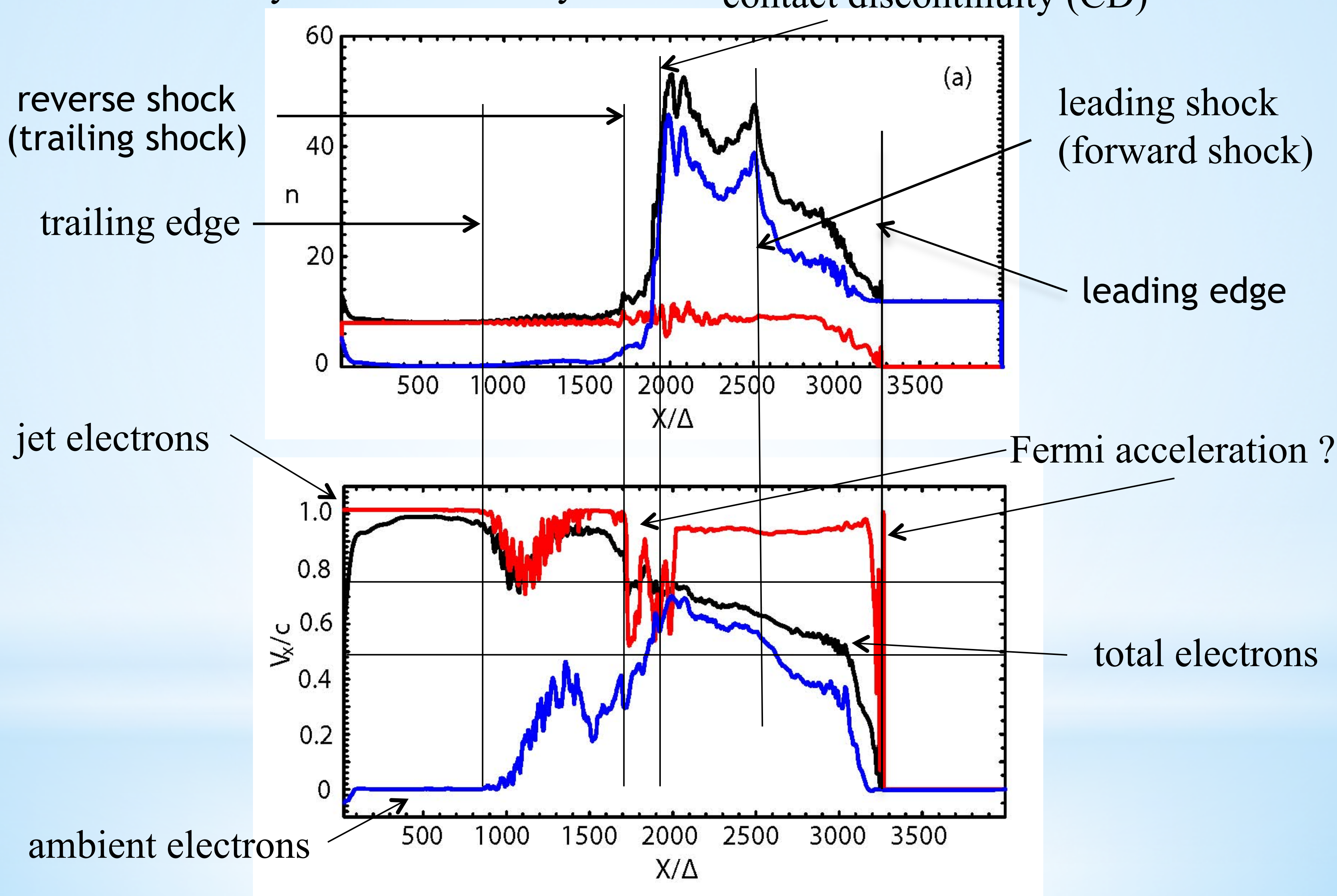

(Nishikawa et al. 2009)

Comparison with different mass ratio (electron-positron and electron-ion)

electron-positron

electron-ion ($m_i/m_e = 20$)

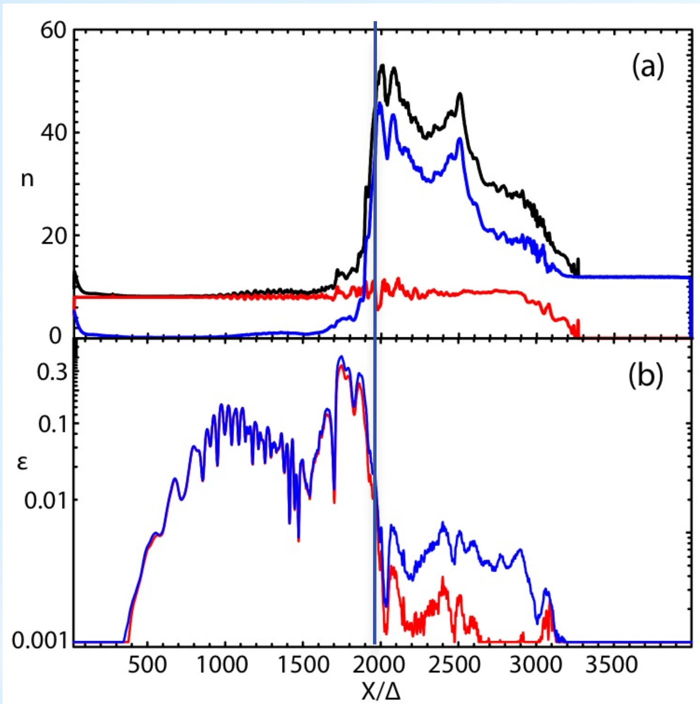

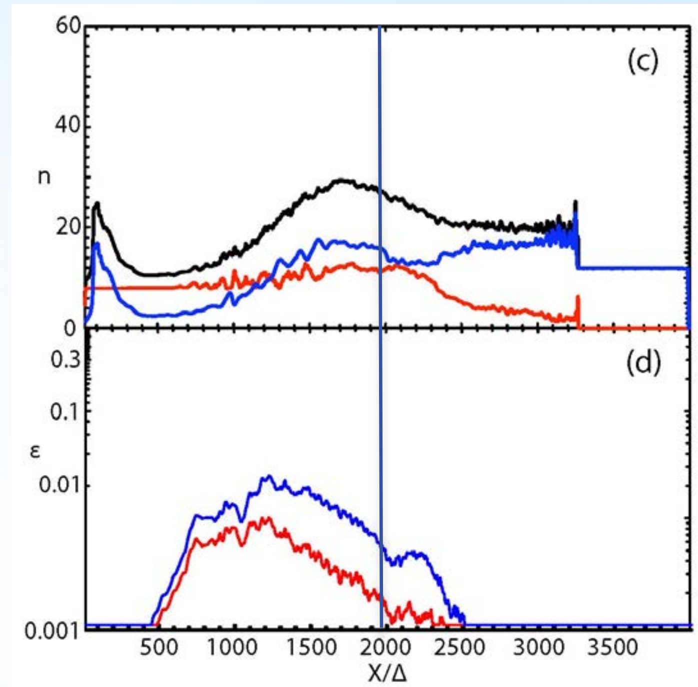

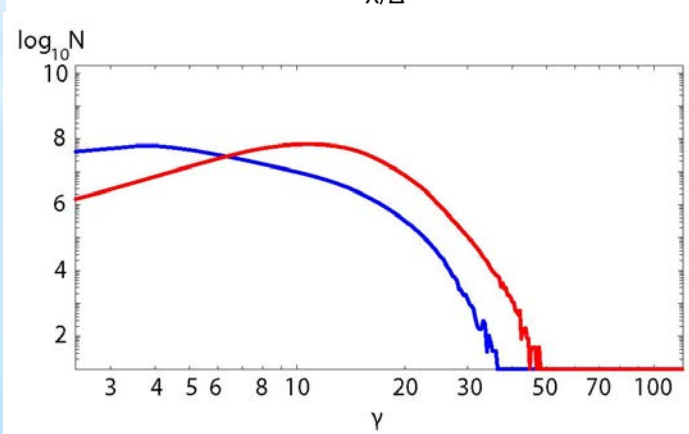

X/Δ>2000

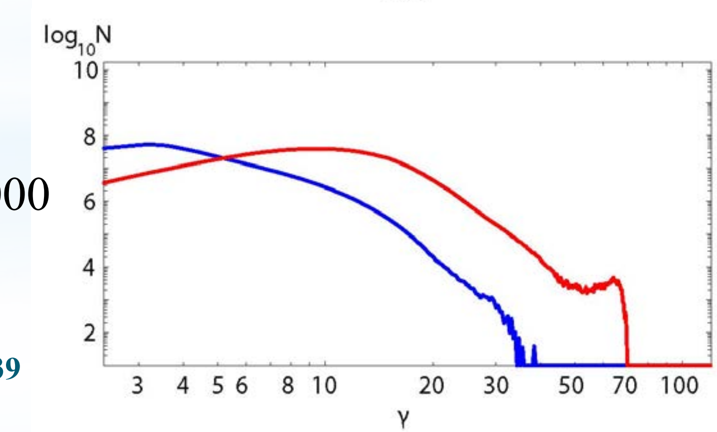

Recent electron-ion simulation (Electrostatic shock and double layer)

$m_i/m_e = 20$

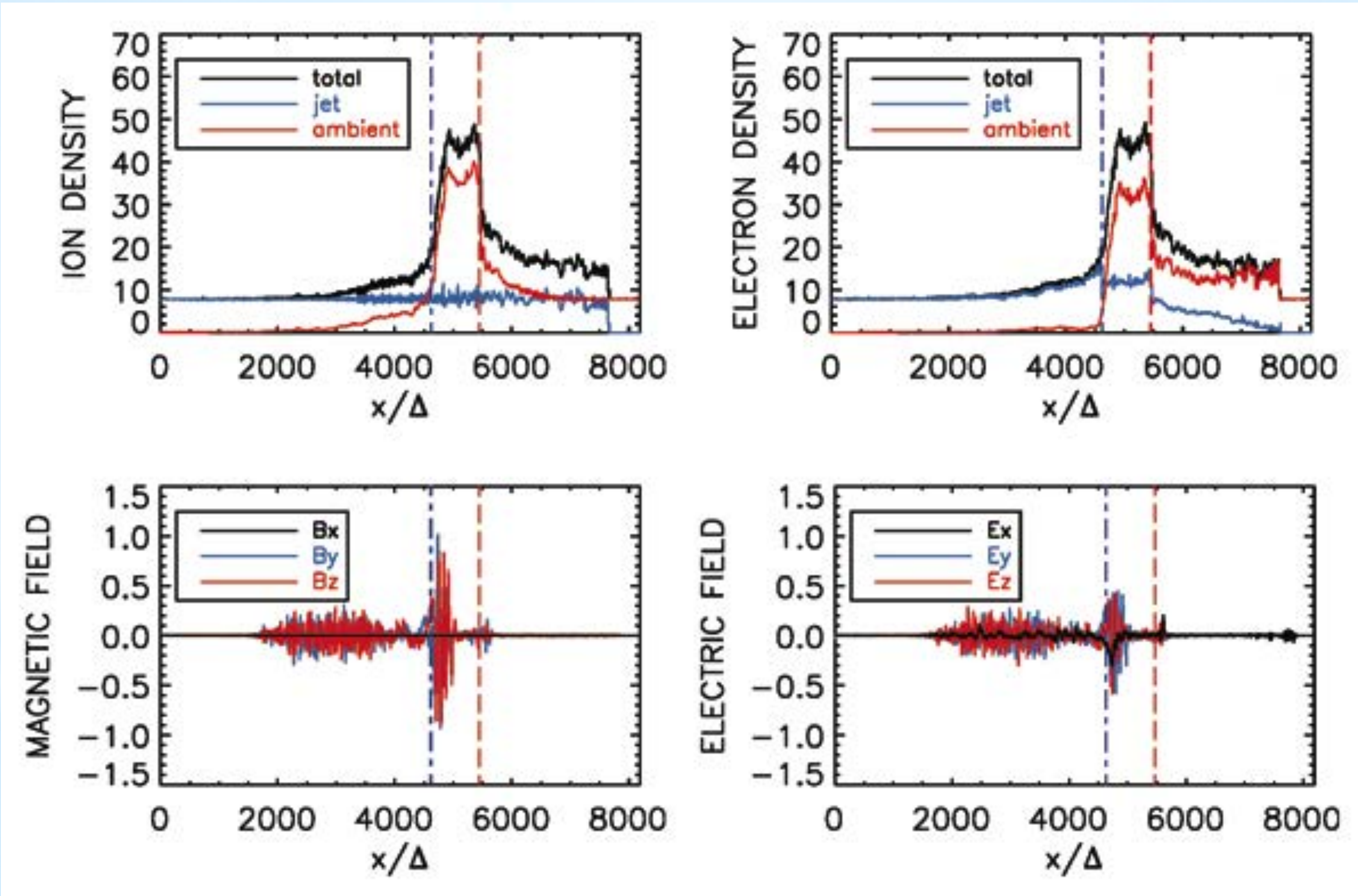

(Choi et al. PhPl, 2014)

Shock formation, forward shock, reverse shock

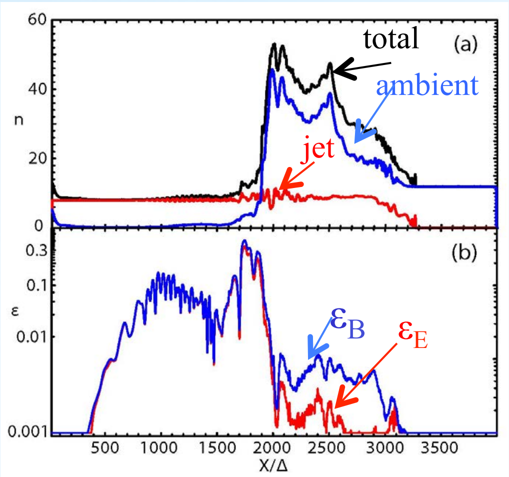

(a) electron density and (b) electromagnetic field energy (ε_B, ε_E) divided by the total kinetic energy at $t = 3250\omega_{pe}^{-1}$

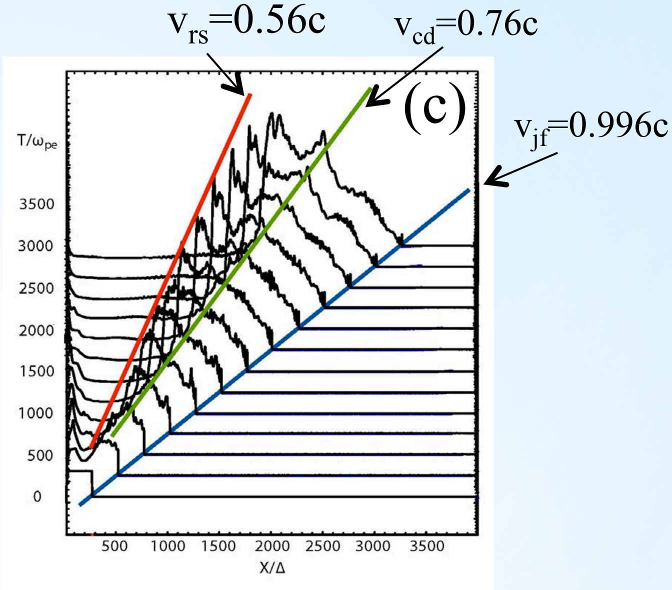

Time evolution of the total electron density. The velocity of the jet front is ~c, the predicted contact discontinuity speed is 0.76c, and the velocity of the reverse shock is 0.56c.

reverse shock region has strong magnetic fields and contributes to radiation

(Nishikawa et al. ApJ, 698, L10, 2009)

Phase space of electrons

red: jet electrons, blue: ambient electrons

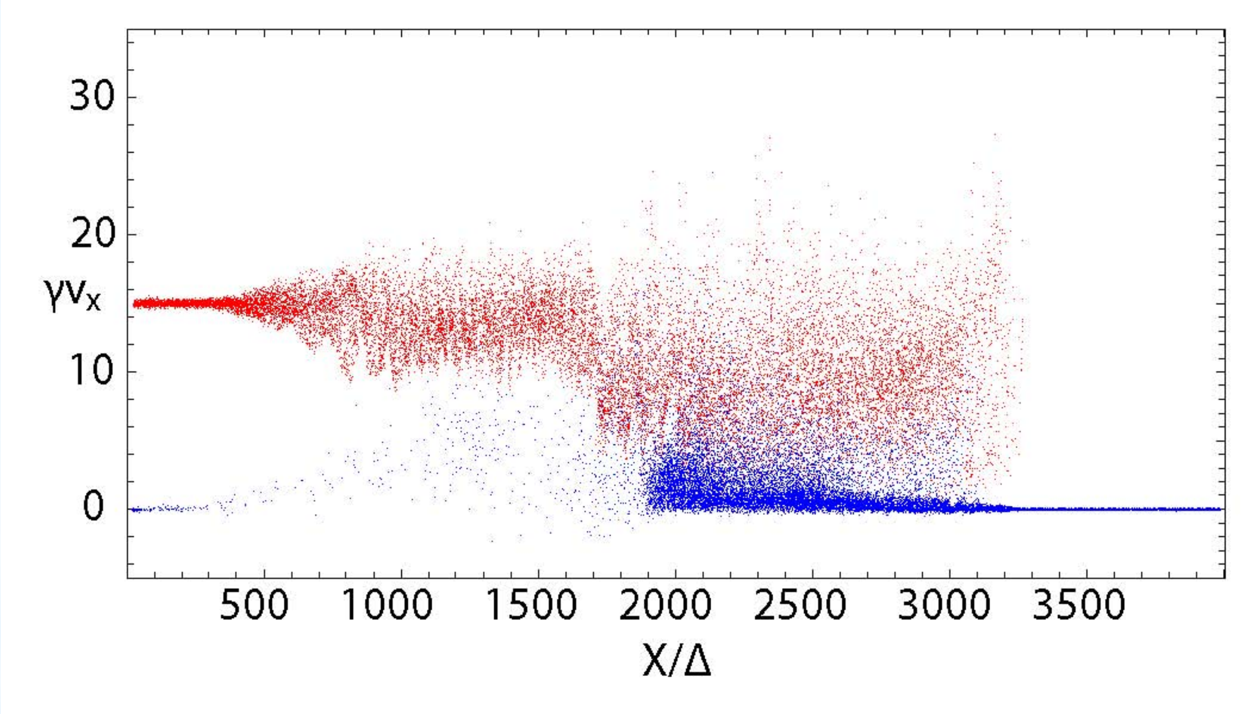

Phase space of electrons in the $x/\Delta - \gamma v_x$ at $t = 3250\omega_{pe}^{-1}$.
Red dots show jet electrons which are injected from the left with $\gamma v_x = 15$

(Nishikawa et al. ApJ, 698, L10, 2009)

see movie dphasvx-x05f.mov

Shock ... *e shock*

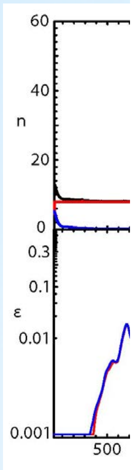

.996c

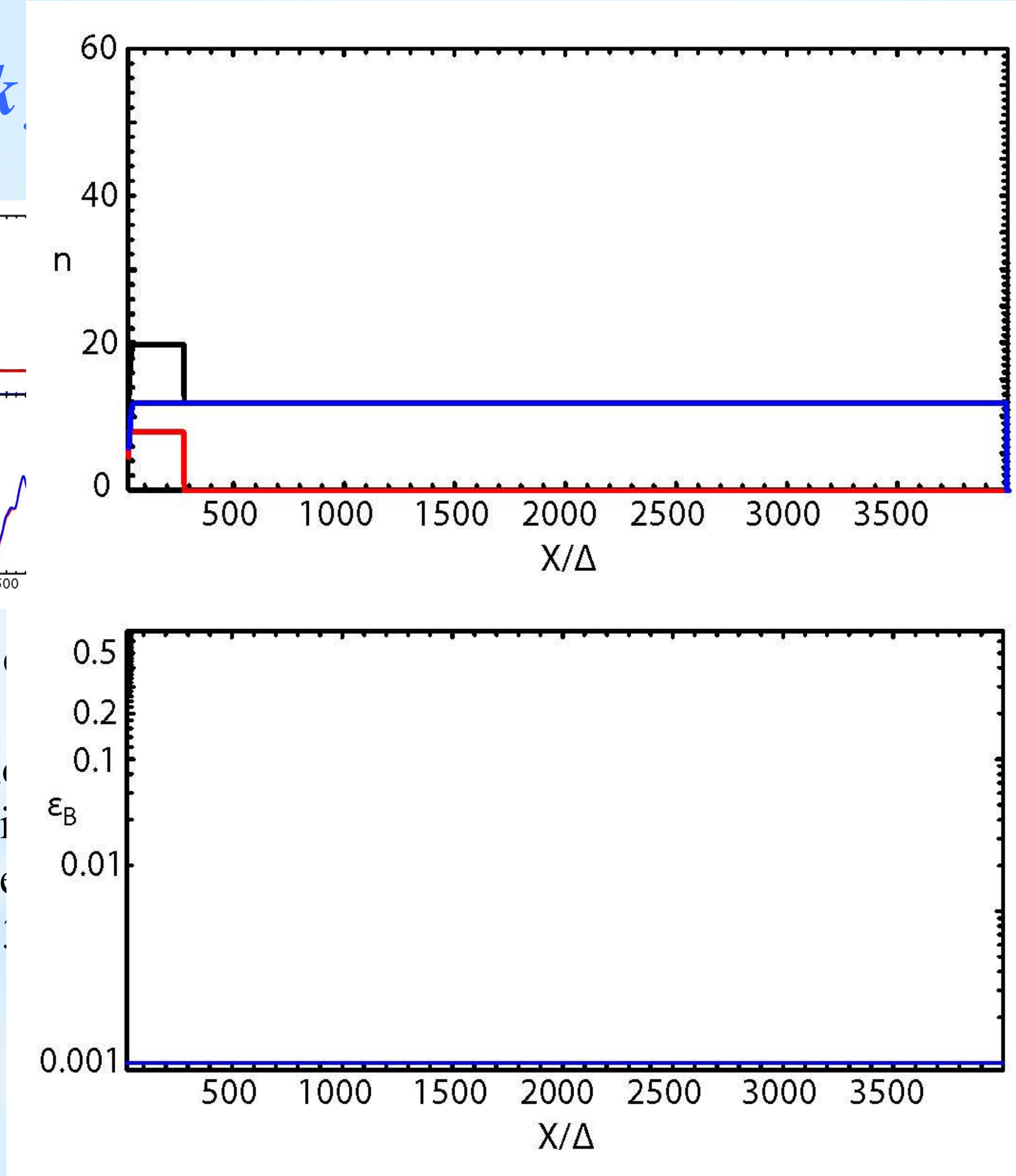

(a)

(b) ... electron

fiel ... jet front is ~c,

divi ... ntinuity speed

kine ... the reverse

t =

Shock velocity and structure based on 1-D HD analysis

moving contact discontinuity (CD)

trailing shock
(reverse shock)

leading shock
(forward shock)

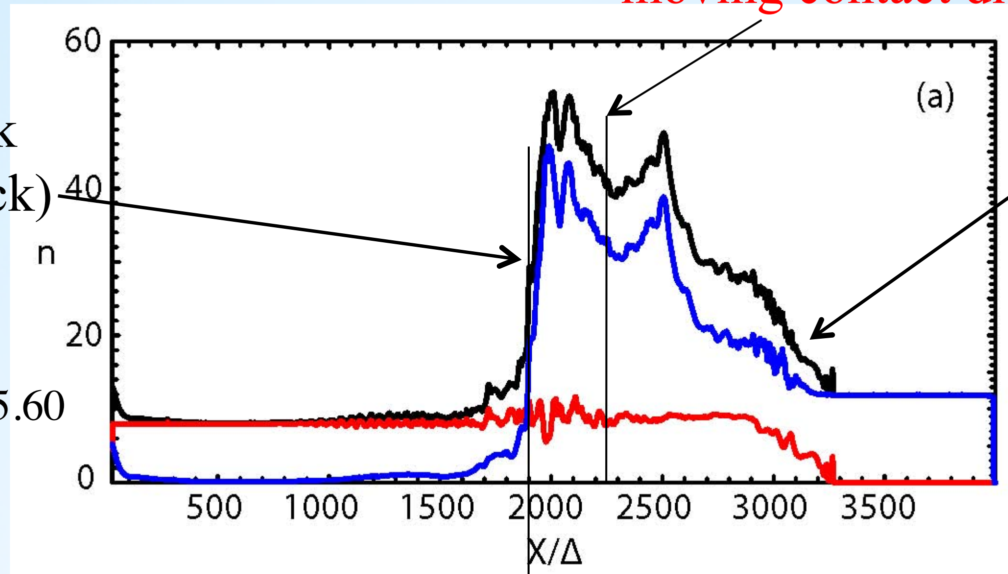

(Nishikawa et al. 2009)

in CD frame

$n_{sj}/\gamma'_{cd}n_j = 3.36$

$\beta_s = 0.417$ $\gamma'_{cd} = 5.60$

$^4\!/_3 < \Gamma = {^3\!/_2} < {^5\!/_3}$

fixed CD

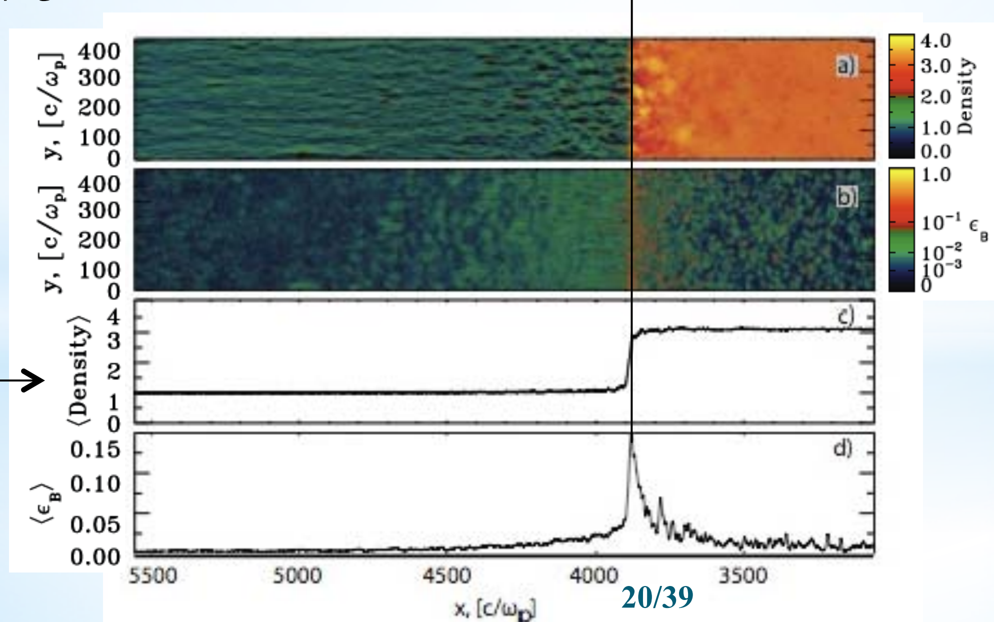

Density

$n_2/\gamma_0 n_1 = 3.13$

$\beta_c = 0.47$

$\gamma_0 = 15$

0

(Spitkovsky 2008 (adapted))

Simulations of Kinetic Kelvin-Helmholtz instability with counter-streaming flows (γ_0 = 3, m_i/m_e=1836)

magnetic field lines

electron density

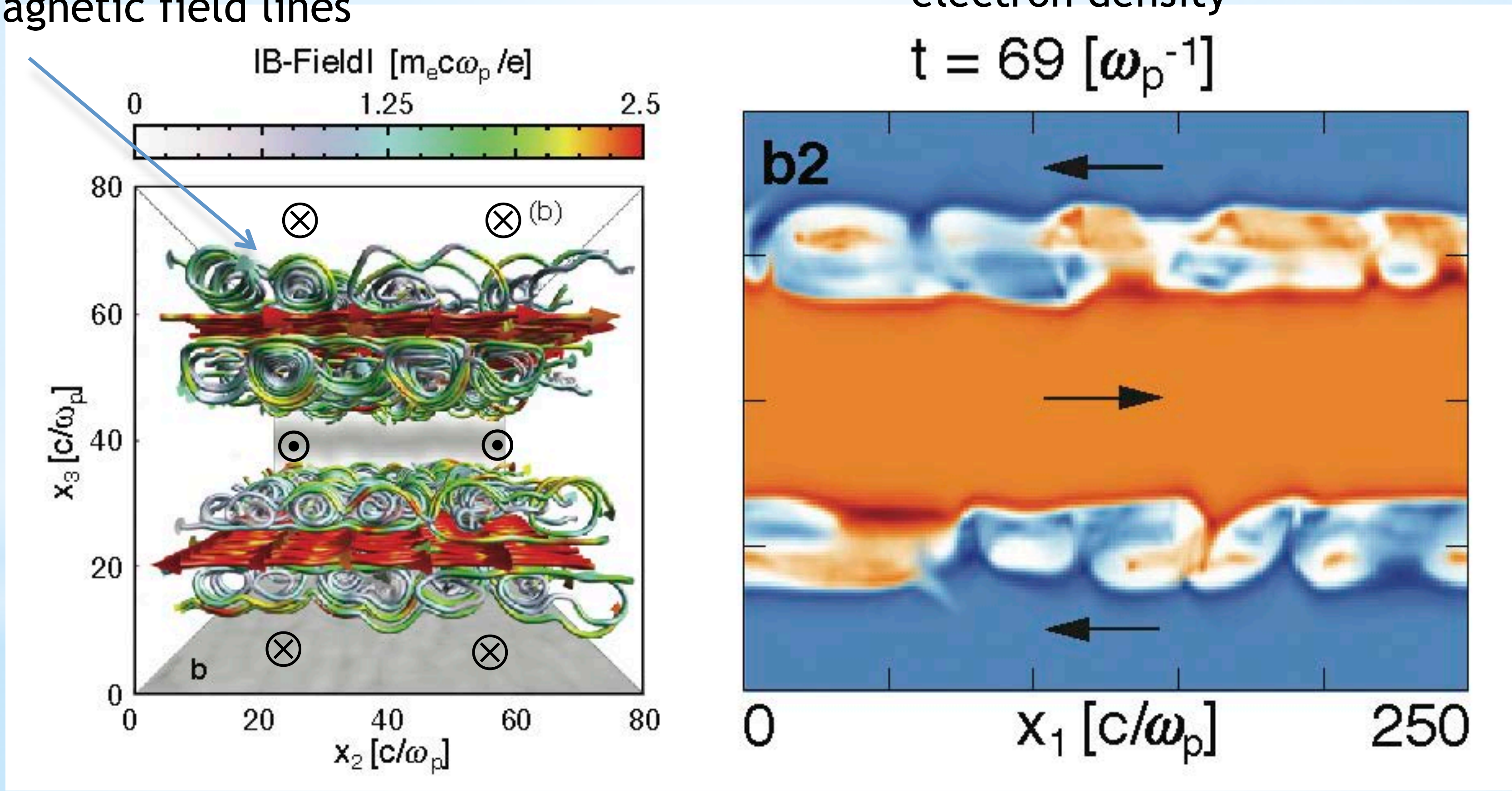

Alves et al. (2012)

Magnetic field lines

(Alves et al. ApJL, 2012)

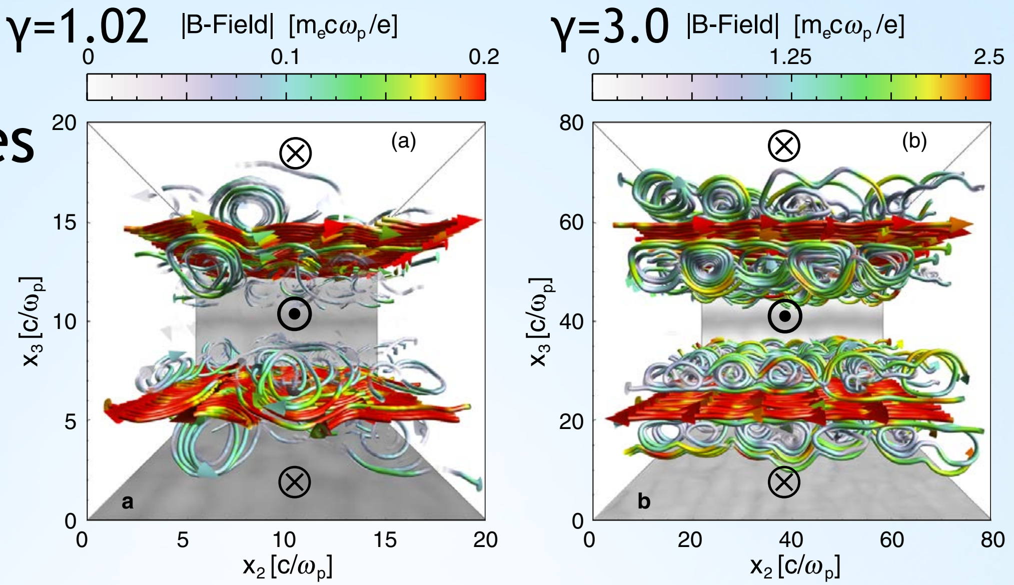

Figure 3. Magnetic field lines generated in (a) the subrelativisitc scenario, and (b) the relativistic scenario, at time $t = 100/\omega_p$.
(A color version of this figure is available in the online journal.)

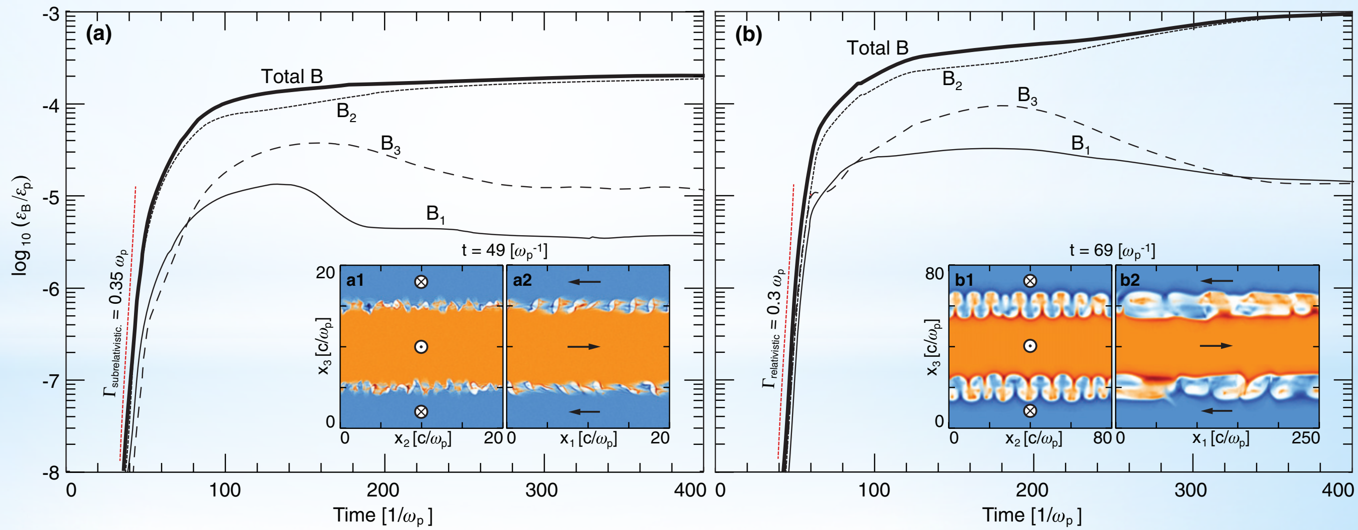

Figure 4. Evolution of the equipartition energy ϵ_B/ϵ_p for a (a) subrelativistic and (b) relativistic shear scenarios. The contribution of each magnetic field component is also depicted. The insets in each frame represent two-dimensional slices of the electron density at $t = 49/\omega_p$ and $t = 69/\omega_p$ for the respective case. The red (blue) color represents the electron density of the plasma that flows in the positive (negative) x_1 direction. Darker regions in the color map indicate high electron density, whereas lighter regions indicate low electron density. Slices for insets (a1), (a2), (b1), and (b2) were taken at the center of the simulation box; (a1) and (b1) are transverse to the flow direction, and slices (a2) and (b2) are longitudinal to the flow direction.

(A color version of this figure is available in the online journal.)

Simulations of KHI with core and sheath jets

slab model

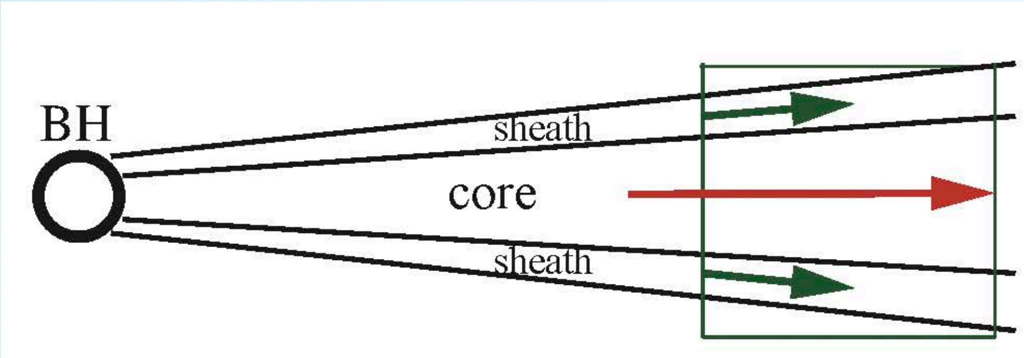

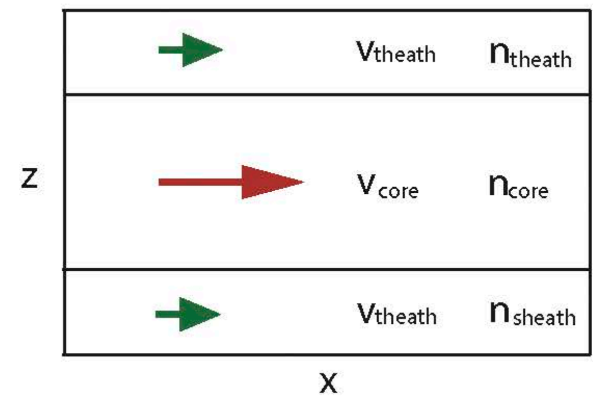

RMHD, no wind ω=0.93, time=60.0

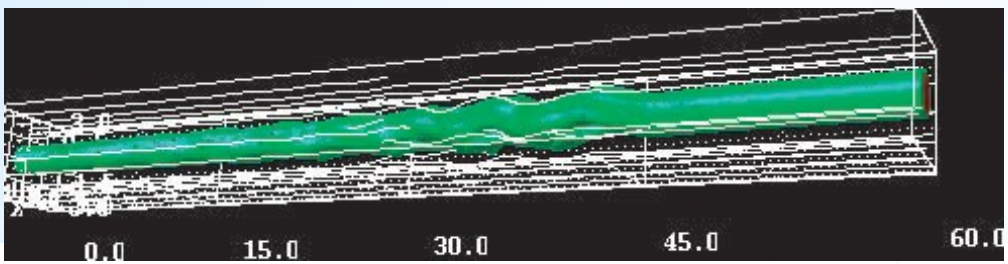

case of V_{theath} = 0

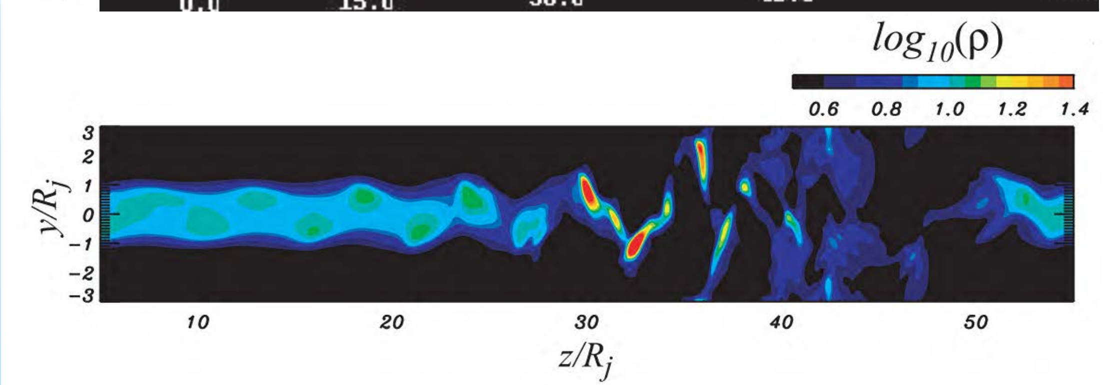

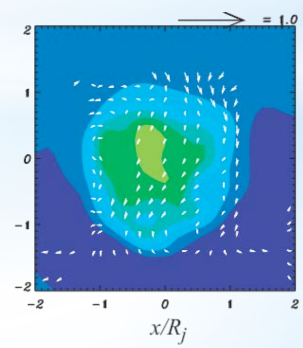

Mizuno, Hardee & Nishikawa, ApJ, 662, 835, 2007

KKHI with Core-sheath plasma scheme

$\gamma_{jt} = 15$ $t = 300\omega_{pe}^{-1}$

B_y

e - p $e^{\pm}$

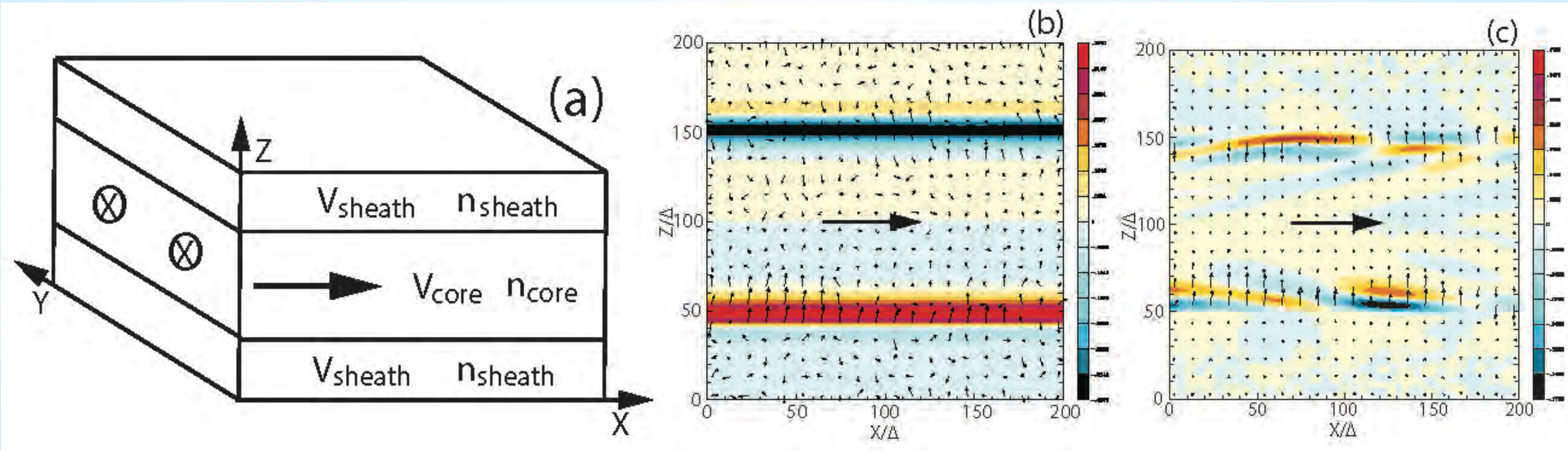

(Nishikawa et al. 2014, ApJ)

New KKHI simulations with core and sheath jets in slab geometry

γ_j = 15, m_i/m_e = 20

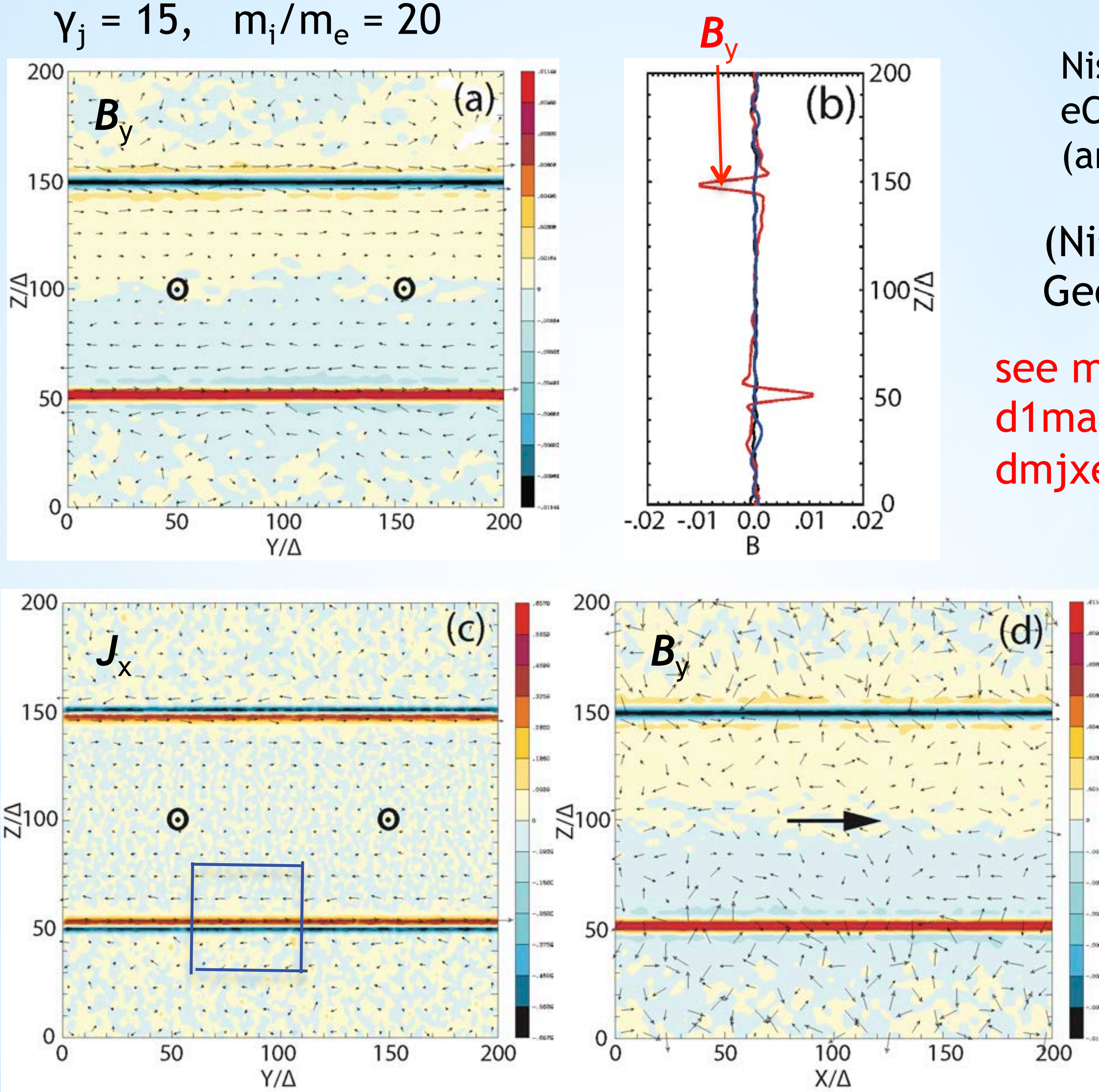

Nishikawa et al. 2013
eConf C121028
(arXiv:1303.2569)

(Nishikawa et al. Ann. Geo, 2013)

see movies
d1magz1a03.mov and
dmjxemyzkhiMn03a,mov

J_x Current structures $\gamma_{jt} = 15$ $t = 300\omega_{pe}^{-1}$

e - p

$e^{\pm}$

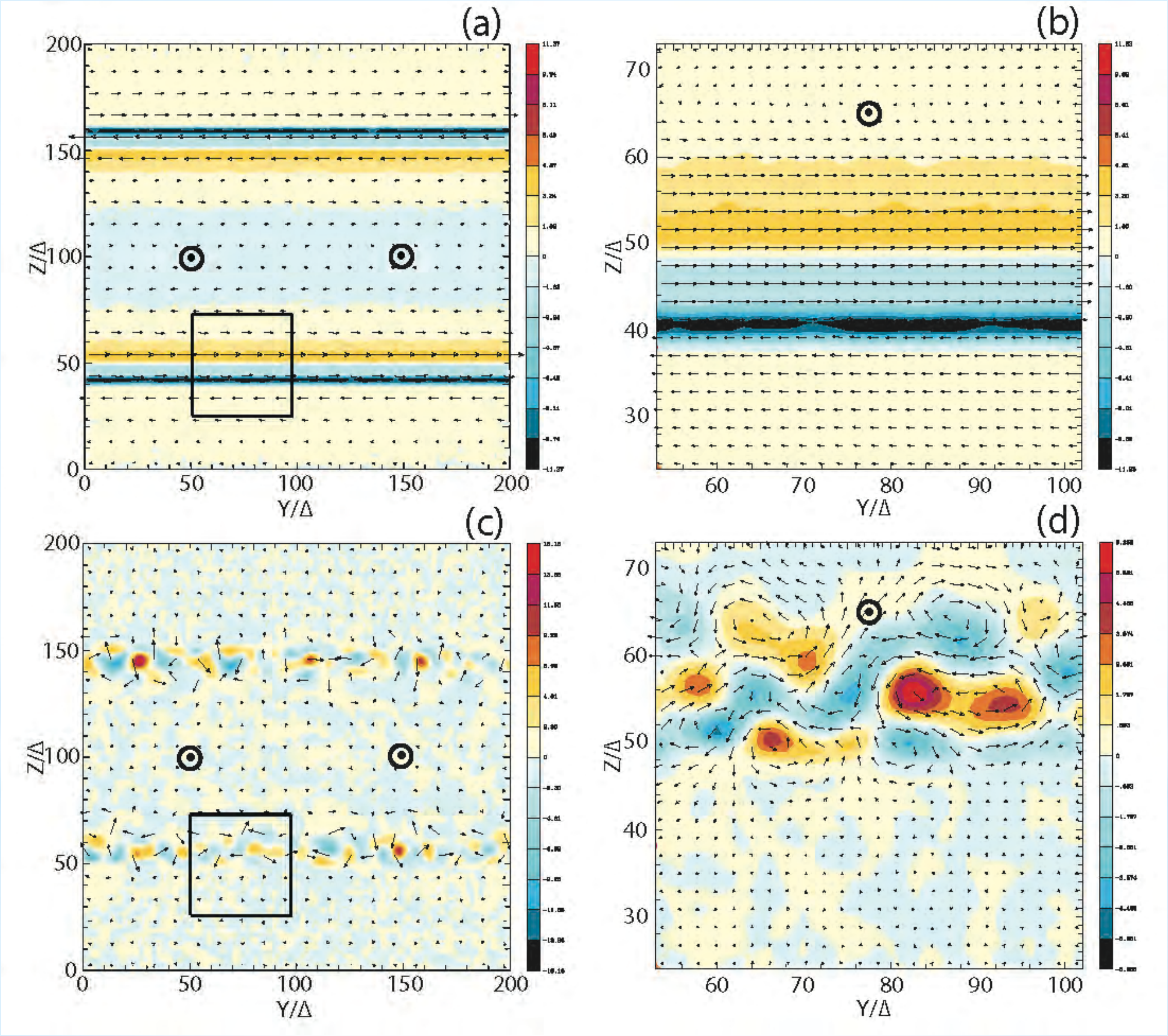

(Nishikawa et al. 2014, arXiv:1405.5247)

3D structure of current filaments and magnetic field

$e_{\pm}$ $\gamma_{jt} = 5$ $t = 250\omega_{pe}^{-1}$

J_x with magnetic field lines B^2 with current streaming lines

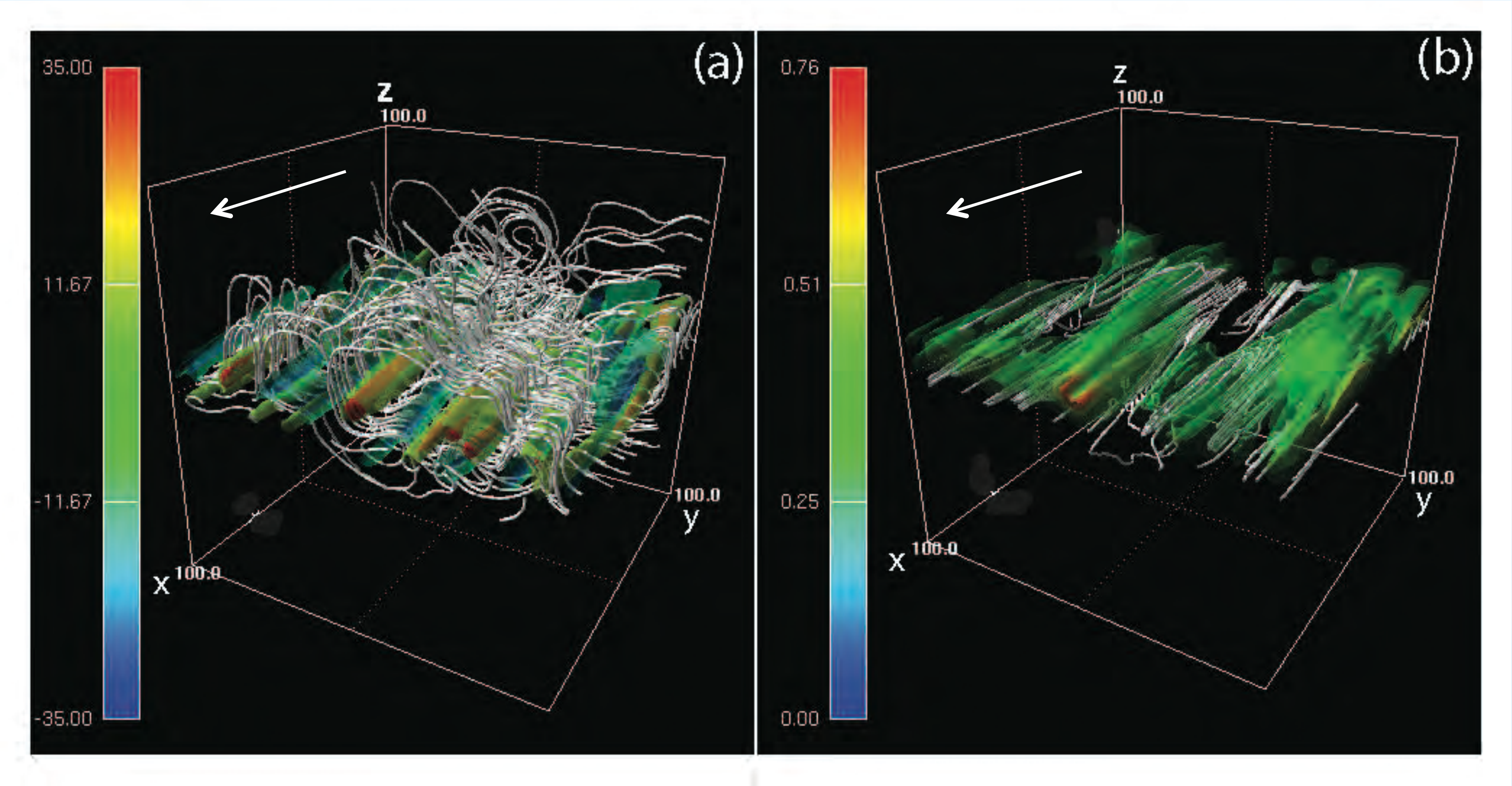

(Nishikawa et al. 2014, arXiv:1405.5247)

Cylindrical kKHI simulations

$\gamma_{jt} = 5$ $\qquad t = 300\omega_{pe}^{-1}$

e - p

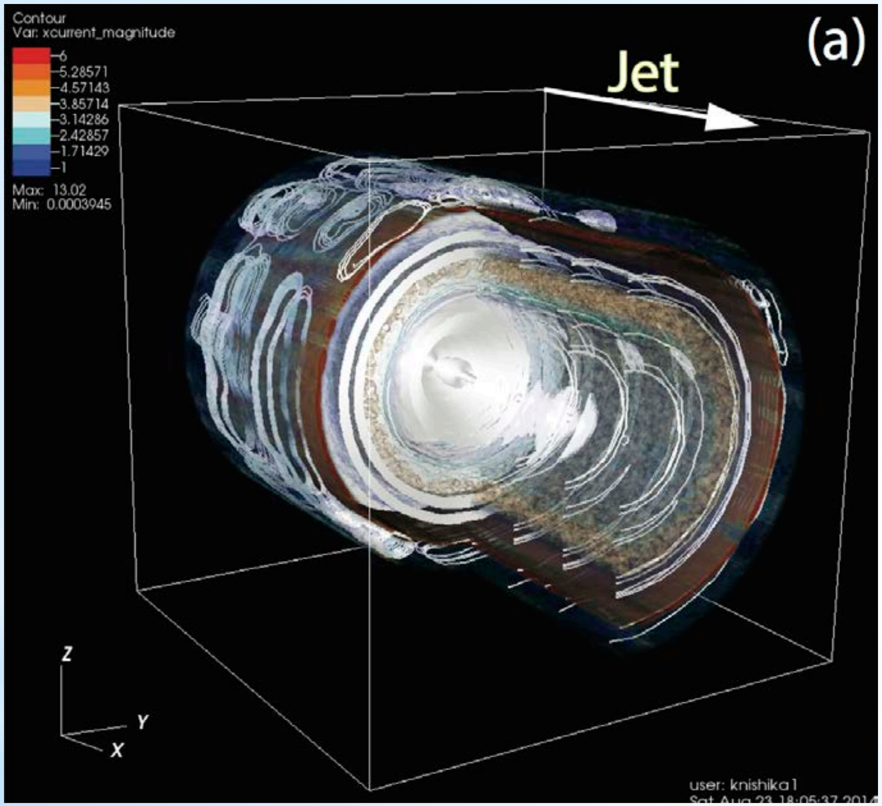

e±

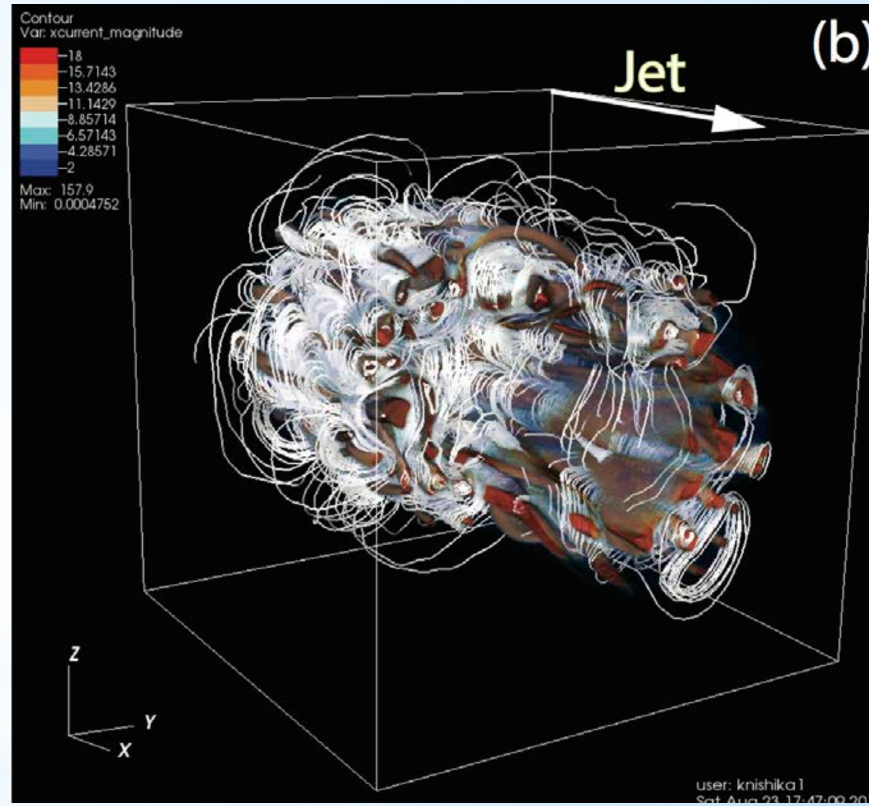

Snap shot of electron density of global jet simulations

$\gamma_{jt} = 5$ $t = 500\omega_{pe}^{-1}$

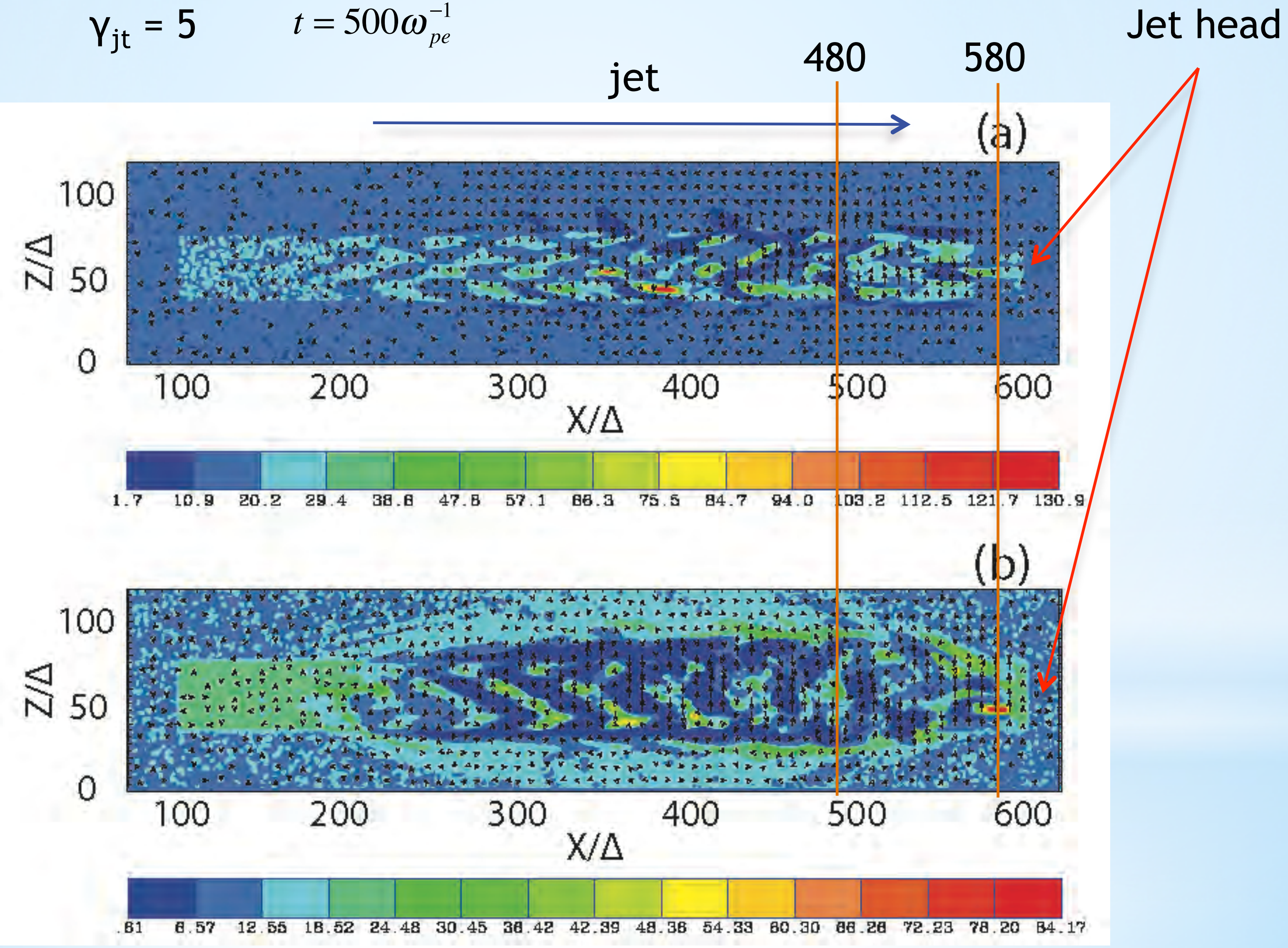

e - p

$e^{\pm}$

(Nishikawa et al. in progress, 2014)

Snap shots of current structures with transverse magnetic fields

$\gamma_{jt} = 5$ $\quad t = 500\omega_{pe}^{-1}$

X/Δ = 480 X/Δ = 580

⊙ Jet center

e - p

$e^{\pm}$

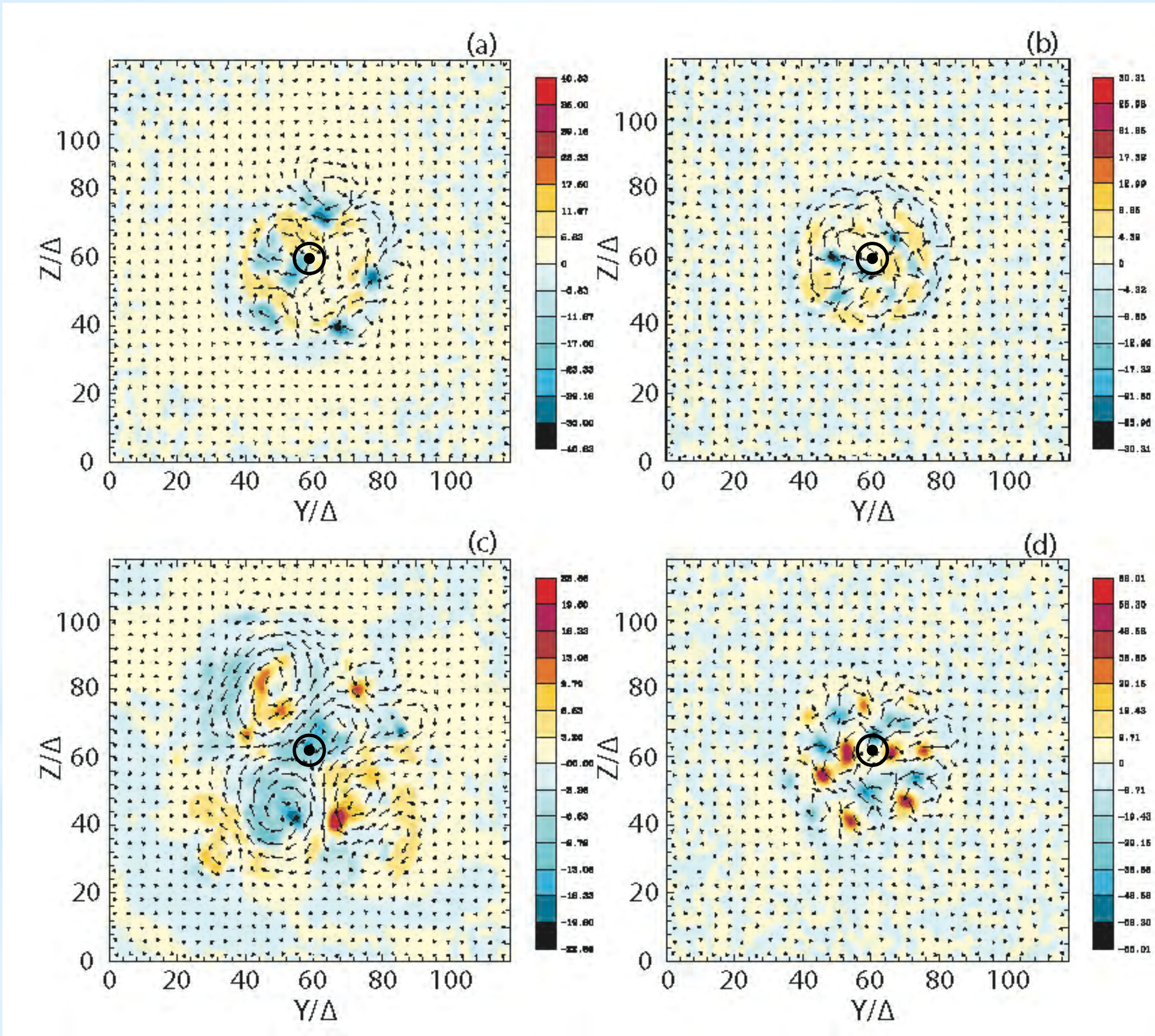

(Nishikawa et al. in progress, 2014)

3D snapshots of current (J_x) isosurfaces with magnetic field lines

Evolution of shock and instability is different for electron-proton γ_{jt} = 5 $t = 500\omega_{pe}^{-1}$
and electron-positron

white lines: magnetic filed lines

e - p

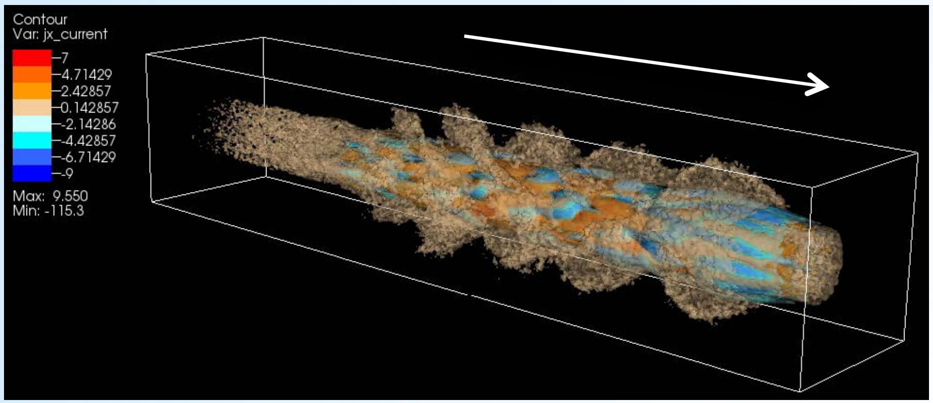

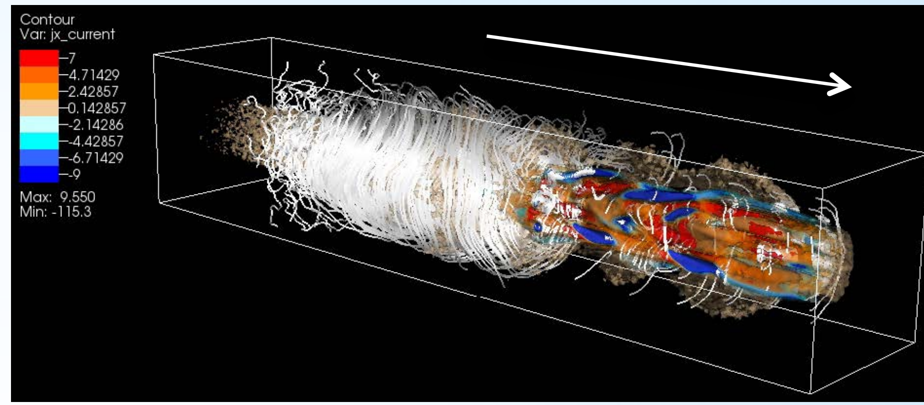

$e^{\pm}$

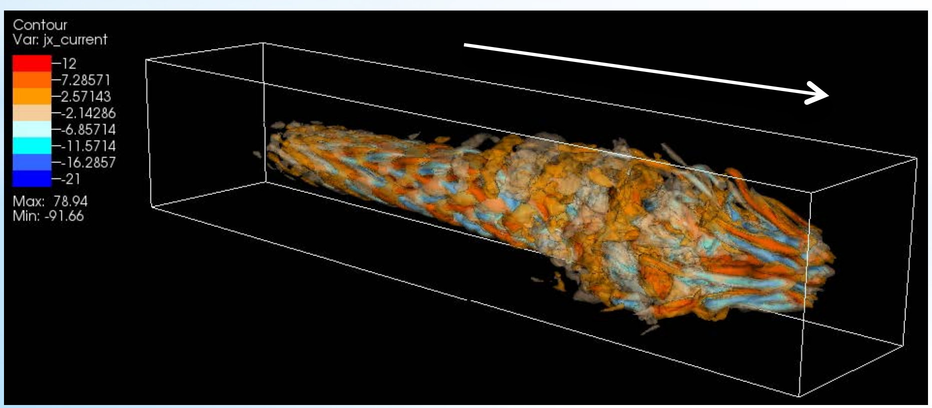

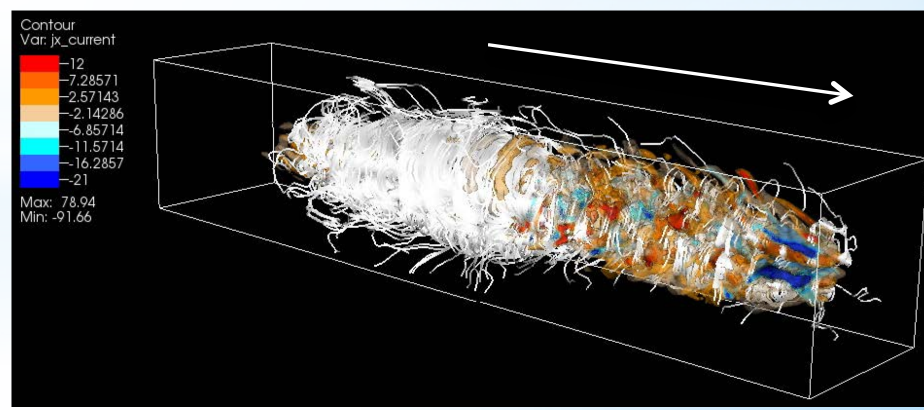

(Nishikawa et al. in progress, 2014)

3D snapshots of current (J_x) isosurfaces with magnetic field lines

Evolution of shock and instability is different for electron-proton and electron-positron $\gamma_{jt} = 15$ $t = 500\omega_{pe}^{-1}$

white lines: magnetic filed lines

e - p

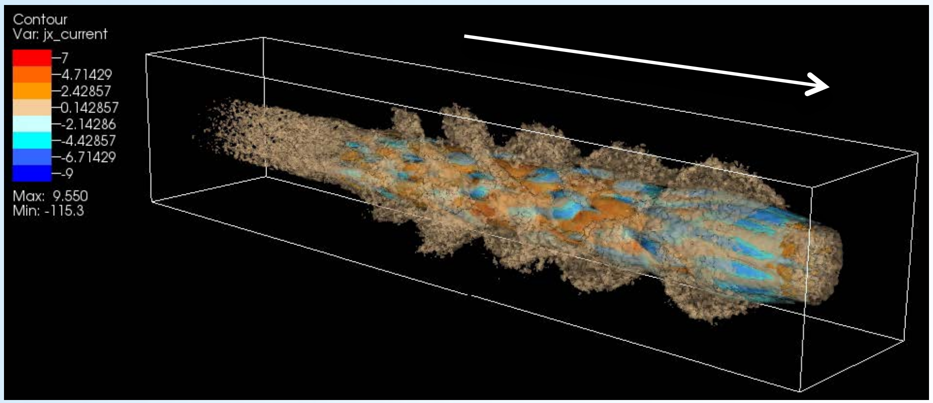

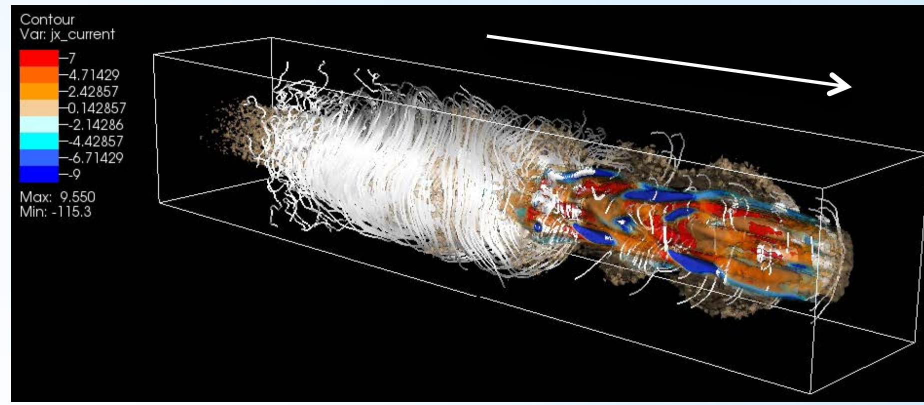

see movies JxBclio03.mov (e-p) and JxBclio02.mov ($e^{\pm}$)

$e^{\pm}$

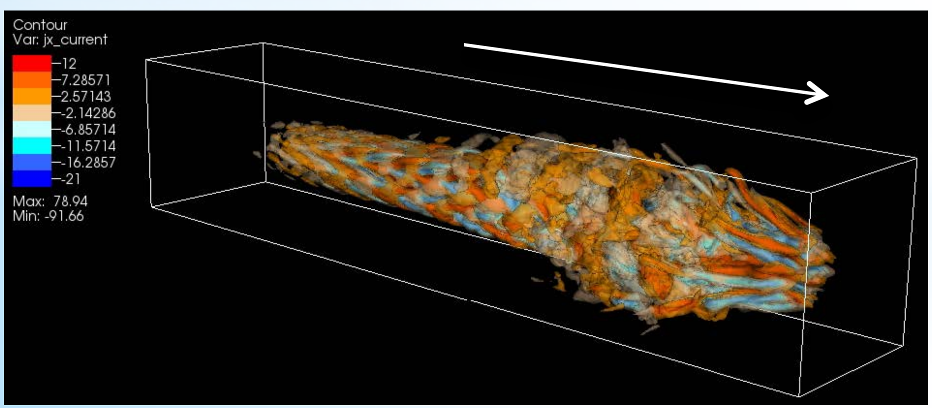

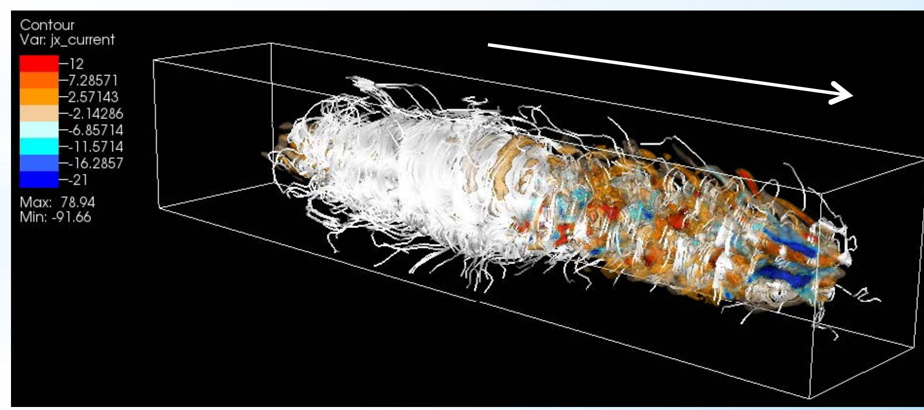

(Nishikawa et al. 2014)

Snap shot of electron density of global jet simulations

$\gamma_{jt} = 15$ $t = 1{,}000\omega_{pe}^{-1}$ $n_{jet} = 0.67 n_{amb}$ arrows: $B_{x,z}$

e-p

e±

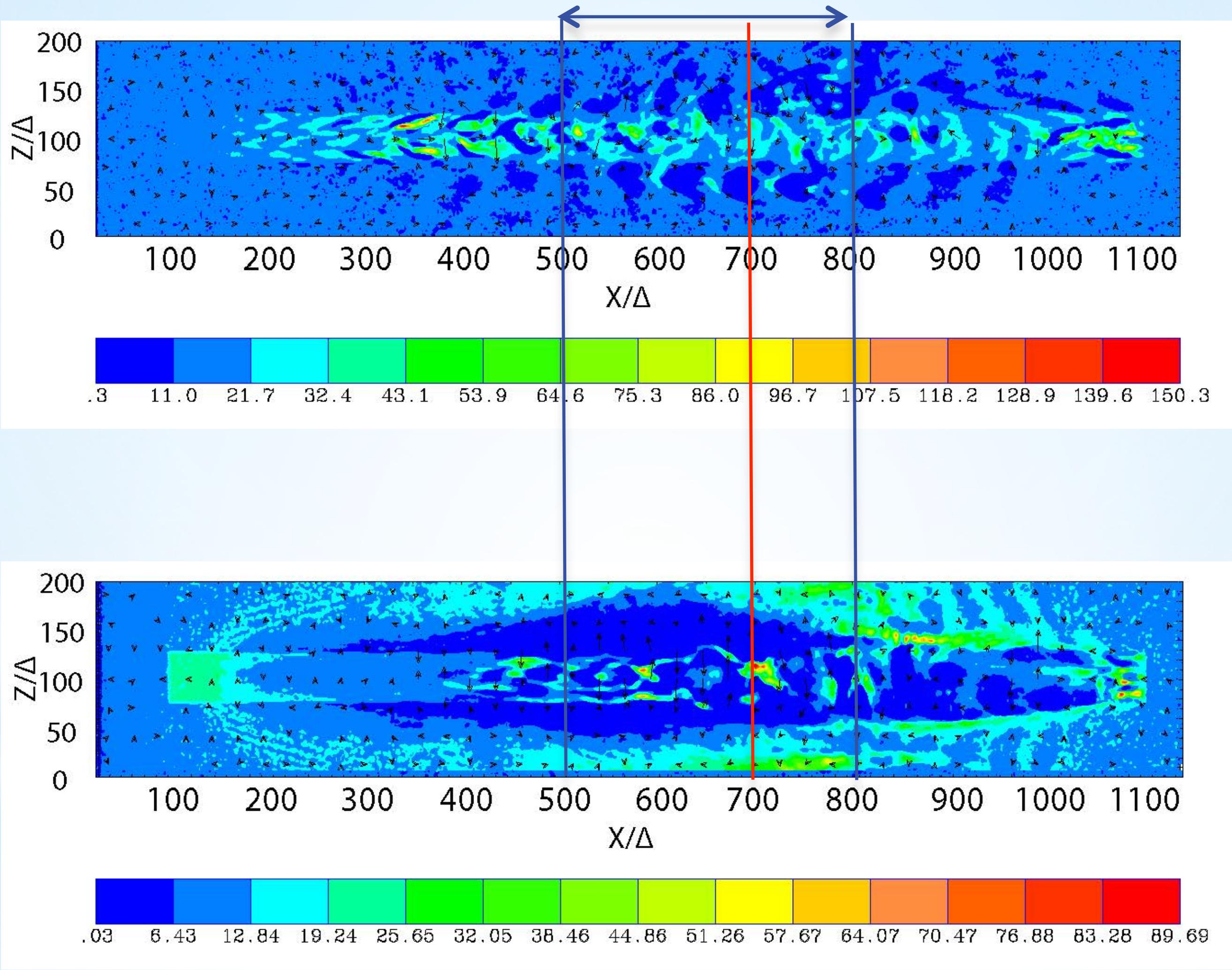

(Nishikawa et al. 2015)

Snap shots of current structures with transverse magnetic fields

$\gamma_{jt} = 15$ $t = 1{,}000\omega_{pe}^{-1}$

X/Δ = 500 X/Δ = 700

e-p

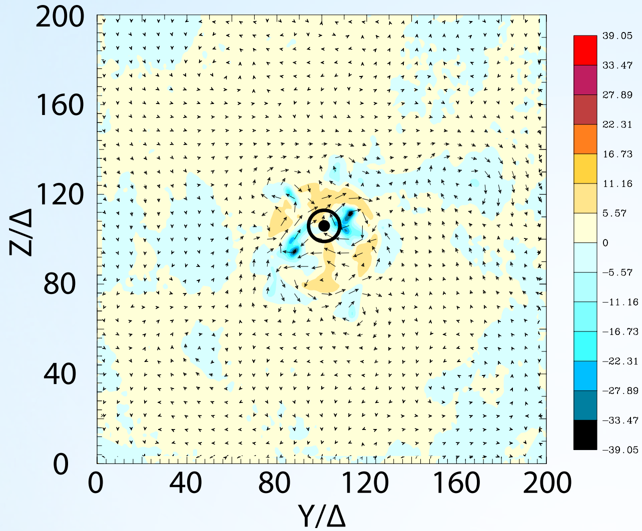

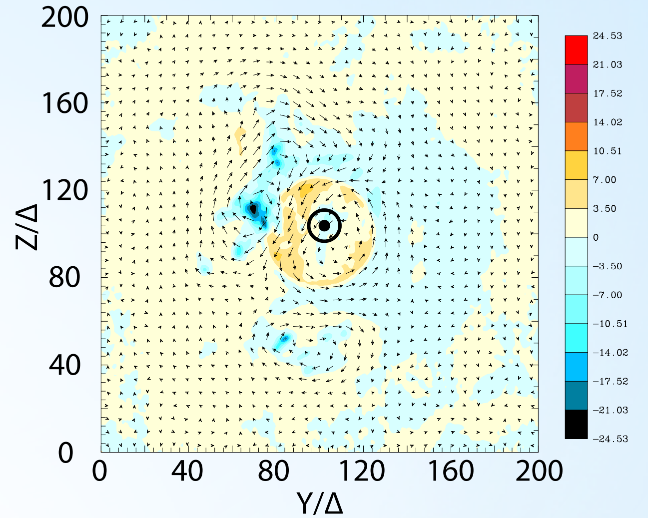

⊙ Jet center

e±

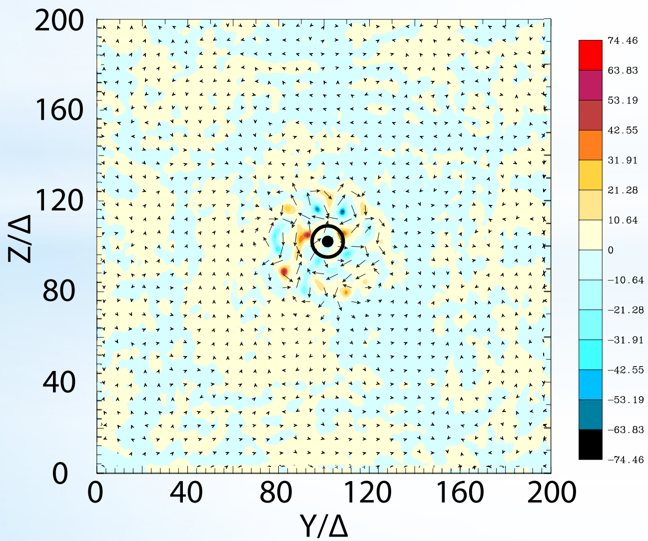

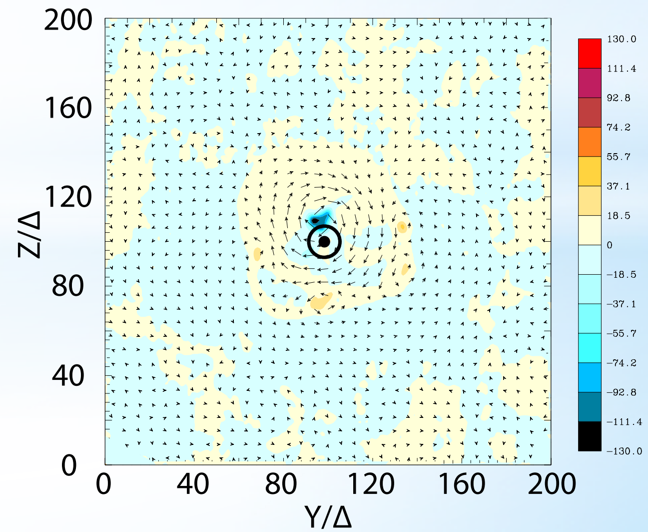

Phase space plot x - γv_x

$\gamma_{jt} = 15$ $t = 3{,}500\omega_{pe}^{-1}$

red: jet electrons blue: ambient electrons

e-p

$e^{\pm}$

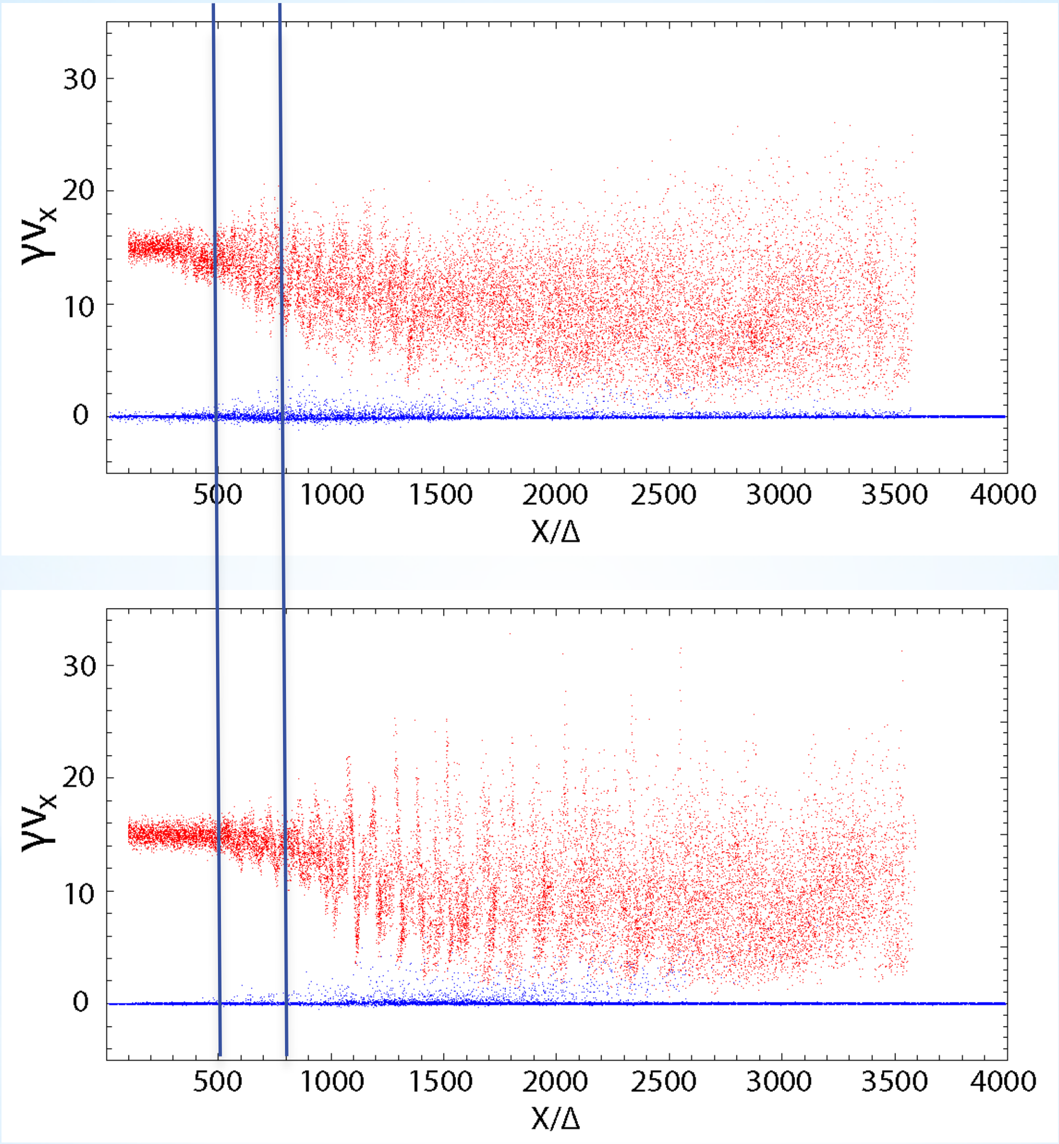

Phase space plot in x - z plane (105<y/Δ<101)

red: jet electrons blue: ambient electrons $\gamma_{jt} = 15$ $t = 3{,}500\omega_{pe}^{-1}$

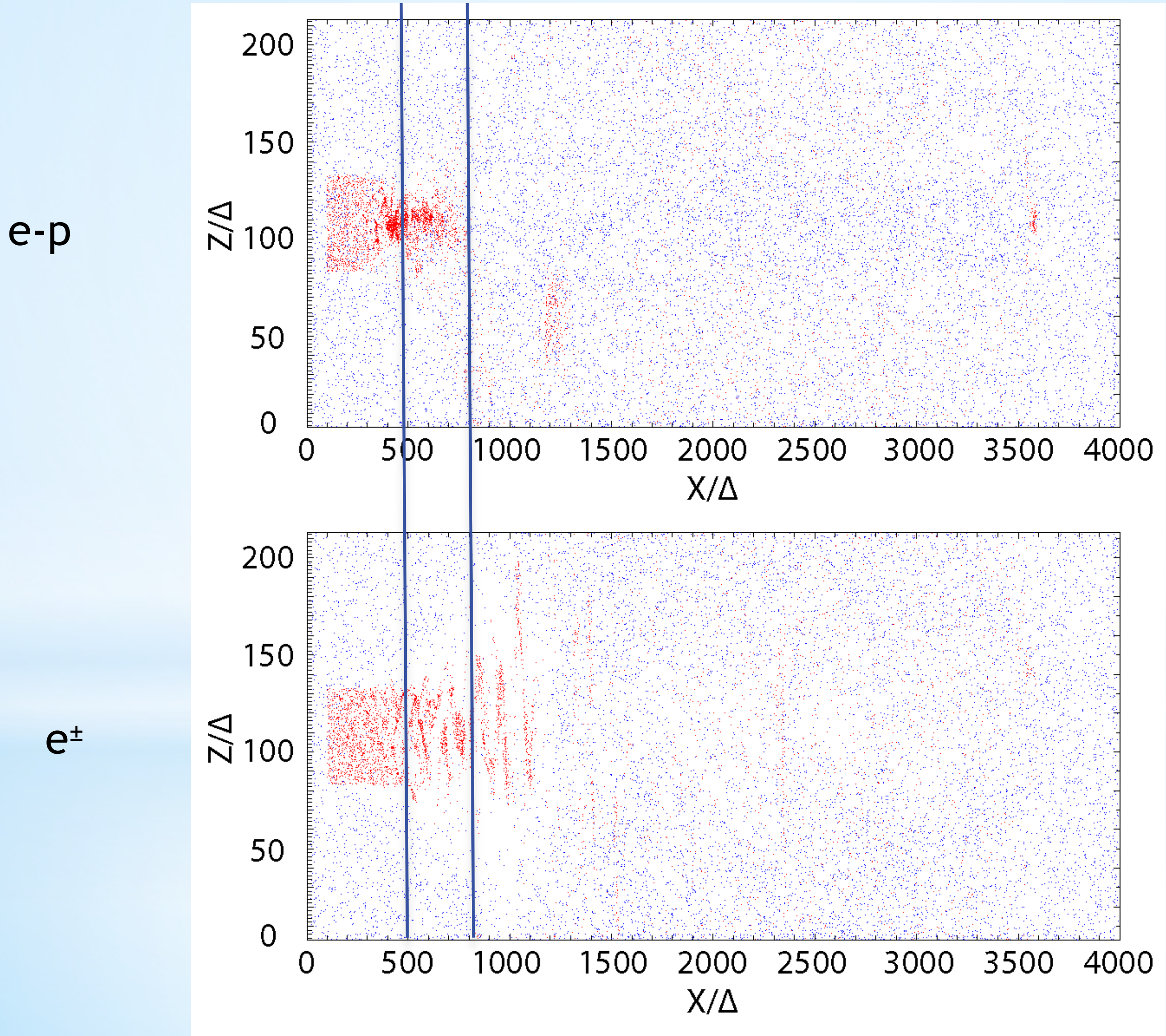

Phase space plot in x -z plane for e-p jet (105<y/Δ<101)

red: jet ions blue: ambient ions $\gamma_{jt} = 15$ $t = 3{,}500\omega_{pe}^{-1}$

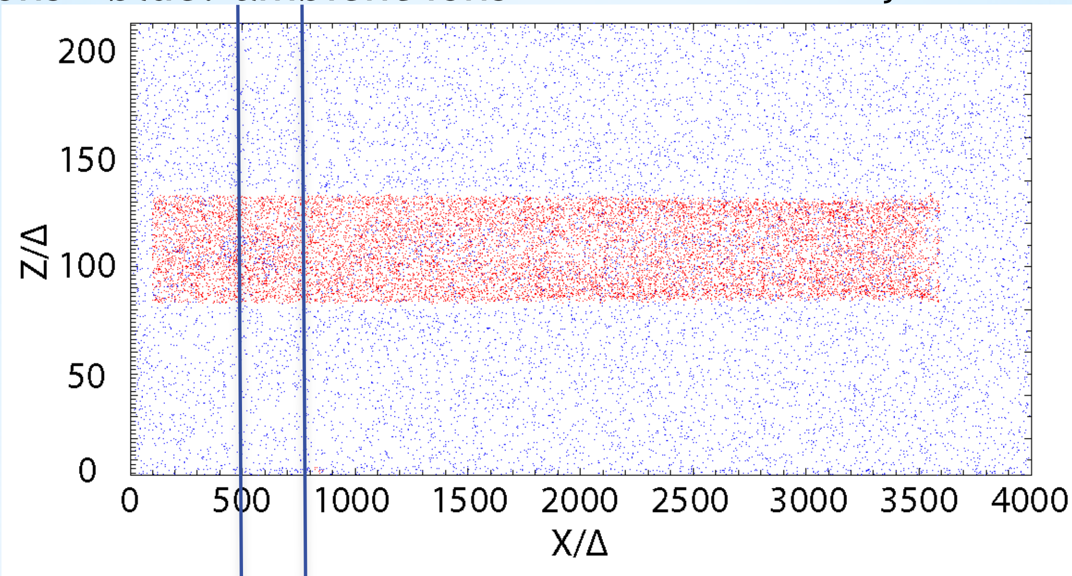

red: jet electrons blue: ambient electrons

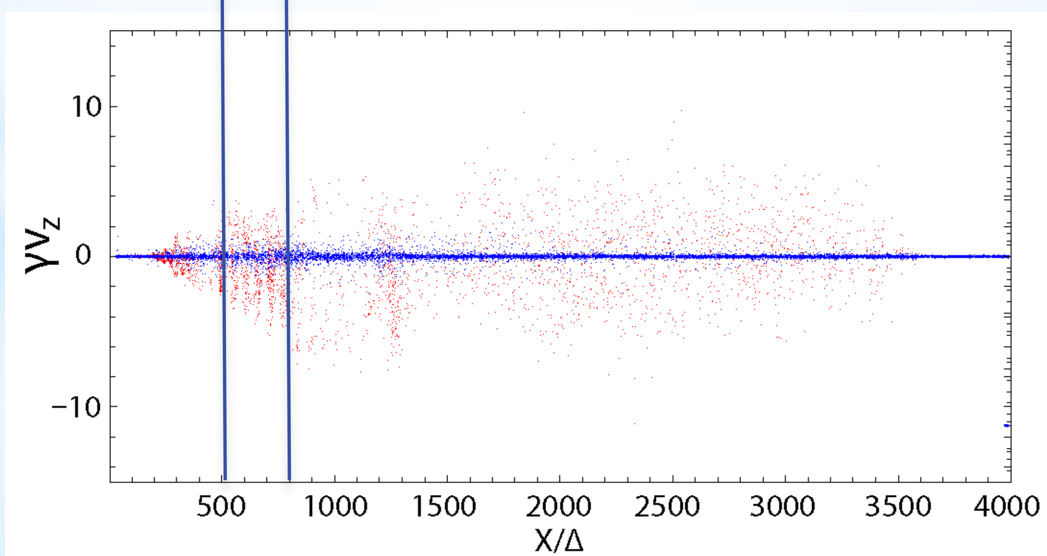

Snap shot of electron density of global jet simulations

$\gamma_{jt} = 15$ $t = 1{,}000\omega_{pe}^{-1}$ $n_{jet} = 0.67n_{amb}$ at the center of the jet

e-p

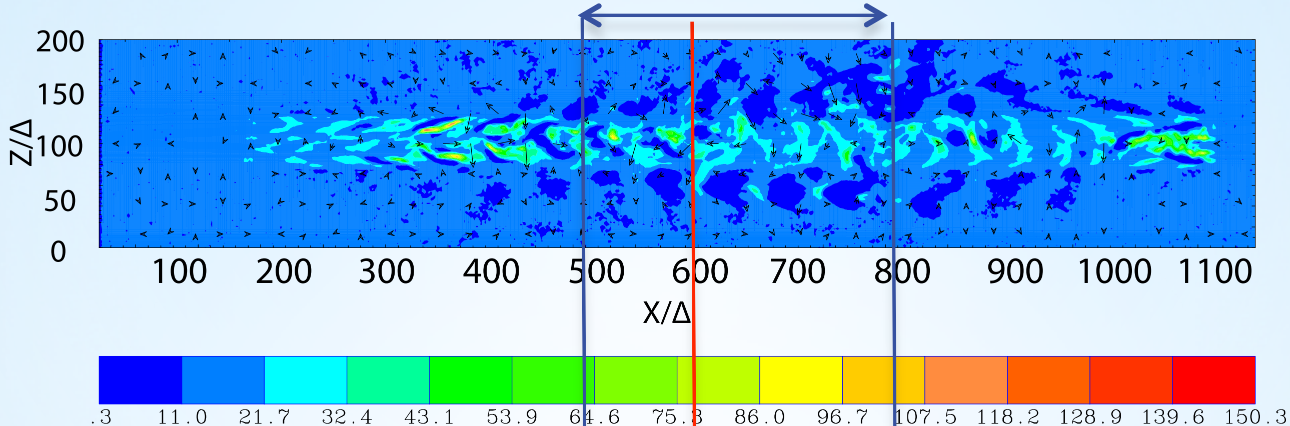

e±

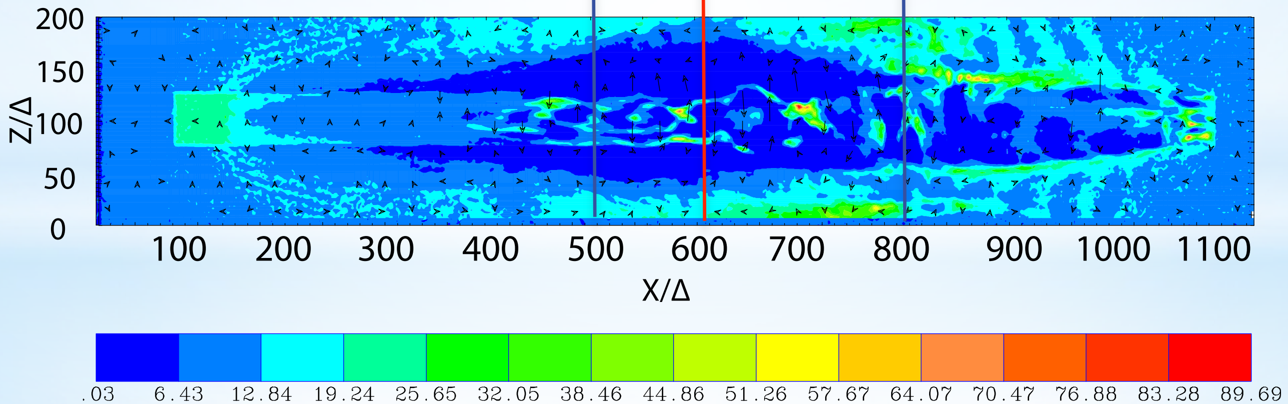

(Nishikawa et al. 2015)

Reconnection in jets?

$t = 1{,}000\omega_{pe}^{-1}$ at the center of the jet

$|B|, B_{x,z}$

electron-proton | electron-positron

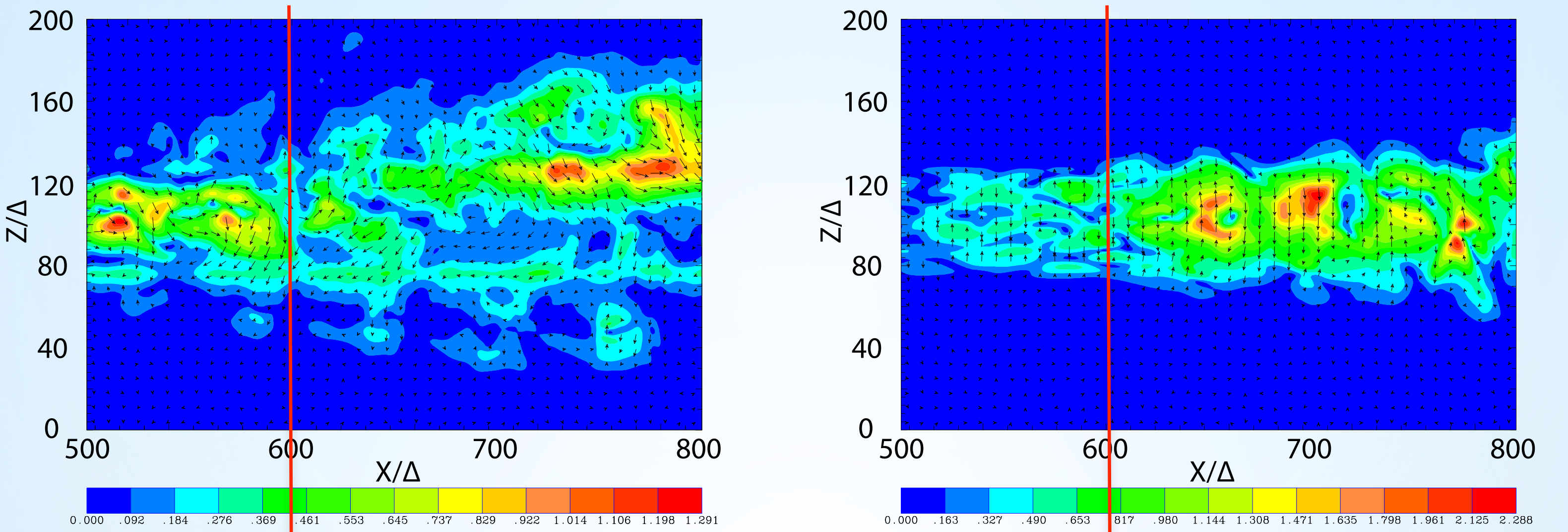

$n_{je}, \mathrm{flux}^{je}_{x,z}$

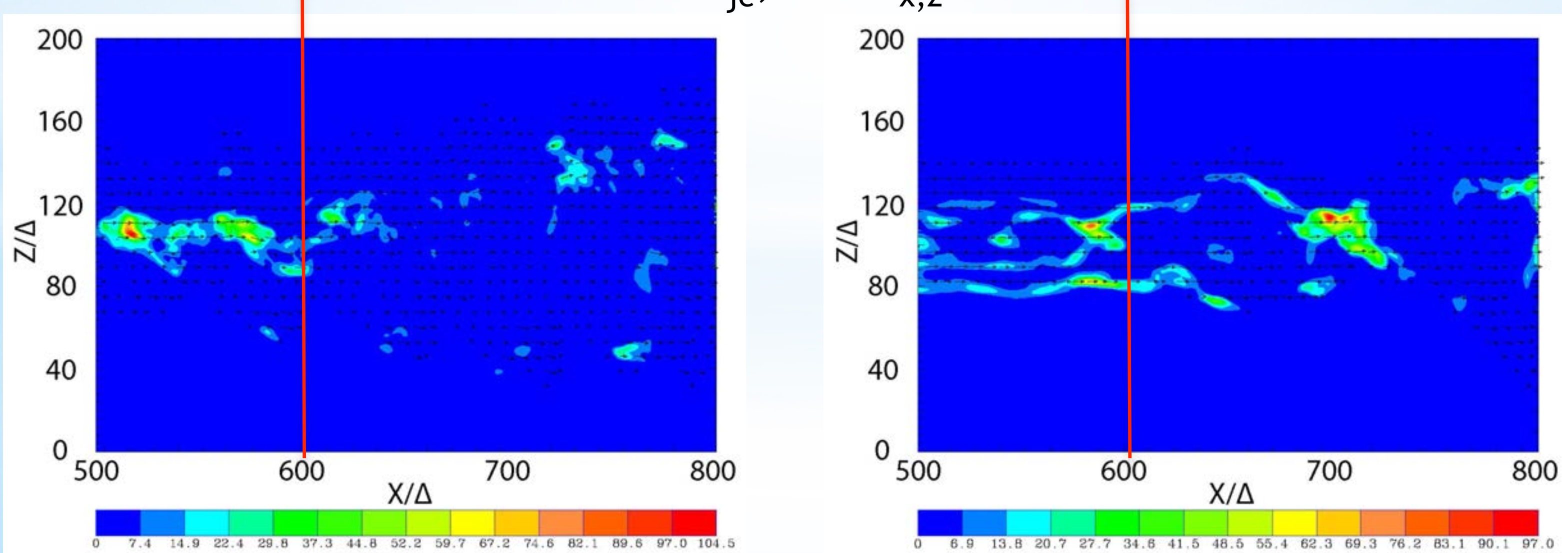

Reconnection in jets?

$t = 1{,}000\omega_{pe}^{-1}$

n_e, $flux^e_{x,z}$

electron-proton

electron-positron

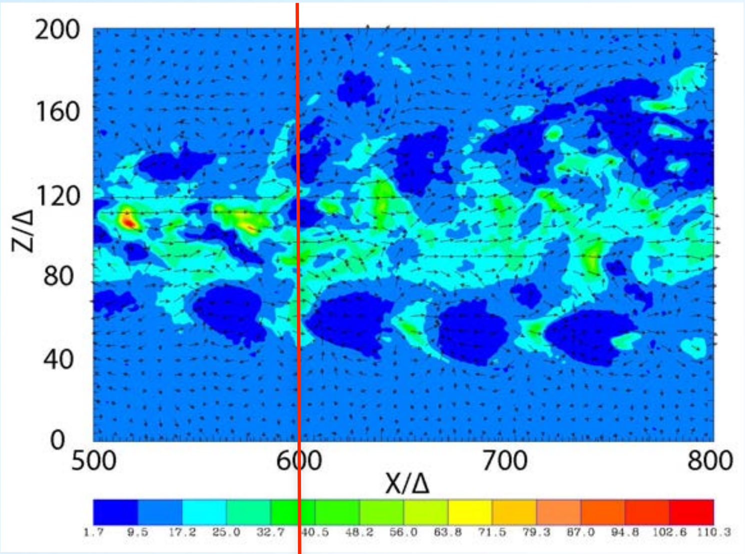

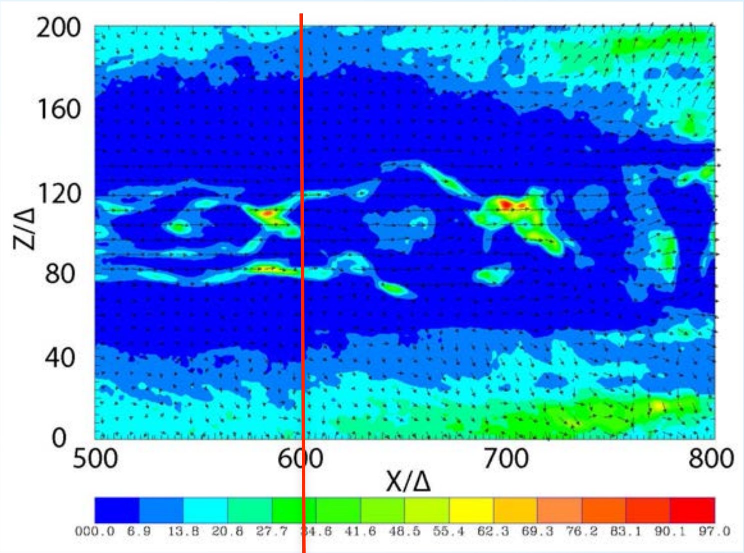

|ExB|, $(ExB)_{x,z}$

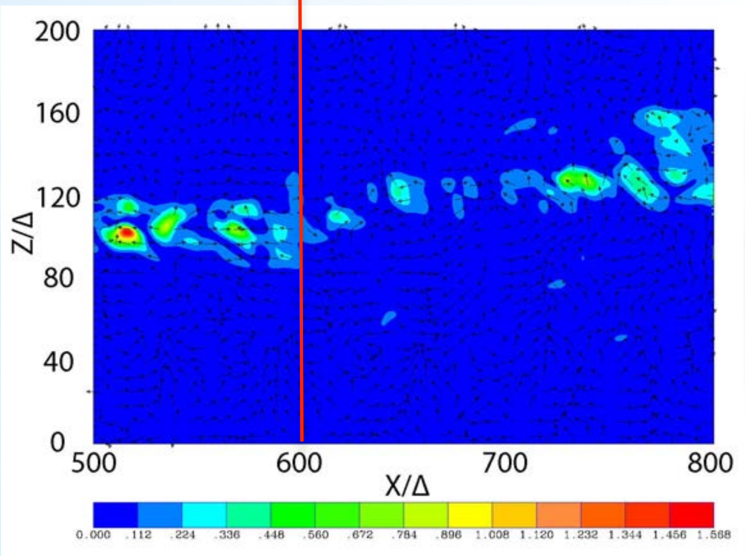

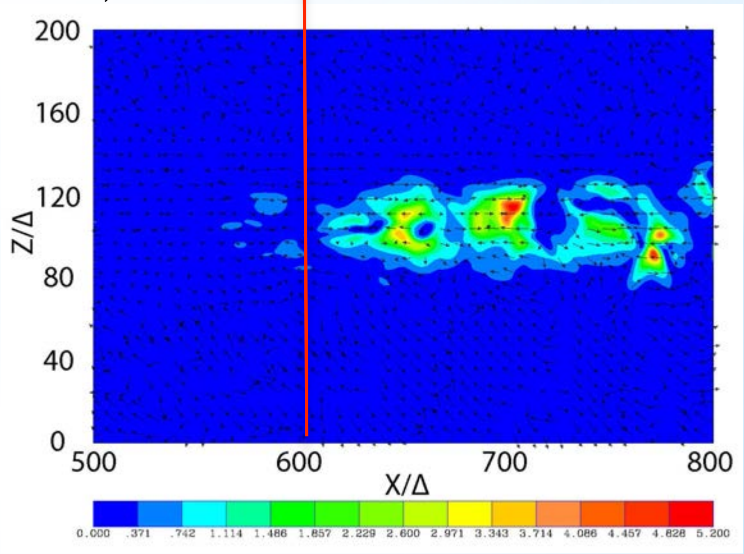

Reconnection in jets?

X/Δ=600 $t = 1{,}000\omega_{pe}^{-1}$

J_x, $B_{y,z}$

electron-proton electron-positron

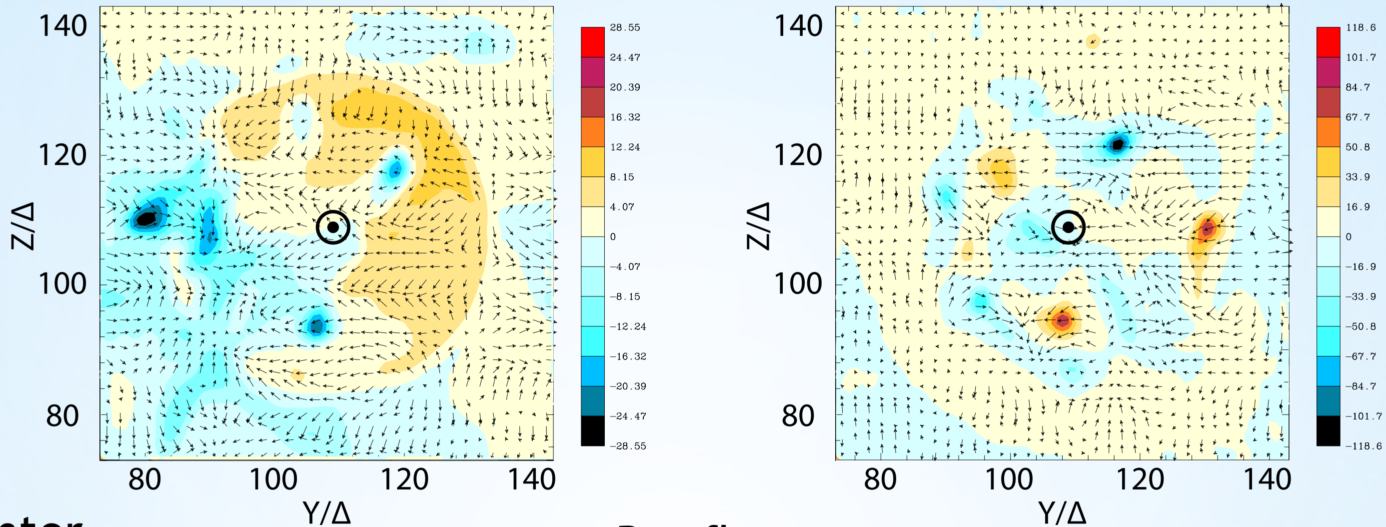

⊙ Jet center

|B|, $flux^e_{y,z}$

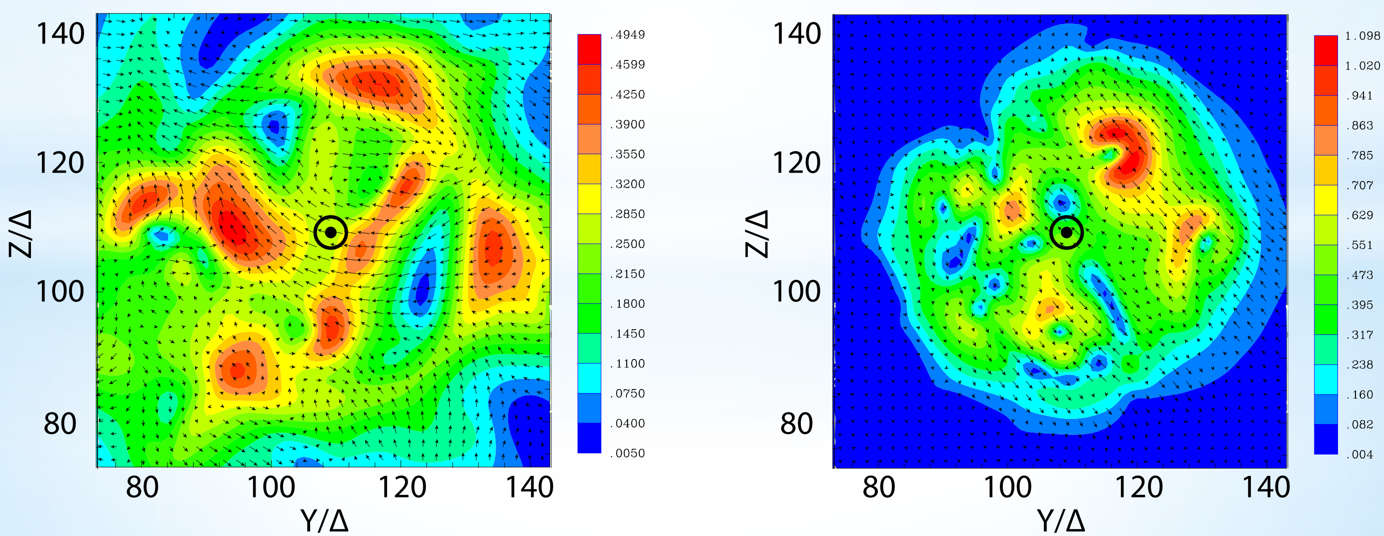

Reconnection in jets?

X/Δ=600 $t = 1{,}000\omega_{pe}^{-1}$

electron-proton |ExB|, $(\text{ExB})_{y,z}$ electron-positron

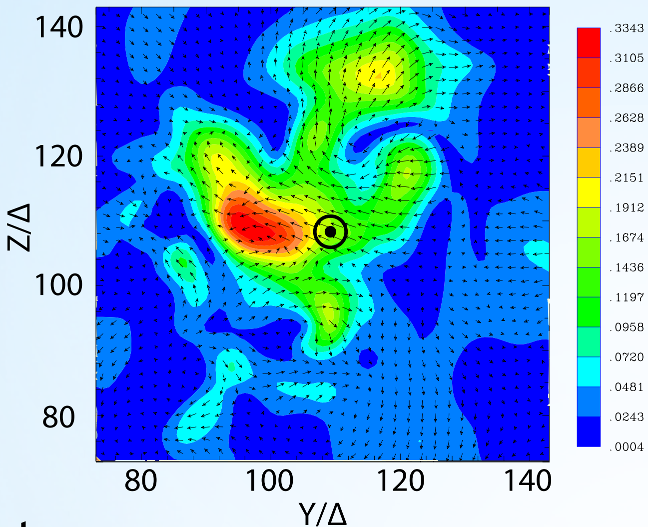

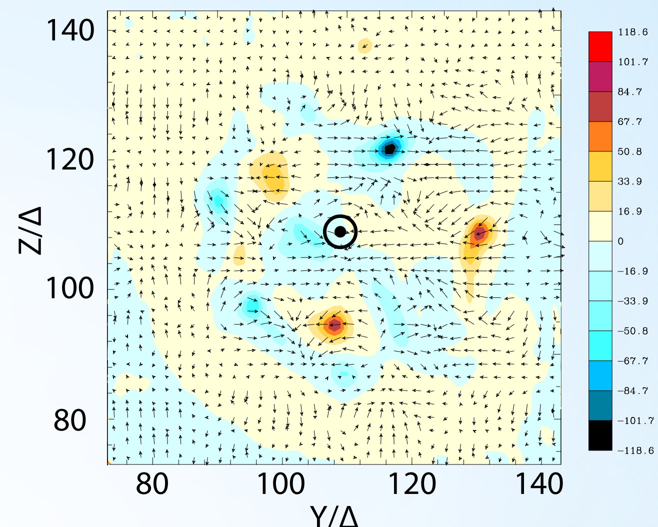

⊙ Jet center

n_e, $\text{flux}^{e}_{y,z}$

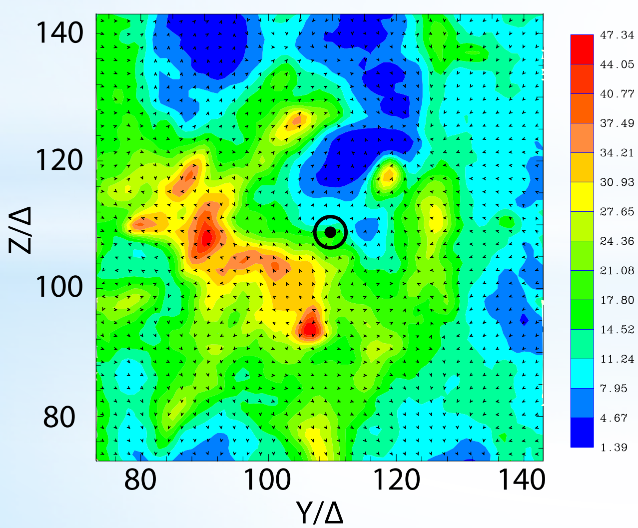

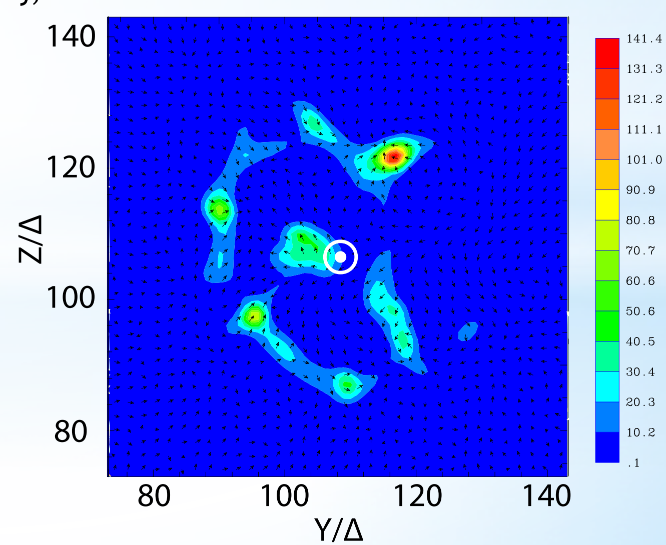

3D snapshots of current (J_x) isosurfaces without magnetic field lines

Evolution of shock and instability is different for electron-proton and electron-positron $\gamma_{jt} = 15$ $t = 1000\omega_{pe}^{-1}$

e-p

e$^{\pm}$

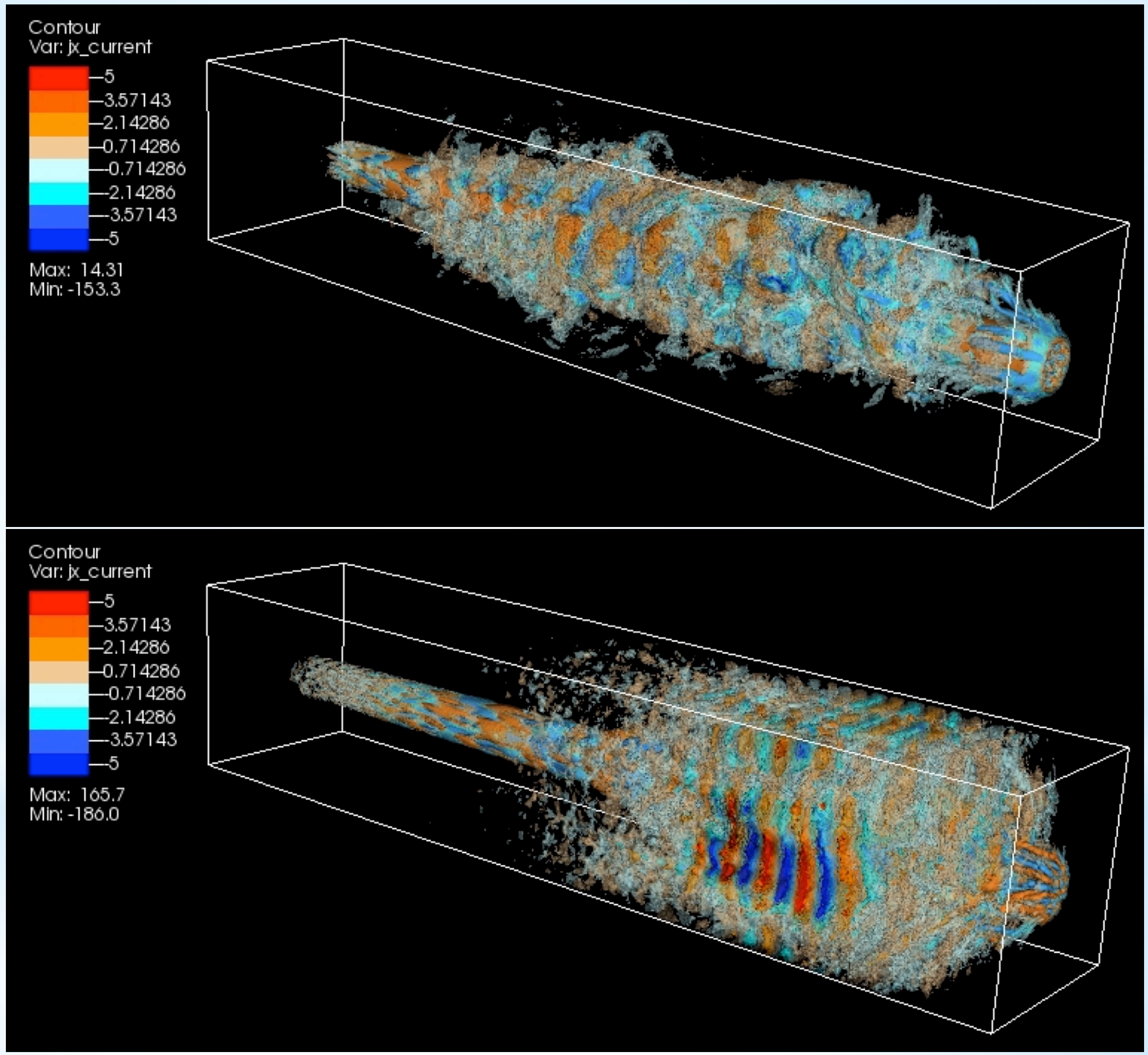

3D snapshots of current (J_x) isosurfaces with magnetic field lines

$\gamma_{jt} = 15 \quad t = 1000\omega_{pe}^{-1}$

e-p

e±

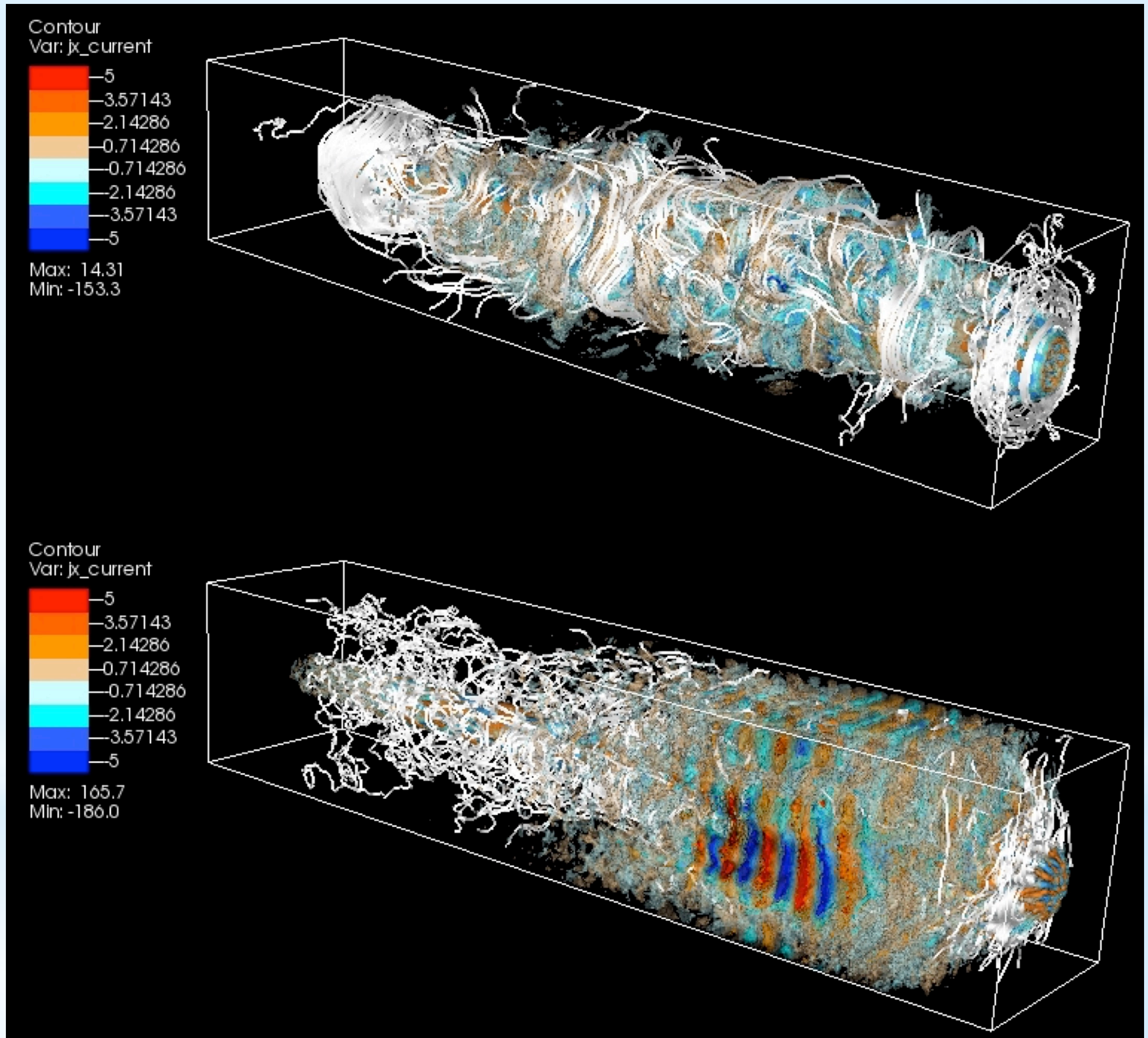

3D snapshots of current (J_x) isosurfaces with magnetic field lines clipped at the center of jet

$\gamma_{jt} = 15$ $t = 1000\omega_{pe}^{-1}$

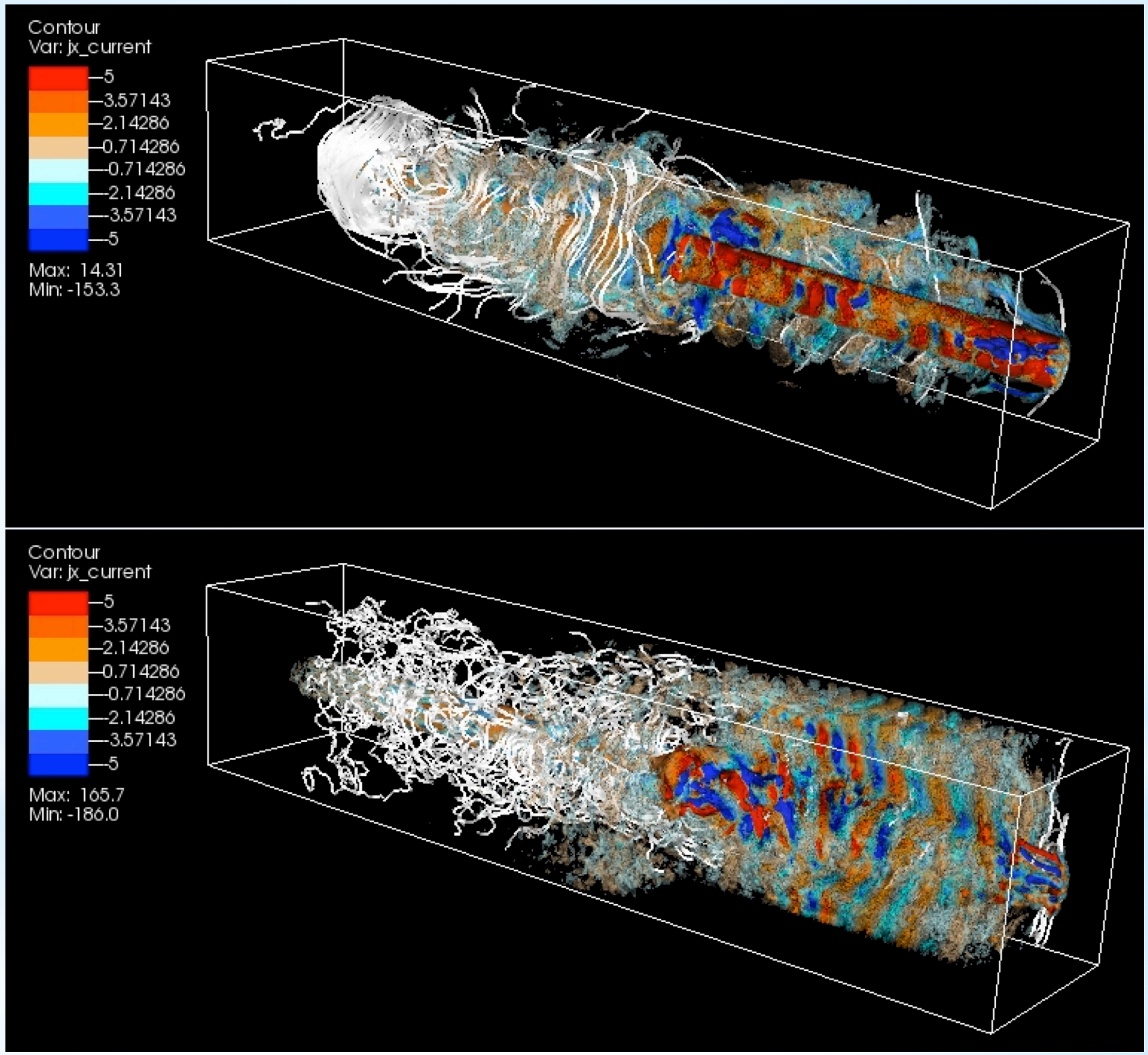

e-p

$e^{\pm}$

3D snapshots of current (J_x) isosurfaces with magnetic field lines clipped at the center of jet (2D plane)

$\gamma_{jt} = 15$ $t = 1000\omega_{pe}^{-1}$

e-p

e±

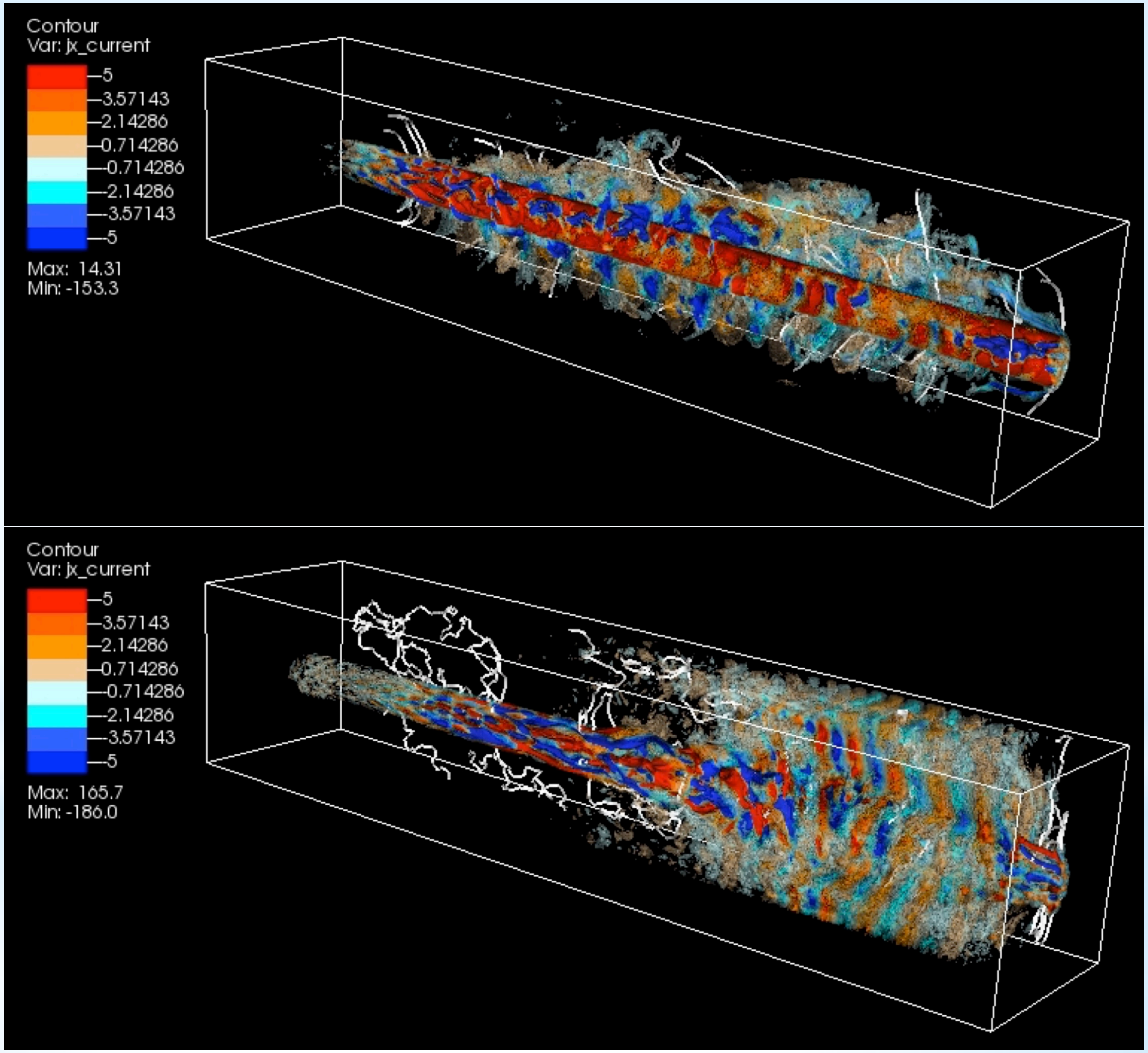

Jet structure at the head of jets

$\gamma_{jt} = 15$ $\quad t = 3500\omega_{pe}^{-1}$

e-p

electron density

$e^{\pm}$

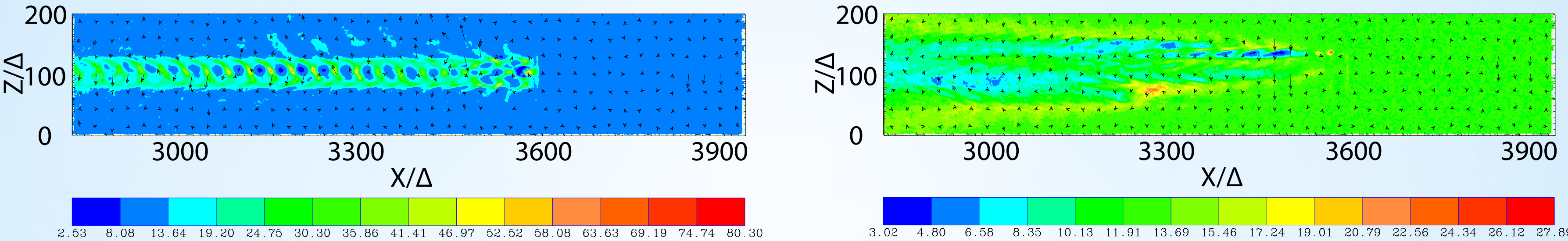

current density

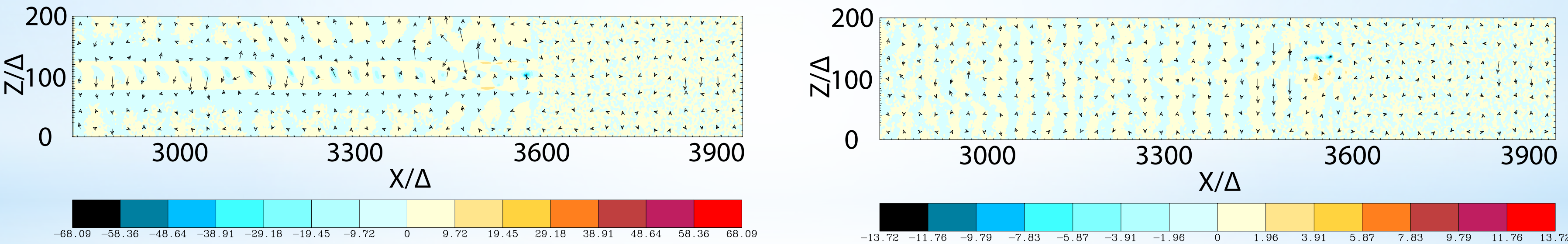

Jet structure at the head of jets in 3D

$\gamma_{jt} = 15$ $t = 3500\omega_{pe}^{-1}$

e-p

electron density

e±

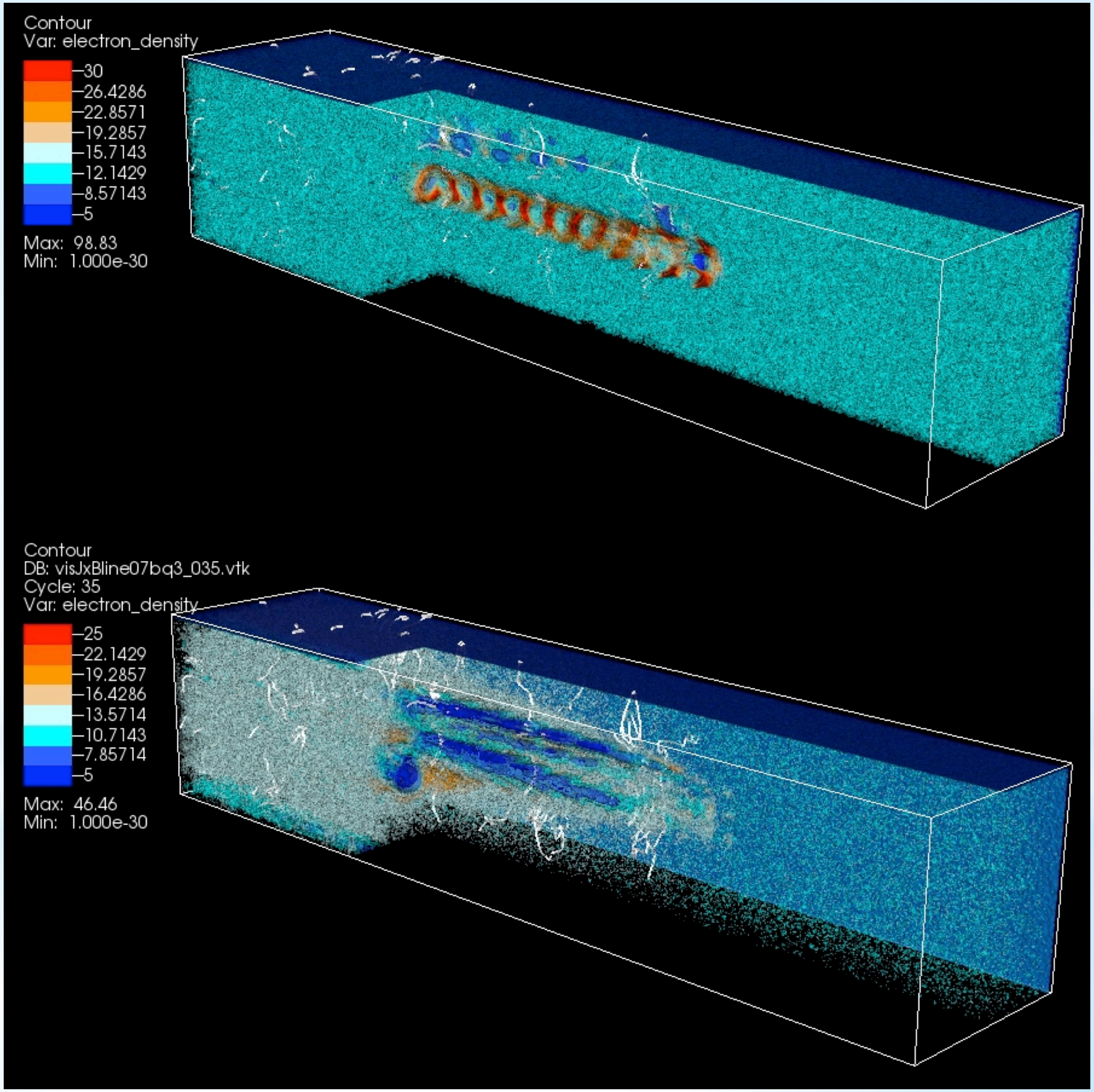

Jet structure at the head of jets in 3D $\gamma_{jt} = 15$ $t = 3500\omega_{pe}^{-1}$

e-p

current density

e±

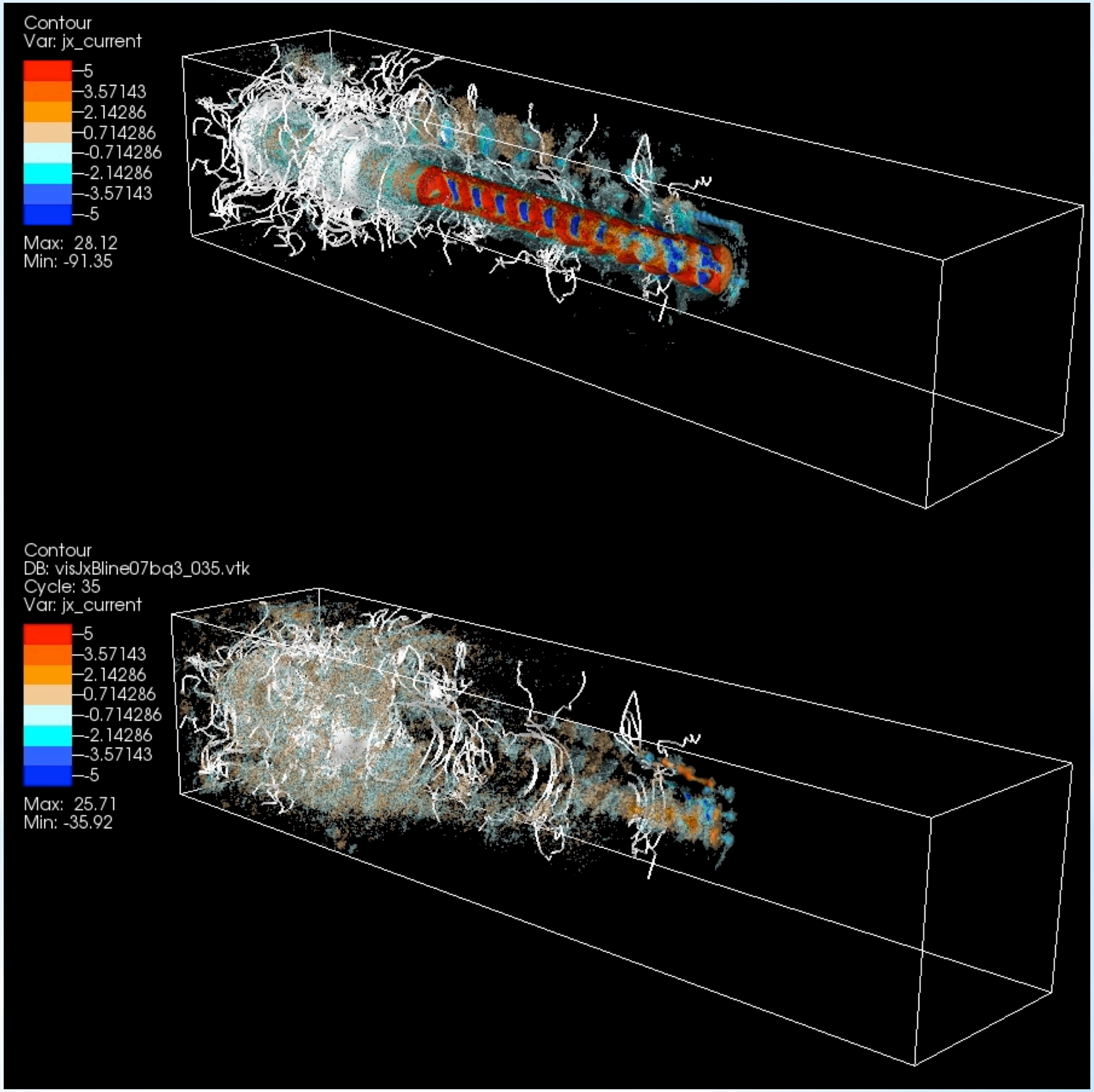

Summary of Kinetic Kelvin-Helmholtz Instability

1. Static electric field grows due to the charge separation by the negative and positive current filaments
2. Current filaments at the velocity shear generate magnetic field transverse to the jet along the velocity shear
3. Jet with high Lorentz factor with core-sheath case generate higher magnetic field even after saturated in the case counter-streaming case with moderately relativistic jet
4. Non-relativistic jet generate KKHI quickly and magnetic field grows faster than the jet with higher Lorentz factor
5. For the jet-sheath case with Lorentz factor 15 the evolution of KKHI does not change with the mass ratio between 20 and 1836
6. Strong magnetic field will affect electron trajectories and create synchrotron-like (jitter) radiation which will be investigated
7. Global jets with combined of Weibel instability and kKHI need to be investigated further and with helical magnetic field

(for detail please see (Nishikawa et al. 2014, ApJ)

Present theory of Synchrotron radiation

- Fermi acceleration (Monte Carlo simulations are not self-consistent; particles are crossing the shock surface many times and remain accelerated, the strengths of turbulent magnetic fields are assumed), Some simulations exhibit Fermi acceleration (Spitkovsky 2008)
- The strength of magnetic fields is estimated based on equipartition - magnetic field energy is comparable to the thermal energy): $\varepsilon_B \sim u(T)$
- The distribution of accelerated electrons is approximated by the power law ($F(\gamma) = \gamma^{-p}$; $p = 2.2$?) (ε_e)
- Synchrotron emission is calculated based on p and ε_B
- There are many assumptions in this calculation!

Synchrotron Emission: radiation from accelerated

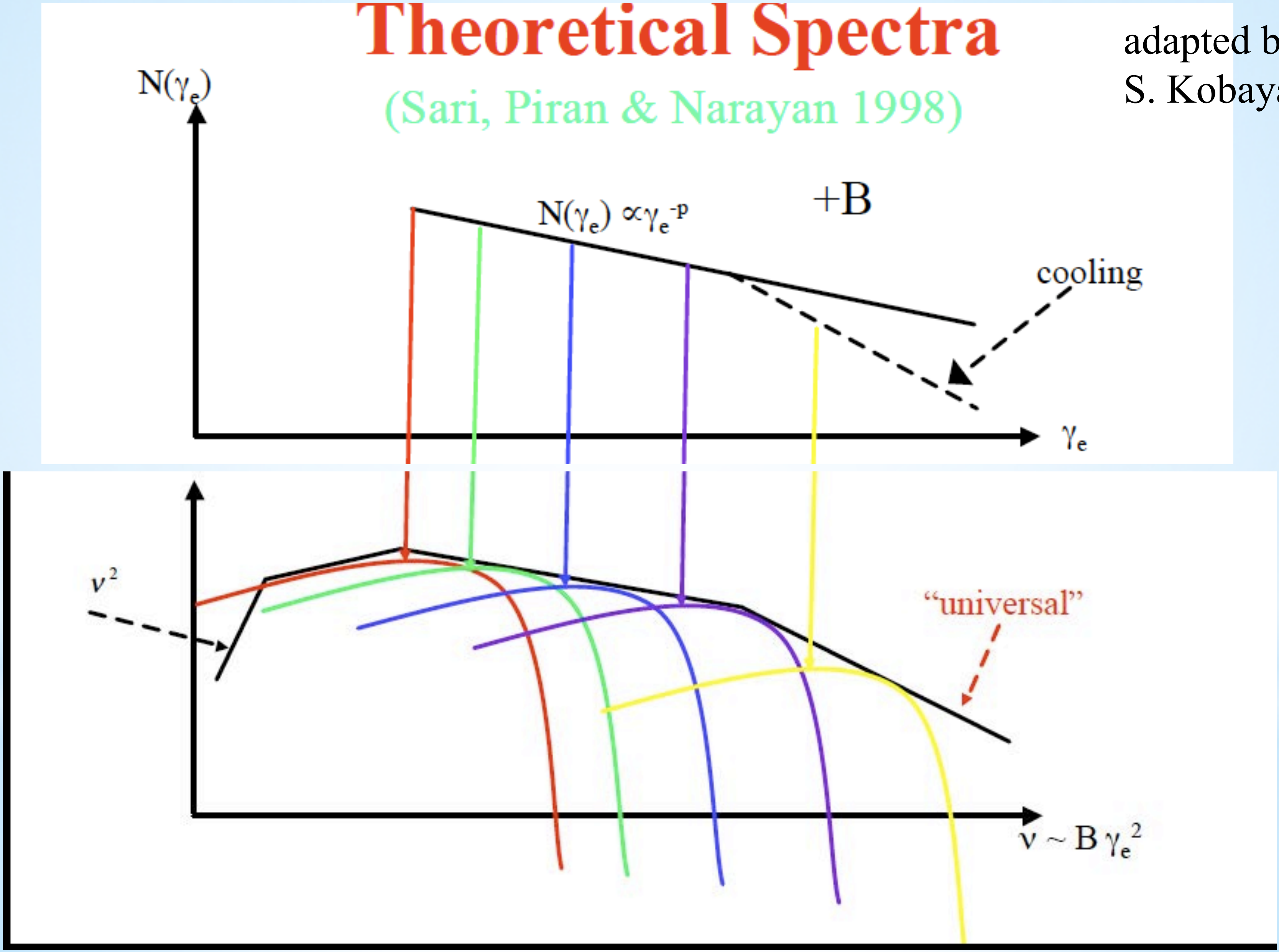

Self-consistent calculation of radiation

- Electrons are accelerated by the electromagnetic field generated by the Weibel instability and KKHI (without the assumption used in test-particle simulations for Fermi acceleration)
- Radiation is calculated using the particle trajectory in the self-consistent turbulent magnetic field
- This calculation includes Jitter radiation (Medvedev 2000, 2006) which is different from standard synchrotron emission
- Radiation from electrons in our simulation is reported in Nishikawa et al. Adv. Sci. Rev, 47, 1434, 2011.

Radiation from particles in collisionless shock

To obtain a spectrum, "just" integrate:

$$\frac{d^2W}{d\Omega d\omega} = \frac{\mu_0 c q^2}{16\pi^3} \left| \int_{-\infty}^{\infty} \frac{\mathbf{n} \times [(\mathbf{n} - \boldsymbol{\beta}) \times \dot{\boldsymbol{\beta}}]}{(1 - \boldsymbol{\beta} \cdot \mathbf{n})^2} e^{i\omega(t' - \mathbf{n} \cdot \mathbf{r}_0(t')/c)} dt' \right|^2$$

where $\mathbf{r}_0$ is the position, β the velocity and $\dot{\beta}$ the acceleration

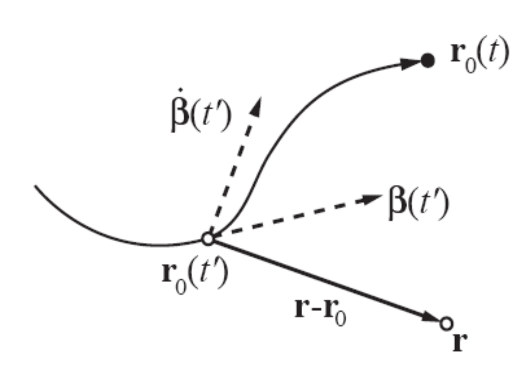

New approach: Calculate radiation from integrating position, velocity, and acceleration of ensemble of particles (electrons and positrons)

Hededal, Thesis 2005 (astro-ph/0506559)
Nishikawa et al. 2008 (astro-ph/0802.2558), 2011
Sironi & Spitkovsky, 2009, ApJ
Martins et al. 2009, Proc. of SPIE Vol. 7359
Frederiksen et al. 2010, ApJL

Synchrotron radiation from propagating electrons in a uniform magnetic field

electron trajectories

radiation electric field observed at long distance

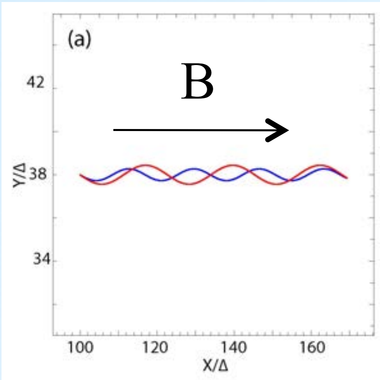

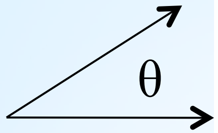

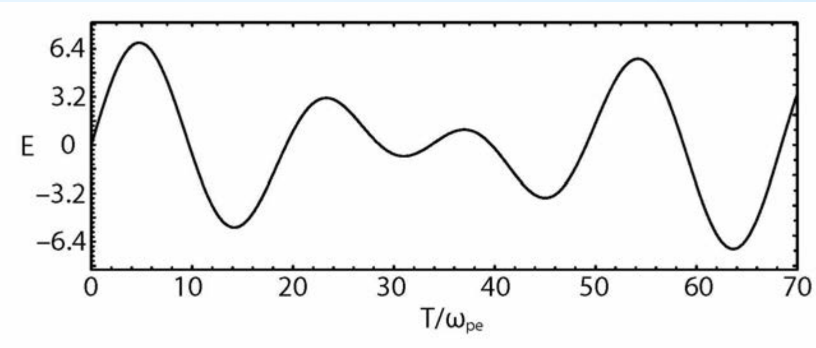

observer

spectra with different viewing angles (helical)

gyrating

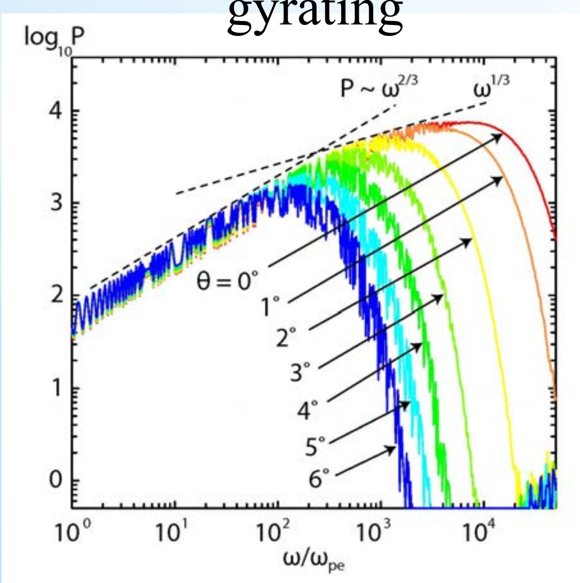

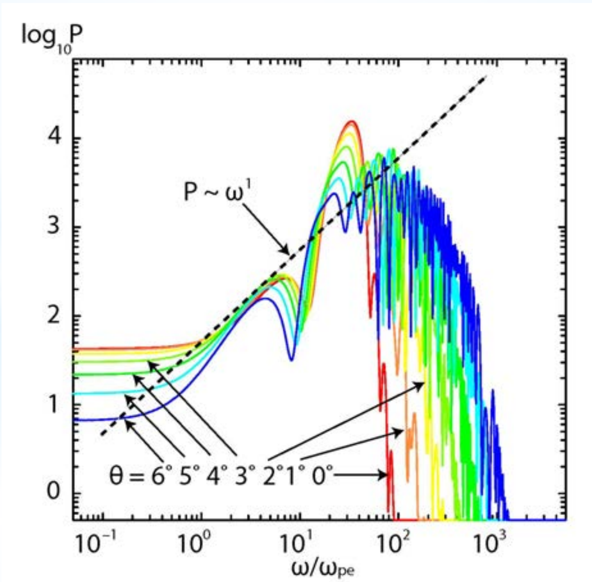

$\theta_\gamma = 4.25°$

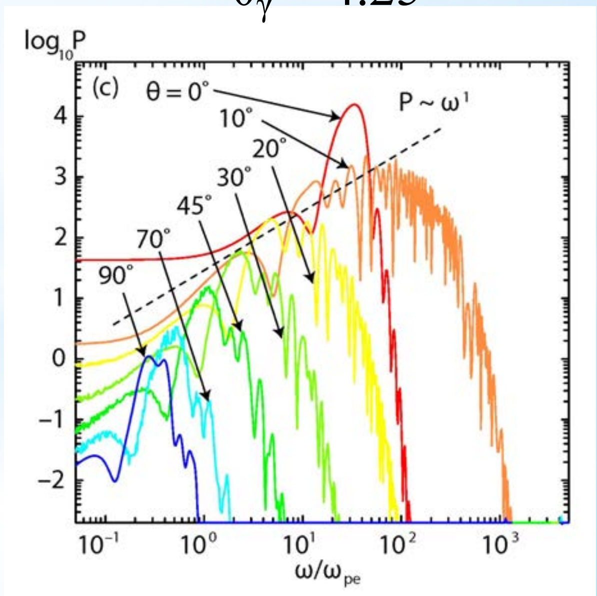

(Nishikawa et al. Advances in Space Research, 2011)

Synchrotron vs. `Jitter'

- (a) Synchrotron emission assumes large-scale homogeneous magnetic fields
- (b) `Jitter' radiation (Medvedev 2000) occurs where the gyro-radius is larger than the randomness of turbulent magnetic fields

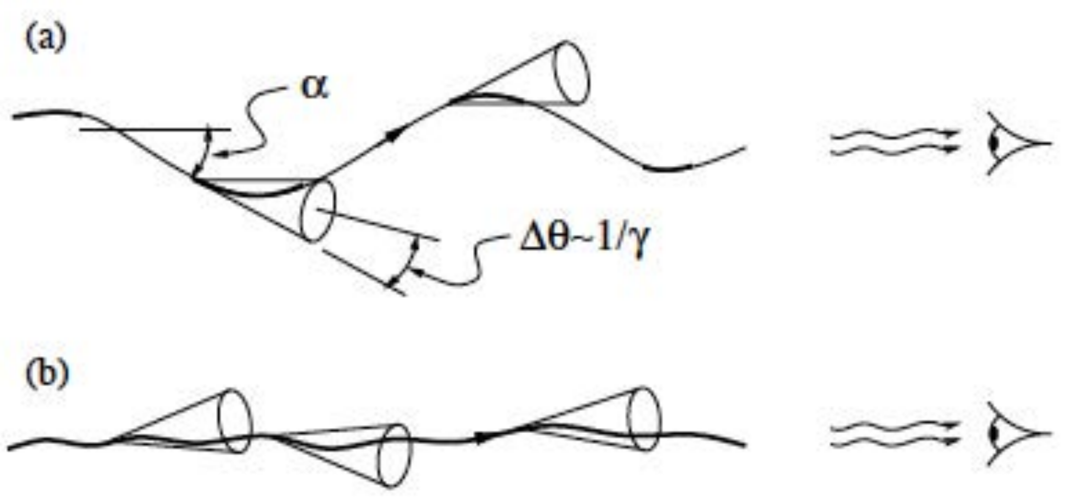

FIG. 1.—Emission from various points along the particle's trajectory. (*a*) $\alpha \gg \Delta\theta$; emission from selected parts (*bold portions*) of the trajectory is seen by an observer. (*b*) $\alpha \ll \Delta\theta$; emission from the entire trajectory is observed.

Observations and numerical spectrum

GRB 080916C

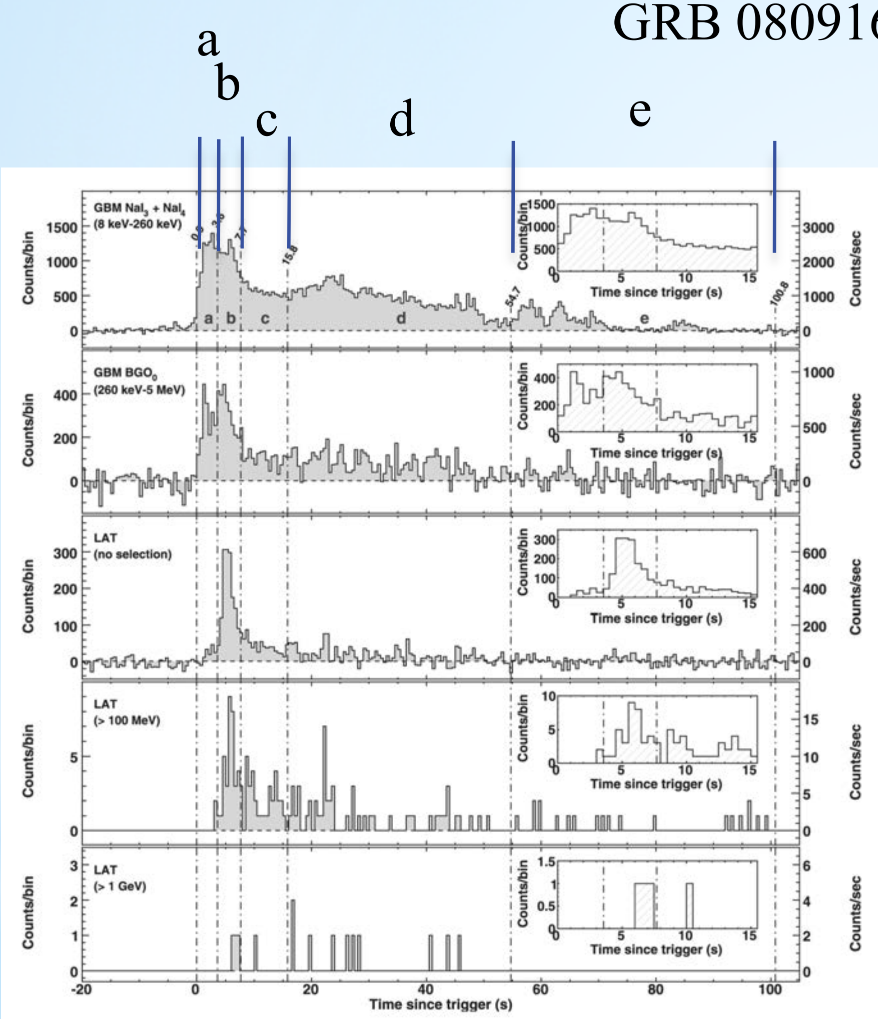

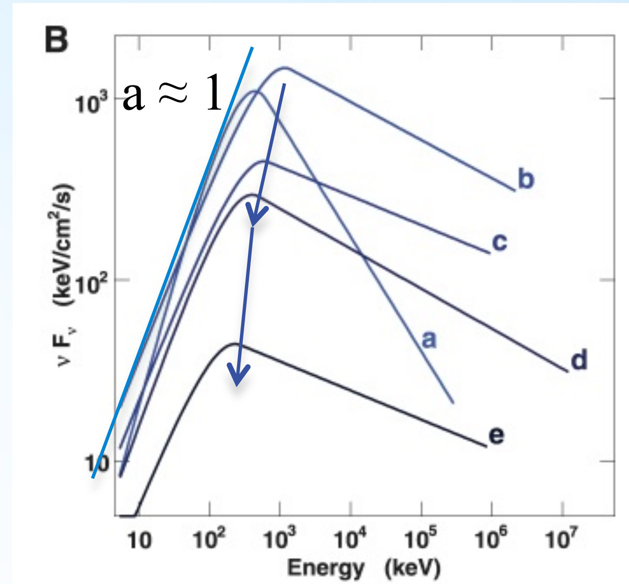

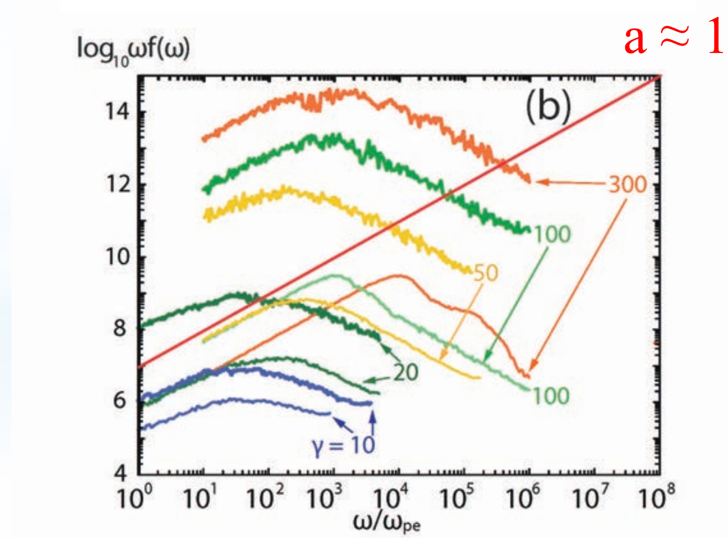

Abdo et al. 2009, Science

(Nishikawa et al. 2012)

Reconnection in jet

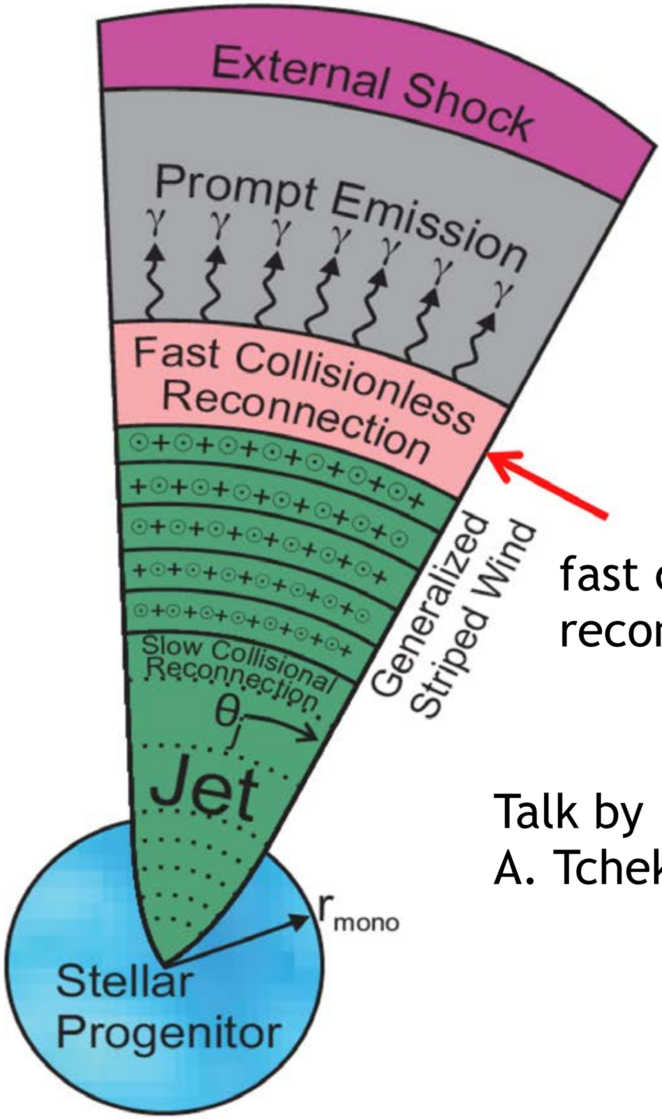

fast collisionless reconnection

Talk by
A. Tchekhovskov

Reconnection switch concept: Collapsar model or some other system produces a jet (with opening half-angle θ_j) corresponding to a generalized stripped wind containing many field reversals that develop into dissipative current sheets (McKinney and Uzdensky, 2012, MNRAS, 419, 573). This reconnection needs to be investigated by resistive RMHD, which is in progress within our research effort.

(see also Bing's talk)

Simulations with magnetic field in jets

no magnetic field   anti-parallel magnetic field

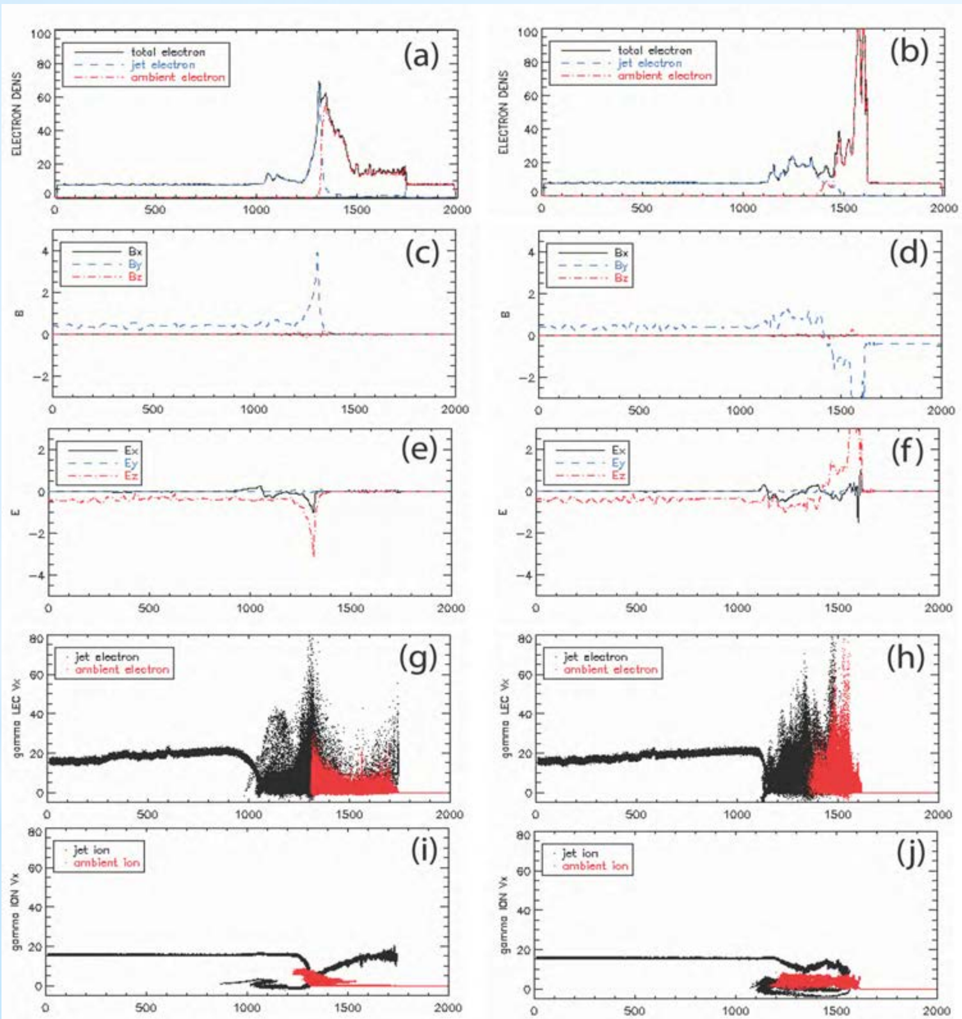

Snapshots for unmagnetized ambient plasma (left column) and anti-parallel magnetic field in the ambient plasma (right column) at t = 1450 ω_{pe}^{-1} (Choi, Min, and Nishikawa, 2012). The averaged values of electron density (a) and (b), magnetic field (c) and (d), electric field (e) and (f), phase space of electrons (g) and (h), and phase space of ions (i) and (j). Reconnection occurs for the case of anti- parallel magnetic fields and is indicated by the positive E_y component in (f).

Choi, Min, KN, 2013 (in progress)

(Nishikawa et al. 2012)

3-D kink instability with helical magnetic field

see movie 3Dprej5b_1.mov

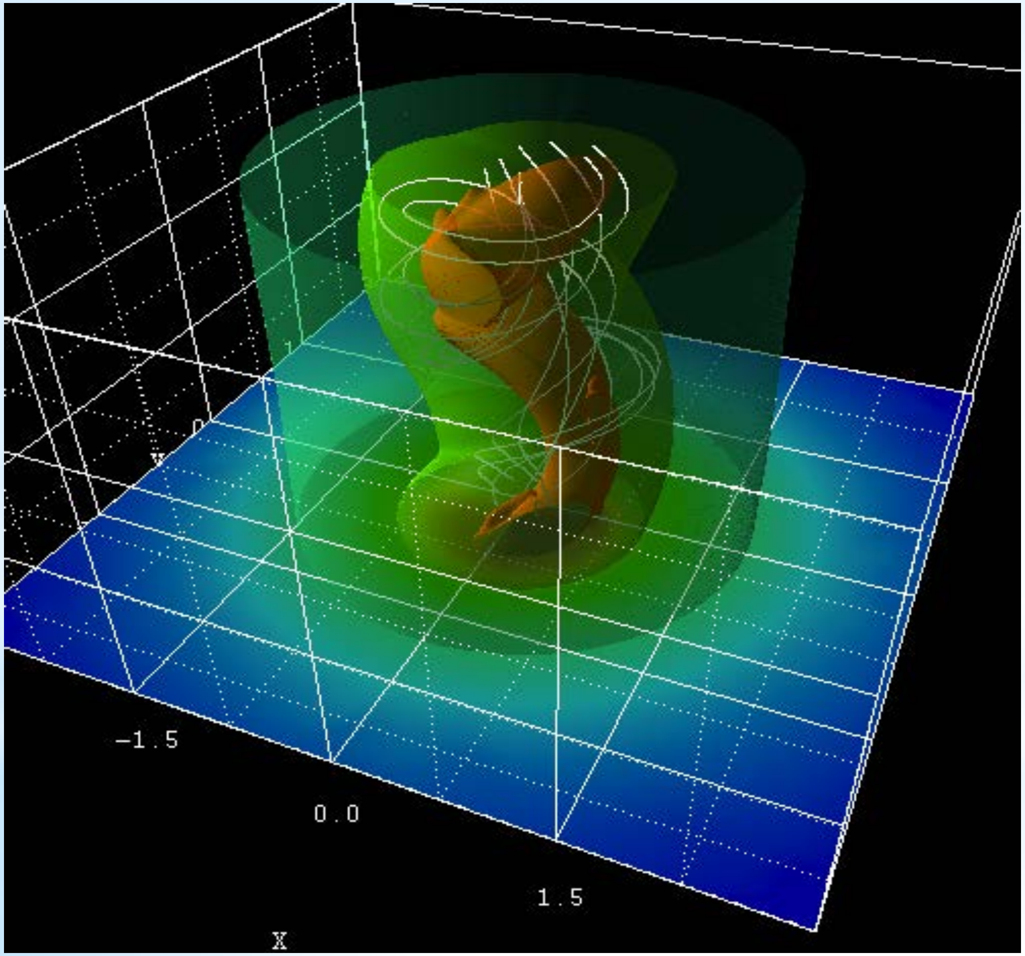

Relativistic jet with helical magnetic field, which leads to the kink instability and subsequent reconnection, can be simulated using resistive relativistic MHD (this simulation was performed with ideal RMHD code).

(Mizuno et al. ApJ, 734:19 (18pp), 2011)

The gas pressure of a jet obtained by RMHD simulation with an initial over-pressure

Series of recolimation shocks

Propagation of perturbed shock

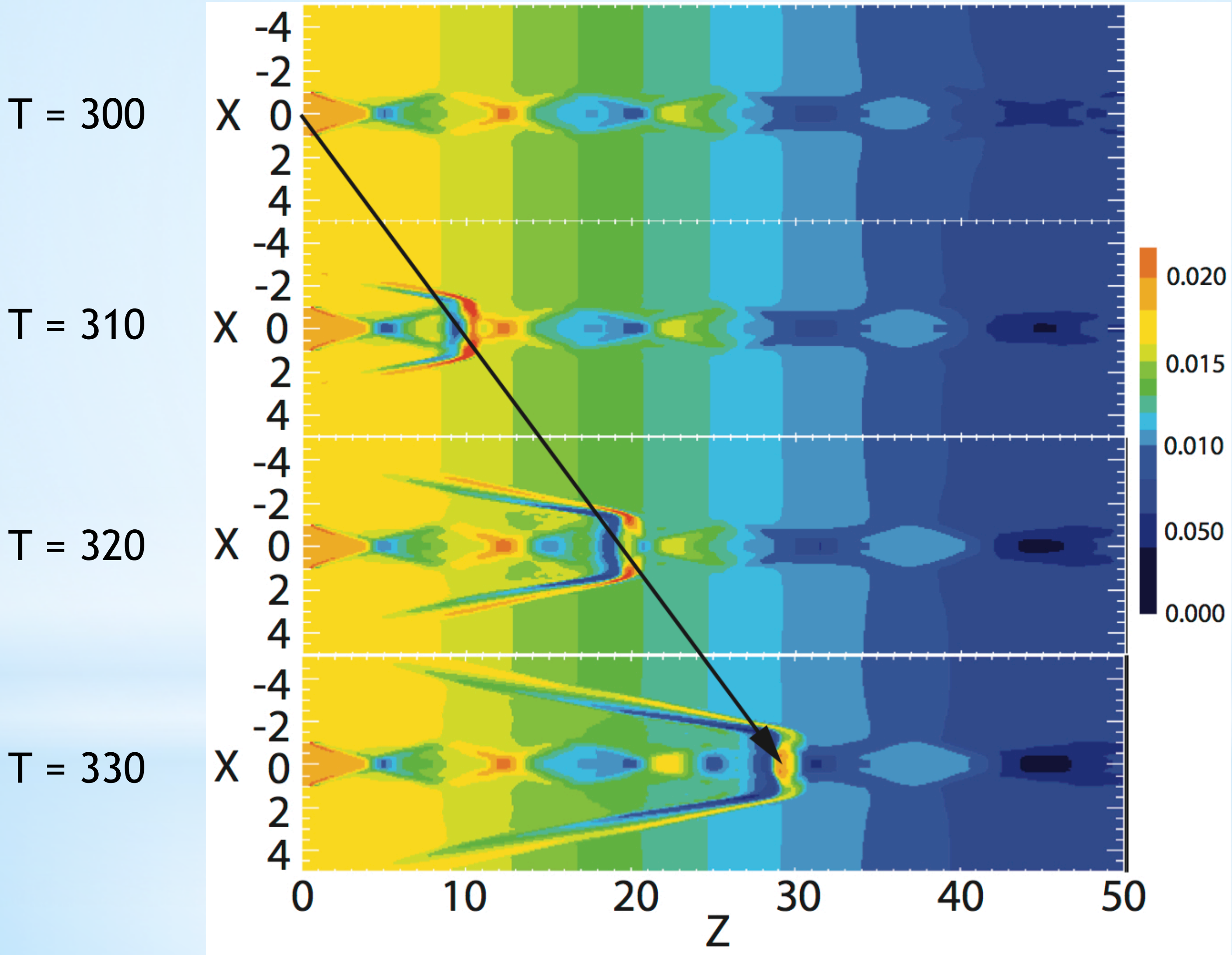

(Mizuno et al. in progress, 2014)

Summary

- Spectra from two electrons were calculated for different conditions.
- The magnetic fields created by the Weibel instability generate highly inhomogeneous magnetic fields, which are responsible for itter radiation (Medvedev, 2000, 2006; Fleishman 2006; Frederiksen et al. 2010, Medvedev et al 2011, Nishikawa et al. 2011)
- Our new numerical approach of calculating radiation from electrons based on self-consistent simulations provides more realistic spectra including jitter radiation
- Need further calculation of synthetic spectra with spectral evolution
- Reconnection is very important to release magnetic field energy to kinetic energy
- Recollimation shock may create gamma-ray flash by moving perturbation

Future plans

- Further simulations with a systematic parameter survey will be performed in order to understand shock dynamics including KKHI and reconnection
- Further simulations will be performed to calculate self-consistent radiation including time evolution of spectrum and time variability using larger systems
- Investigate radiation processes from the accelerated electrons in turbulent magnetic fields and compare with observations using global simulation of shock, KKHI and reconnection with helical magnetic field in jet (GRBs, SNRs, AGNs, etc)
- Particle acceleration and radiation in recollimation shocks

GRB progenitor (collapsar, merger, magnetar)

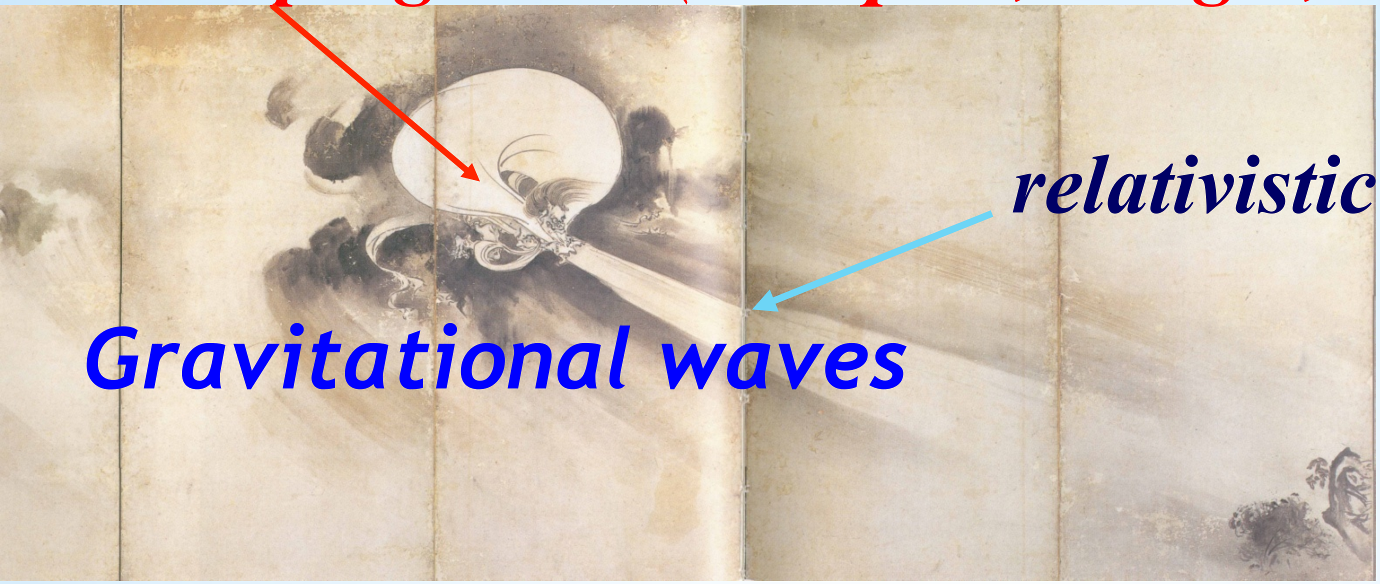

relativistic jet

Gravitational waves

Fushin

(god of wind)

EM emission

(shocks, acceleration)

Raishin

(god of lightning)

(Tanyu Kano 1657)

Emission Lines from Tori

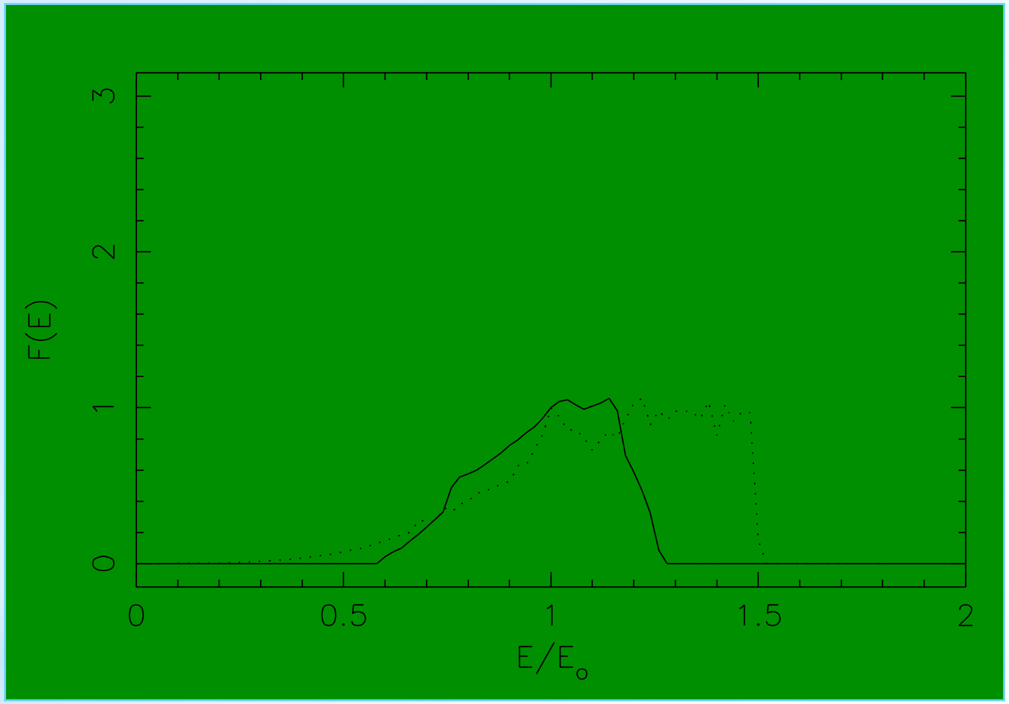

- Inner most region is obscured – weakening the red and blue wings.
- A broad emission line centered at 6.4keV results.
- This may explain why not many sources with asymmetric lines like MCG-6-30-15 are observed.

Comparison of emission line between accretion torus (solid) and disk (dotted) inclined at 85^o.

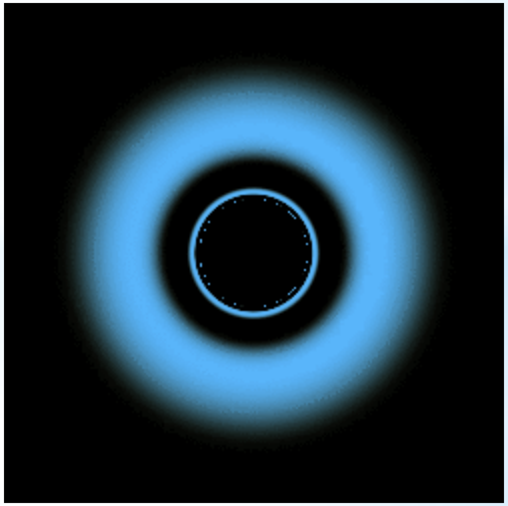

Partially transparent torus around a Kerr Black Hole.

(Fuerst & Wu 2004, A&A, 424, 733)

*Relativistic Radiation Transfer

Fuerst, Mizuno, Nishikawa, & Wu, 2007, ApJL, submitted

• We have calculated the thermal free-free emission and thermal synchrotron emission from a relativistic flows in black hole systems based on the results of our 2D GRMHD simulations (rotating BH cases).
• We consider a general relativistic radiation transfer formulation (Fuerst & Wu 2004, A&A, 424, 733) and solve the transfer equation using a ray-tracing algorithm.
• In this algorithm, we treat general relativistic effect (light bending, gravitational lensing, gravitational redshift, frame-dragging effect etc.).

Image of Emission, absorption & scattering

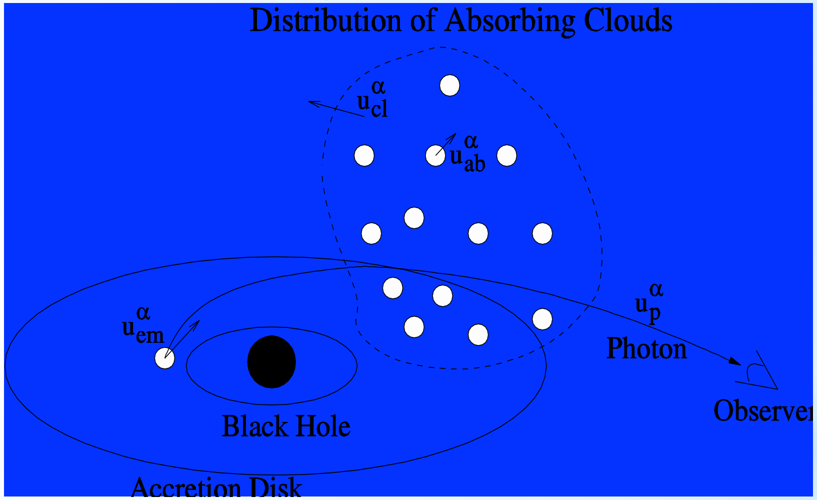

*Relativistic Radiation Transfer

Project image of thermal emission (<20 rs)

2D GRMHD simulations (*old version)* (a = 0.95, B = 0.1 $(\rho c^2)^{-2}$)

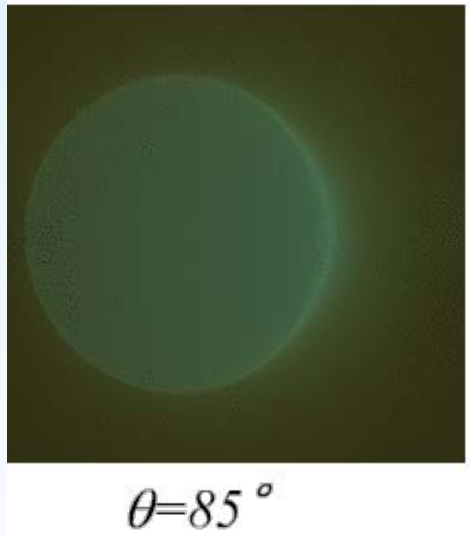

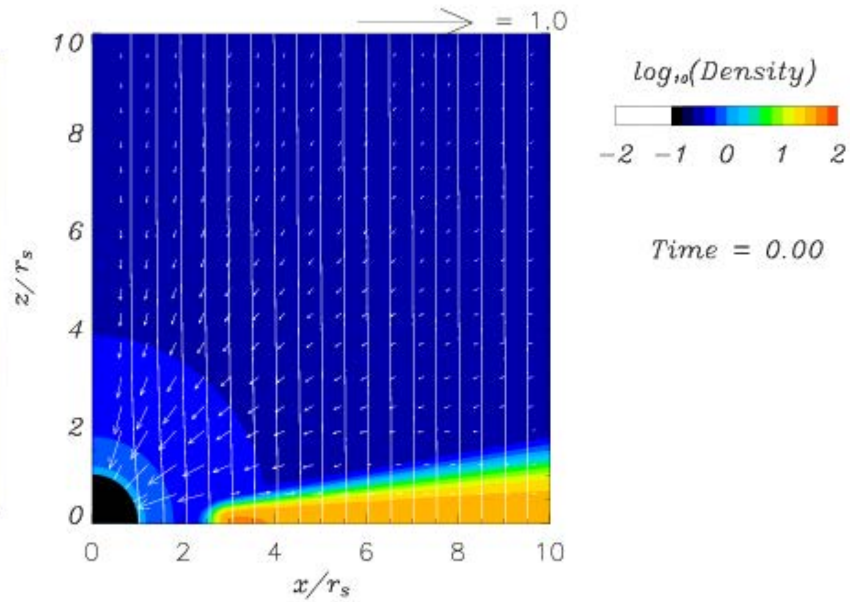

- The radiation image shows the front side of the accretion disk and the other side of the disk at the top and bottom regions.
- It is because the general relativistic effects.

- We can see the propagation of waves and the strong radiation from geometrically thick disk near the BHs.
- The jet generated in GRMHD simulation is not visible in the radiation image.
- This is because we assume the thermal free-free emission. It has a strong density dependence and the jet is less dense than the disk.
- If we calculate the emission with weaker dependence on the density, such as non-thermal process or Compton scattering, the jet would be visible.

(Wu et al. 2008)

* Radiation images of black hole-disk system

• The radiation image shows the front side of the accretion disk and the other side of the disk at the top and bottom regions because the general relativistic effects.

• We can see the formation of two-component jet based on synchrotron emission and the strong thermal radiation from hot dense gas near the BHs.

• A beaming synchrotron emission (green-spark) is seen the surface of the disk (time-dependent). It would be a origin of QPOs?

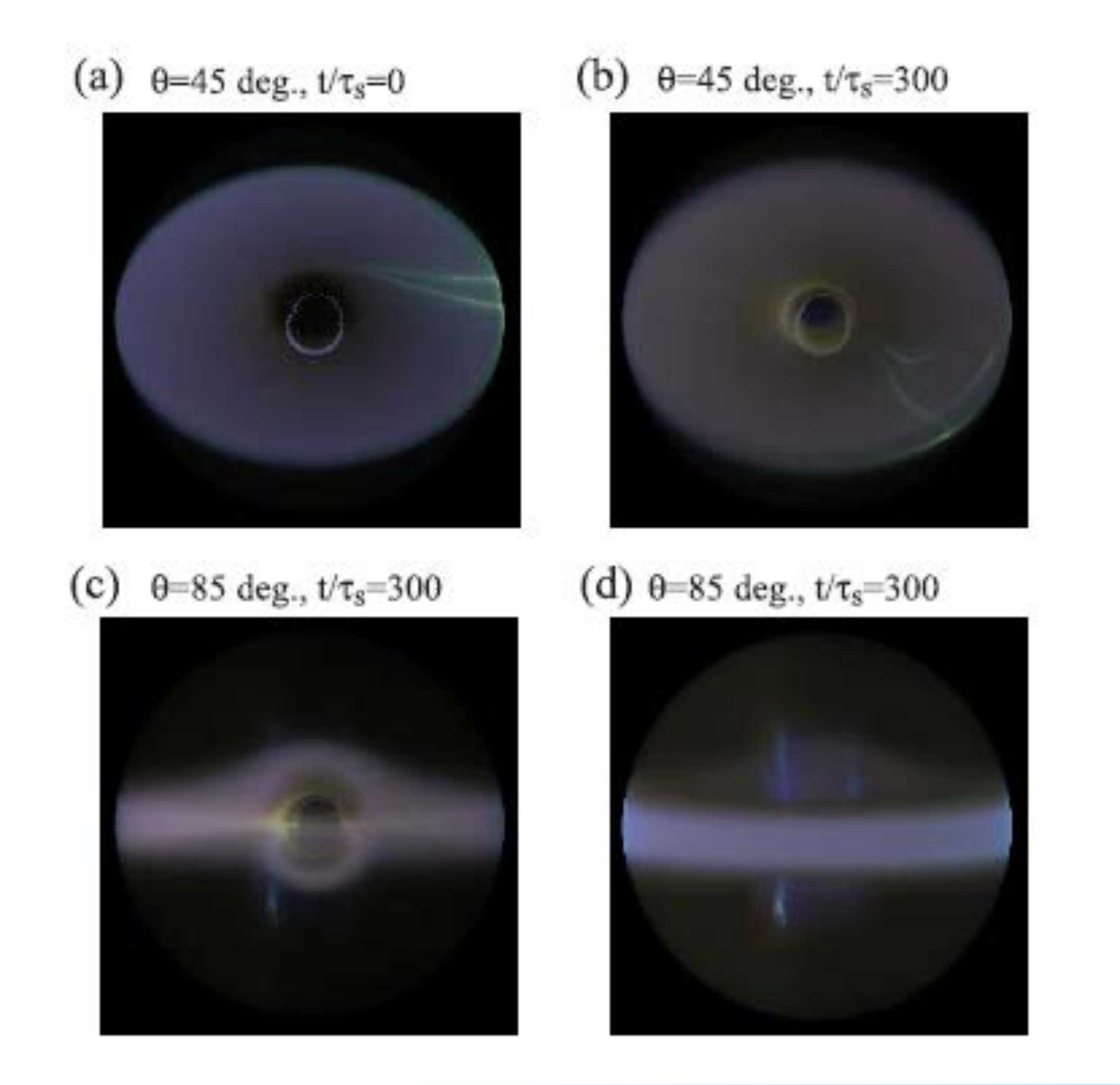

Fuerst, Mizuno, Nishikawa, & Wu, 2007, ApJL, submitted

* Summary

* Simulation results show electromagnetic stream instability driven by streaming $e^{\pm}$ pairs are responsible for the excitation of near-equipartition, turbulent magnetic fields and a structure with leading and trailing shocks.
* Shock is similar to the shock in simulations with the constant contact discontinuity.
* The spectrum from jet electrons in a weak magnetic field in a small system shows a Bremsstrahlung like spectrum with higher frequency enhancement with turbulent magnetic field.
* The magnetic fields created by Weibel instability generate highly inhomogeneous magnetic fields, which is responsible for jitter radiation (Medvedev, 2000, 2006; Fleishman 2006).

Future plans of our simulations of relativistic jets

- **Calculate radiation with larger 3-D systems for different parameters including magnetic fields in order to compare with observational data**
- **Include inverse Compton emission beside synchrotron radiation to obtain high frequency radiation**
- **Simulations with magnetic fields including turbulent magnetic fields with pair plasma and electron-ion plasma**
- **Reconnection simulations for additional acceleration mechanism including magnetic reconnection**
- **Non-relativistic jet simulations for understanding SNRs**

* Gamma-Ray Large Area Space Telescope (FERMI) (launched on June 11, 2008) http://www-glast.stanford.edu/

Compton Gamma-Ray Observatory (CGRO)

Burst And Transient Source Experiment (BATSE) (1991-2000)

PI: Jerry Fishman

→

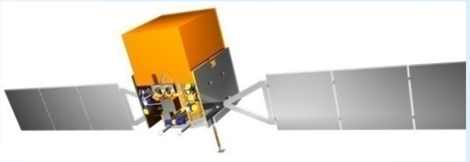

Fermi (GLAST)

All sky monitor

* Large Area Telescope (LAT) PI: Peter Michaelson: gamma-ray energies between 20 MeV to about 300 GeV
* Fermi Gamma-ray Burst Monitor (GBM) PI: Bill Paciaas (UAH) (Chip Meegan (Retired;USRA)): X-rays and gamma rays with energies between 8 keV and 25 MeV

(http://gammaray.nsstc.nasa.gov/gbm/)

The combination of the GBM and the LAT provides a powerful tool for studying radiation from relativistic jets and gamma-ray bursts, particularly for time-resolved spectral studies over very large energy band.

* Jet formation in general relativistic PIC simulation

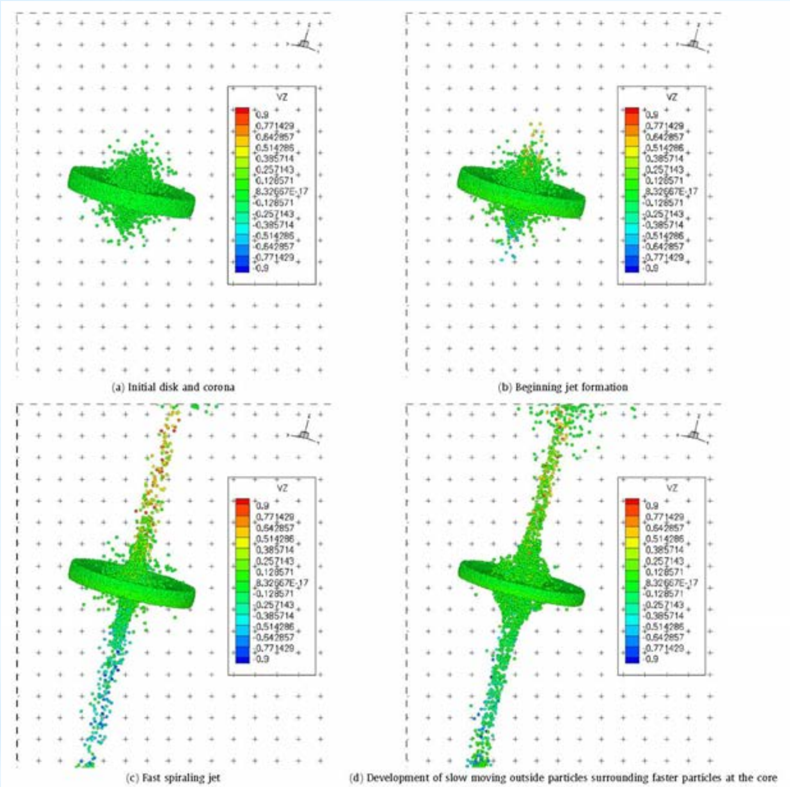

Fig. 5. Bipolar jet formations are shown at the times $t = 0$, 100, 300, and 500.

Keplerian motion of electrons and positrons may excite charge separation instability, then generate jet

see movie jetbig.avi

A method for incorporating the Kerr–Schild metric in electromagnetic particle-in-cell code, M. Watson & K.-I. Nishikawa, Computer Physics Communications 181 (2010) 1750–1757

Summary

- We have developed a new three-dimensional general relativistic magnetohydrodynamic (GRMHD) code ``RAISHIN" (RelAtivIStic magnetoHydrodynamic sImulatioN, RAISHIN is the Japanese ancient god of lightning) by using a conservative, high-resolution shock-capturing scheme.
- The flux-interpolated, constrained transport scheme is used to maintain a divergence-free magnetic field.
- We have performed simulations of jet formation from a geometrically thin accretion disk near both non-rotating and rotating black holes. Similar to previous results (Koide et al. 2000, Nishikawa et al. 2005a) we find magnetically driven jets.
- It appears that the rotating black hole creates a second, faster, and more collimated inner outflow. Kinematic jet structure could be a sensitive function of the black hole spin parameter and magnetic field strength.
- GRPIC simulations will be complementary to GRMHD simulations.

* Standard radiation model by E. Waxman (2006)

- the luminosity and spectrum of synchrotron radiation, the strength of the magnetic field and the energy distribution of the electrons
- Due to the lack of a first principles theory of collisionless shocks, we present in this section a purely phenomenological approach to the model of afterglow radiation emission
- we simply assume that a fraction ε_B of the post-shock thermal energy density is carried by the magnetic field, that a fraction ε_e is carried by electrons, and that the energy distribution of the electrons is a power-law, $\mathbf{d}\log n_e/\mathbf{d}\log \boldsymbol{\varepsilon} = \mathbf{p}$ (above some minimum energy $\boldsymbol{\varepsilon}_0$ which is determined by ε_e and **p**)
- $\boldsymbol{\varepsilon}_B$, $\boldsymbol{\varepsilon}_e$ and **p** are treated as free parameters, to be determined by observations
- the constraints implied on these parameters by observations are independent of any assumptions regarding the nature of the afterglow shock and the processes responsible for particle acceleration or magnetic field generation
- The parameters ε_B, $\boldsymbol{\varepsilon}_e$ and **p**, together with the parameters **E** and **n** which determine the shock dynamics, completely determine the magnetic field strength and electron distribution (including their temporal and spatial dependence).

Fermi Observations of High-Energy Gamma-Ray Emission from GRB 080916C

*Light curves for GRB 080916C observed with the GBM and the LAT (*Abdo et al. 2009)

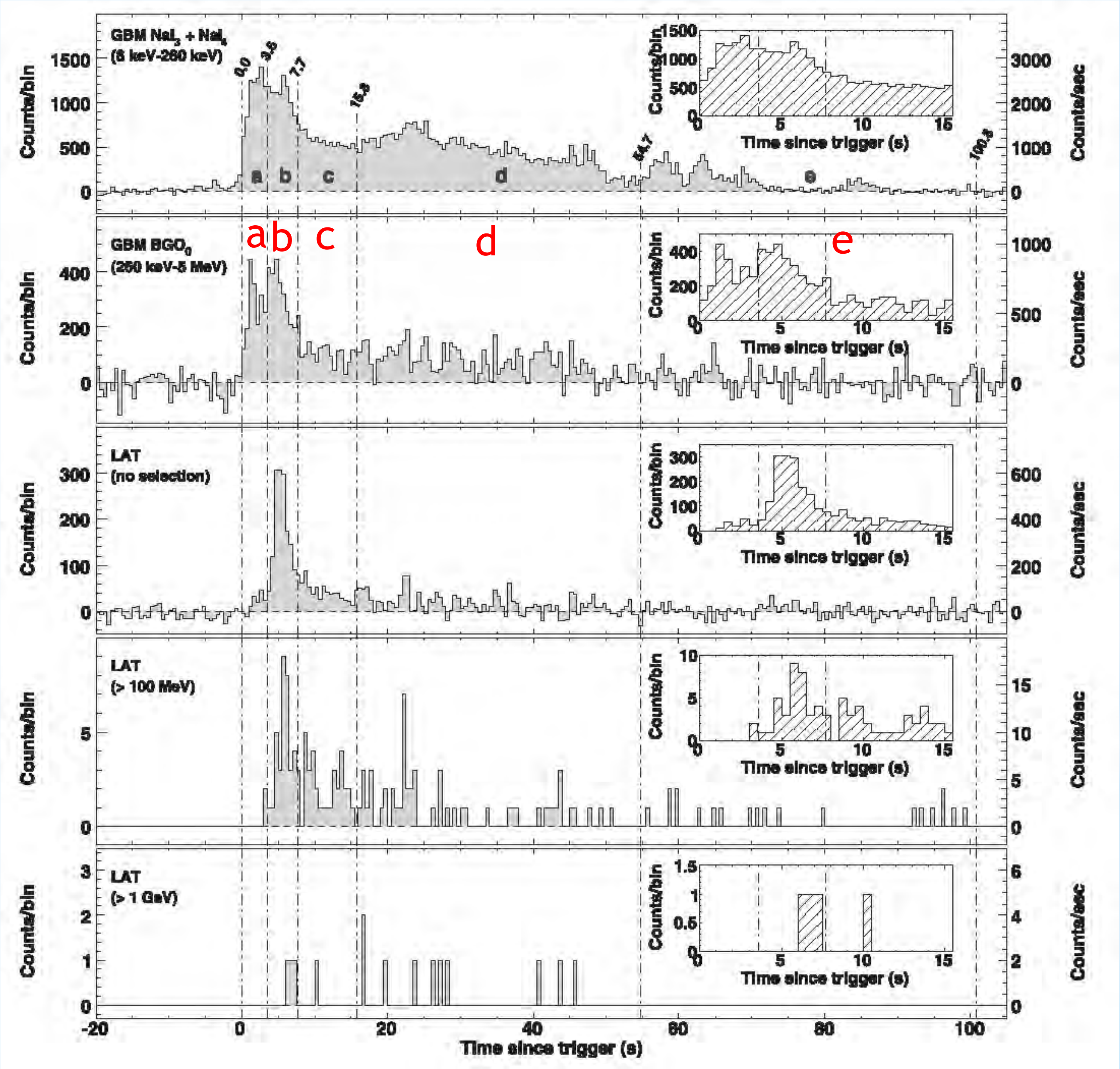

Synthetic spectra with different Lorentz factors with cold and warm thermal temperatures

synthetic spectra

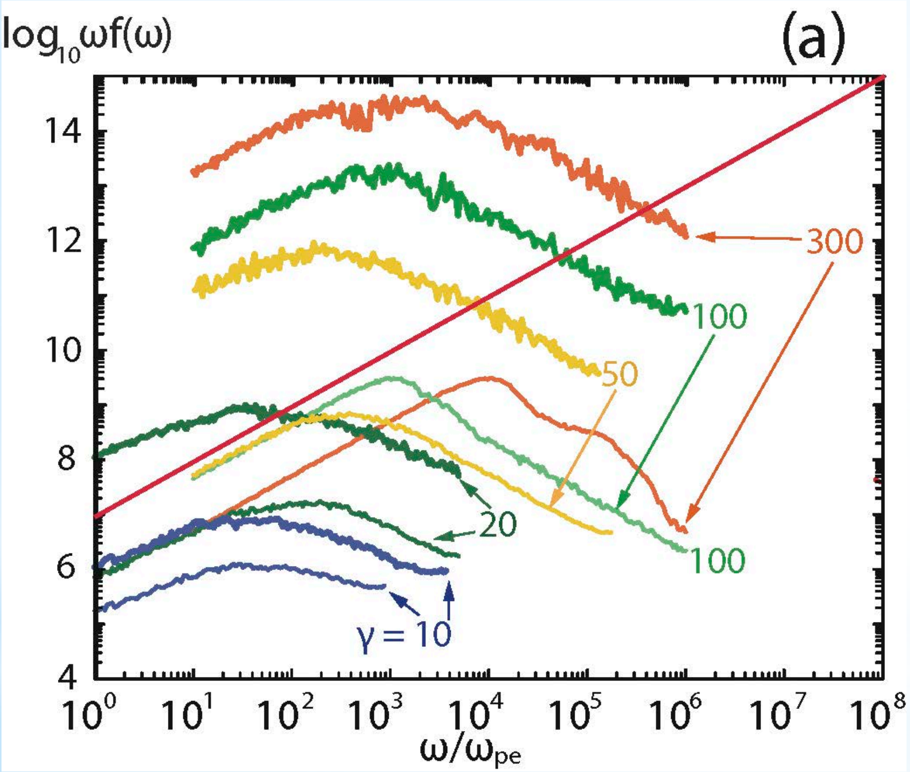

modeled Fermi spectra in vF units

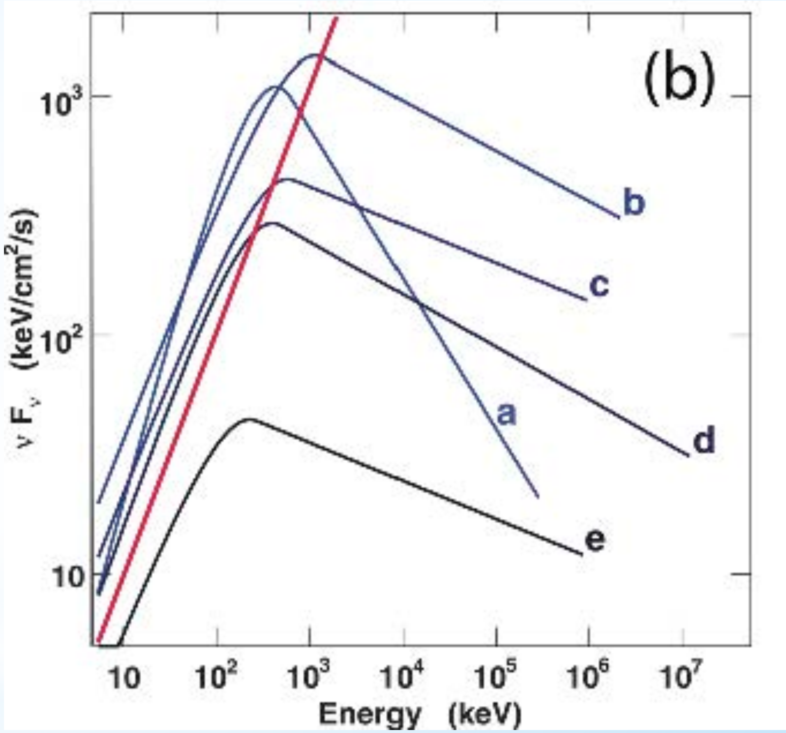

(thin lines) and warm (thick lines) electron jets.
The red lines indicate slope in vF ~ 1

(Abdo et al. 2009)

(Nishikawa et al. 2012)